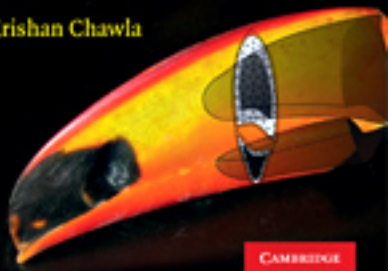


Mechanical Behavior of **MATERIALS**

SECOND EDITION

Marc Meyers and Krishan Chawla



CAMBRIDGE

CAMBRIDGE

www.cambridge.org/9780521866750

This page intentionally left blank

Mechanical Behavior of Materials

A balanced mechanics-materials approach and coverage of the latest developments in biomaterials and electronic materials, the new edition of this popular text is the most thorough and modern book available for upper-level undergraduate courses on the mechanical behavior of materials. Kept mathematically simple and with no extensive background in materials assumed, this is an accessible introduction to the subject.

New to this edition:

Every chapter has been revised, reorganised and updated to incorporate modern materials whilst maintaining a logical flow of theory to follow in class.

Mechanical principles of biomaterials, including cellular materials, and electronic materials are emphasized throughout.

A new chapter on environmental effects is included, describing the key relationship between conditions, microstructure and behaviour.

New homework problems included at the end of every chapter.

Providing a conceptual understanding by emphasizing the fundamental mechanisms that operate at micro- and nano-meter level across a wide-range of materials, reinforced through the extensive use of micrographs and illustrations this is the perfect textbook for a course in mechanical behavior of materials in mechanical engineering and materials science.

Marc André Meyers is a Professor in the Department of Mechanical and Aerospace Engineering at the University of California, San Diego. He was Co-Founder and Co-Chair of the EXPLOMET Conferences and won the TMS Distinguished Materials Scientist/Engineer Award in 2003.

Krishan Kumar Chawla is a Professor and former Chair in the Department of Materials Science and Engineering, University of Alabama at Birmingham, and also won their Presidential Award for Excellence in Teaching in 2006.

Mechanical Behavior of Materials

Marc André Meyers
University of California, San Diego

Krishan Kumar Chawla
University of Alabama at Birmingham



CAMBRIDGE UNIVERSITY PRESS
Cambridge, New York, Melbourne, Madrid, Cape Town, Singapore, São Paulo

Cambridge University Press
The Edinburgh Building, Cambridge CB2 8RU, UK
Published in the United States of America by Cambridge University Press, New York

www.cambridge.org

Information on this title: www.cambridge.org/9780521866750

© Cambridge University Press 2009

This publication is in copyright. Subject to statutory exception and to the provision of relevant collective licensing agreements, no reproduction of any part may take place without the written permission of Cambridge University Press.

First published in print format 2008

ISBN-13 978-0-511-45557-5 eBook (EBL)

ISBN-13 978-0-521-86675-0 hardback

Cambridge University Press has no responsibility for the persistence or accuracy of urls for external or third-party internet websites referred to in this publication, and does not guarantee that any content on such websites is, or will remain, accurate or appropriate.

Lovingly dedicated to the memory of my parents,
Henri and Marie-Anne.

Marc André Meyers

Lovingly dedicated to the memory of my parents,
Manohar L. and Sumitra Chawla.

Krishan Kumar Chawla

We dance round in a ring and suppose.
But the secret sits in the middle and knows.
Robert Frost

Contents

<i>Preface to the First Edition</i>	<i>page xvii</i>
<i>Preface to the Second Edition</i>	<i>xxi</i>
<i>A Note to the Reader</i>	<i>xxiii</i>

Chapter 1	Materials: Structure, Properties, and Performance	1
1.1	Introduction	1
1.2	Monolithic, Composite, and Hierarchical Materials	3
1.3	Structure of Materials	15
1.3.1	Crystal Structures	16
1.3.2	Metals	19
1.3.3	Ceramics	25
1.3.4	Glasses	30
1.3.5	Polymers	31
1.3.6	Liquid Crystals	39
1.3.7	Biological Materials and Biomaterials	40
1.3.8	Porous and Cellular Materials	44
1.3.9	Nano- and Microstructure of Biological Materials	45
1.3.10	The Sponge Spicule: An Example of a Biological Material	56
1.3.11	Active (or Smart) Materials	57
1.3.12	Electronic Materials	58
1.3.13	Nanotechnology	60
1.4	Strength of Real Materials	61
	Suggested Reading	64
	Exercises	65
Chapter 2	Elasticity and Viscoelasticity	71
2.1	Introduction	71
2.2	Longitudinal Stress and Strain	72
2.3	Strain Energy (or Deformation Energy) Density	77
2.4	Shear Stress and Strain	80
2.5	Poisson's Ratio	83
2.6	More Complex States of Stress	85
2.7	Graphical Solution of a Biaxial State of Stress: the Mohr Circle	89
2.8	Pure Shear: Relationship between G and E	95
2.9	Anisotropic Effects	96
2.10	Elastic Properties of Polycrystals	107
2.11	Elastic Properties of Materials	110
2.11.1	Elastic Properties of Metals	111
2.11.2	Elastic Properties of Ceramics	111
2.11.3	Elastic Properties of Polymers	116
2.11.4	Elastic Constants of Unidirectional Fiber Reinforced Composite	117

2.12	Viscoelasticity	120
2.12.1	Storage and Loss Moduli	124
2.13	Rubber Elasticity	126
2.14	Mooney–Rivlin Equation	131
2.15	Elastic Properties of Biological Materials	134
2.15.1	Blood Vessels	134
2.15.2	Articular Cartilage	137
2.15.3	Mechanical Properties at the Nanometer Level	140
2.16	Elastic Properties of Electronic Materials	143
2.17	Elastic Constants and Bonding	145
	Suggested Reading	155
	Exercises	155
<hr/>		
Chapter 3	Plasticity	161
3.1	Introduction	161
3.2	Plastic Deformation in Tension	163
3.2.1	Tensile Curve Parameters	171
3.2.2	Necking	172
3.2.3	Strain Rate Effects	176
3.3	Plastic Deformation in Compression Testing	183
3.4	The Bauschinger Effect	187
3.5	Plastic Deformation of Polymers	188
3.5.1	Stress–Strain Curves	188
3.5.2	Glassy Polymers	189
3.5.3	Semicrystalline Polymers	190
3.5.4	Viscous Flow	191
3.5.5	Adiabatic Heating	192
3.6	Plastic Deformation of Glasses	193
3.6.1	Microscopic Deformation Mechanism	195
3.6.2	Temperature Dependence and Viscosity	197
3.7	Flow, Yield, and Failure Criteria	199
3.7.1	Maximum-Stress Criterion (Rankine)	200
3.7.2	Maximum-Shear-Stress Criterion (Tresca)	200
3.7.3	Maximum-Distortion-Energy Criterion (von Mises)	201
3.7.4	Graphical Representation and Experimental Verification of Rankine, Tresca, and von Mises Criteria	201
3.7.5	Failure Criteria for Brittle Materials	205
3.7.6	Yield Criteria for Ductile Polymers	209
3.7.7	Failure Criteria for Composite Materials	211
3.7.8	Yield and Failure Criteria for Other Anisotropic Materials	213
3.8	Hardness	214
3.8.1	Macroindentation Tests	216
3.8.2	Microindentation Tests	221
3.8.3	Nanoindentation	225
3.9	Formability: Important Parameters	229
3.9.1	Plastic Anisotropy	231

3.9.2	Punch–Stretch Tests and Forming-Limit Curves (or Keeler–Goodwin Diagrams)	232
3.10	Muscle Force	237
3.11	Mechanical Properties of Some Biological Materials	241
	Suggested Reading	245
	Exercises	246

Chapter 4	Imperfections: Point and Line Defects	251
4.1	Introduction	251
4.2	Theoretical Shear Strength	252
4.3	Atomic or Electronic Point Defects	254
4.3.1	Equilibrium Concentration of Point Defects	256
4.3.2	Production of Point Defects	259
4.3.3	Effect of Point Defects on Mechanical Properties	260
4.3.4	Radiation Damage	261
4.3.5	Ion Implantation	265
4.4	Line Defects	266
4.4.1	Experimental Observation of Dislocations	270
4.4.2	Behavior of Dislocations	273
4.4.3	Stress Field Around Dislocations	275
4.4.4	Energy of Dislocations	278
4.4.5	Force Required to Bow a Dislocation	282
4.4.6	Dislocations in Various Structures	284
4.4.7	Dislocations in Ceramics	293
4.4.8	Sources of Dislocations	298
4.4.9	Dislocation Pileups	302
4.4.10	Intersection of Dislocations	304
4.4.11	Deformation Produced by Motion of Dislocations (Orowan’s Equation)	306
4.4.12	The Peierls–Nabarro Stress	309
4.4.13	The Movement of Dislocations: Temperature and Strain Rate Effects	310
4.4.14	Dislocations in Electronic Materials	313
	Suggested Reading	316
	Exercises	317

Chapter 5	Imperfections: Interfacial and Volumetric Defects	321
5.1	Introduction	321
5.2	Grain Boundaries	321
5.2.1	Tilt and Twist Boundaries	326
5.2.2	Energy of a Grain Boundary	328
5.2.3	Variation of Grain-Boundary Energy with Misorientation	330
5.2.4	Coincidence Site Lattice (CSL) Boundaries	332
5.2.5	Grain-Boundary Triple Junctions	334

5.2.6	Grain-Boundary Dislocations and Ledges	334
5.2.7	Grain Boundaries as a Packing of Polyhedral Units	336
5.3	Twinning and Twin Boundaries	336
5.3.1	Crystallography and Morphology	337
5.3.2	Mechanical Effects	341
5.4	Grain Boundaries in Plastic Deformation (Grain-size Strengthening)	345
5.4.1	Hall-Petch Theory	348
5.4.2	Cottrell's Theory	349
5.4.3	Li's Theory	350
5.4.4	Meyers-Ashworth Theory	351
5.5	Other Internal Obstacles	353
5.6	Nanocrystalline Materials	355
5.7	Volumetric or Tridimensional Defects	358
5.8	Imperfections in Polymers	361
	Suggested Reading	364
	Exercises	364
<hr/>		
Chapter 6	Geometry of Deformation and Work-Hardening	369
6.1	Introduction	369
6.2	Geometry of Deformation	373
6.2.1	Stereographic Projections	373
6.2.2	Stress Required for Slip	374
6.2.3	Shear Deformation	380
6.2.4	Slip in Systems and Work-Hardening	381
6.2.5	Independent Slip Systems in Polycrystals	384
6.3	Work-Hardening in Polycrystals	384
6.3.1	Taylor's Theory	386
6.3.2	Seeger's Theory	388
6.3.3	Kuhlmann-Wilsdorf's Theory	388
6.4	Softening Mechanisms	392
6.5	Texture Strengthening	395
	Suggested Reading	399
	Exercises	399
<hr/>		
Chapter 7	Fracture: Macroscopic Aspects	404
7.1	Introduction	404
7.2	Theoretical Tensile Strength	406
7.3	Stress Concentration and Griffith Criterion of Fracture	409
7.3.1	Stress Concentrations	409
7.3.2	Stress Concentration Factor	409
7.4	Griffith Criterion	416
7.5	Crack Propagation with Plasticity	419
7.6	Linear Elastic Fracture Mechanics	421
7.6.1	Fracture Toughness	422

7.6.2	Hypotheses of LEFM	423
7.6.3	Crack-Tip Separation Modes	423
7.6.4	Stress Field in an Isotropic Material in the Vicinity of a Crack Tip	424
7.6.5	Details of the Crack-Tip Stress Field in Mode I	425
7.6.6	Plastic-Zone Size Correction	428
7.6.7	Variation in Fracture Toughness with Thickness	431
7.7	Fracture Toughness Parameters	434
7.7.1	Crack Extension Force G	434
7.7.2	Crack Opening Displacement	437
7.7.3	J Integral	440
7.7.4	R Curve	443
7.7.5	Relationships among Different Fracture Toughness Parameters	444
7.8	Importance of K_{Ic} in Practice	445
7.9	Post-Yield Fracture Mechanics	448
7.10	Statistical Analysis of Failure Strength	449
	Appendix: Stress Singularity at Crack Tip	458
	Suggested Reading	460
	Exercises	460
Chapter 8 Fracture: Microscopic Aspects		466
8.1	Introduction	466
8.2	Fracture in Metals	468
8.2.1	Crack Nucleation	468
8.2.2	Ductile Fracture	469
8.2.3	Brittle, or Cleavage, Fracture	480
8.3	Fracture in Ceramics	487
8.3.1	Microstructural Aspects	487
8.3.2	Effect of Grain Size on Strength of Ceramics	494
8.3.3	Fracture of Ceramics in Tension	496
8.3.4	Fracture in Ceramics Under Compression	499
8.3.5	Thermally Induced Fracture in Ceramics	504
8.4	Fracture in Polymers	507
8.4.1	Brittle Fracture	507
8.4.2	Crazing and Shear Yielding	508
8.4.3	Fracture in Semicrystalline and Crystalline Polymers	512
8.4.4	Toughness of Polymers	513
8.5	Fracture and Toughness of Biological Materials	517
8.6	Fracture Mechanism Maps	521
	Suggested Reading	521
	Exercises	521
Chapter 9 Fracture Testing		525
9.1	Introduction	525
9.2	Impact Testing	525
9.2.1	Charpy Impact Test	526

9.2.2	Drop-Weight Test	529
9.2.3	Instrumented Charpy Impact Test	531
9.3	Plane-Strain Fracture Toughness Test	532
9.4	Crack Opening Displacement Testing	537
9.5	J-Integral Testing	538
9.6	Flexure Test	540
9.6.1	Three-Point Bend Test	541
9.6.2	Four-Point Bending	542
9.6.3	Interlaminar Shear Strength Test	543
9.7	Fracture Toughness Testing of Brittle Materials	545
9.7.1	Chevron Notch Test	547
9.7.2	Indentation Methods for Determining Toughness	549
9.8	Adhesion of Thin Films to Substrates	552
	Suggested Reading	553
	Exercises	553
<hr/>		
Chapter 10	Solid Solution, Precipitation, and Dispersion Strengthening	558
10.1	Introduction	558
10.2	Solid-Solution Strengthening	559
10.2.1	Elastic Interaction	560
10.2.2	Other Interactions	564
10.3	Mechanical Effects Associated with Solid Solutions	564
10.3.1	Well-Defined Yield Point in the Stress–Strain Curves	565
10.3.2	Plateau in the Stress–Strain Curve and Lüders Band	566
10.3.3	Strain Aging	567
10.3.4	Serrated Stress–Strain Curve	568
10.3.5	Snoek Effect	569
10.3.6	Blue Brittleness	570
10.4	Precipitation- and Dispersion-Hardening	571
10.5	Dislocation–Precipitate Interaction	579
10.6	Precipitation in Microalloyed Steels	585
10.7	Dual-Phase Steels	590
	Suggested Reading	590
	Exercises	591
<hr/>		
Chapter 11	Martensitic Transformation	594
11.1	Introduction	594
11.2	Structures and Morphologies of Martensite	594
11.3	Strength of Martensite	600
11.4	Mechanical Effects	603
11.5	Shape-Memory Effect	608
11.5.1	Shape-Memory Effect in Polymers	614
11.6	Martensitic Transformation in Ceramics	614
	Suggested Reading	618
	Exercises	619

Chapter 12	Special Materials: Intermetallics and Foams	621
12.1	Introduction	621
12.2	Silicides	621
12.3	Ordered Intermetallics	622
12.3.1	Dislocation Structures in Ordered Intermetallics	624
12.3.2	Effect of Ordering on Mechanical Properties	628
12.3.3	Ductility of Intermetallics	634
12.4	Cellular Materials	639
12.4.1	Structure	639
12.4.2	Modeling of the Mechanical Response	639
12.4.3	Comparison of Predictions and Experimental Results	645
12.4.4	Syntactic Foam	645
12.4.5	Plastic Behavior of Porous Materials	646
	Suggested Reading	650
	Exercises	650
<hr/>		
Chapter 13	Creep and Superplasticity	653
13.1	Introduction	653
13.2	Correlation and Extrapolation Methods	659
13.3	Fundamental Mechanisms Responsible for Creep	665
13.4	Diffusion Creep	666
13.5	Dislocation (or Power Law) Creep	670
13.6	Dislocation Glide	673
13.7	Grain-Boundary Sliding	675
13.8	Deformation-Mechanism (Weertman–Ashby) Maps	676
13.9	Creep-Induced Fracture	678
13.10	Heat-Resistant Materials	681
13.11	Creep in Polymers	688
13.12	Diffusion-Related Phenomena in Electronic Materials	695
13.13	Superplasticity	697
	Suggested Reading	705
	Exercises	705
<hr/>		
Chapter 14	Fatigue	713
14.1	Introduction	713
14.2	Fatigue Parameters and <i>S</i> – <i>N</i> (Wöhler) Curves	714
14.3	Fatigue Strength or Fatigue Life	716
14.4	Effect of Mean Stress on Fatigue Life	719
14.5	Effect of Frequency	721
14.6	Cumulative Damage and Life Exhaustion	721
14.7	Mechanisms of Fatigue	725

14.7.1	Fatigue Crack Nucleation	725
14.7.2	Fatigue Crack Propagation	730
14.8	Linear Elastic Fracture Mechanics Applied to Fatigue	735
14.8.1	Fatigue of Biomaterials	744
14.9	Hysteretic Heating in Fatigue	746
14.10	Environmental Effects in Fatigue	748
14.11	Fatigue Crack Closure	748
14.12	The Two-Parameter Approach	749
14.13	The Short-Crack Problem in Fatigue	750
14.14	Fatigue Testing	751
14.14.1	Conventional Fatigue Tests	751
14.14.2	Rotating Bending Machine	751
14.14.3	Statistical Analysis of <i>S-N</i> Curves	753
14.14.4	Nonconventional Fatigue Testing	753
14.14.5	Servohydraulic Machines	755
14.14.6	Low-Cycle Fatigue Tests	756
14.14.7	Fatigue Crack Propagation Testing	757
	Suggested Reading	758
	Exercises	759
Chapter 15 Composite Materials		765
15.1	Introduction	765
15.2	Types of Composites	765
15.3	Important Reinforcements and Matrix Materials	767
15.3.1	Microstructural Aspects and Importance of the Matrix	769
15.4	Interfaces in Composites	770
15.4.1	Crystallographic Nature of the Fiber–Matrix Interface	771
15.4.2	Interfacial Bonding in Composites	772
15.4.3	Interfacial Interactions	773
15.5	Properties of Composites	774
15.5.1	Density and Heat Capacity	775
15.5.2	Elastic Moduli	775
15.5.3	Strength	780
15.5.4	Anisotropic Nature of Fiber Reinforced Composites	783
15.5.5	Aging Response of Matrix in MMCs	785
15.5.6	Toughness	785
15.6	Load Transfer from Matrix to Fiber	788
15.6.1	Fiber and Matrix Elastic	789
15.6.2	Fiber Elastic and Matrix Plastic	792
15.7	Fracture in Composites	794
15.7.1	Single and Multiple Fracture	795
15.7.2	Failure Modes in Composites	796
15.8	Some Fundamental Characteristics of Composites	799
15.8.1	Heterogeneity	799

15.8.2	Anisotropy	799
15.8.3	Shear Coupling	801
15.8.4	Statistical Variation in Strength	802
15.9	Functionally Graded Materials	803
15.10	Applications	803
15.10.1	Aerospace Applications	803
15.10.2	Nonaerospace Applications	804
15.11	Laminated Composites	806
	Suggested Reading	809
	Exercises	810
<hr/> Chapter 16 Environmental Effects		815
16.1	Introduction	815
16.2	Electrochemical Nature of Corrosion in Metals	815
16.2.1	Galvanic Corrosion	816
16.2.2	Uniform Corrosion	817
16.2.3	Crevice corrosion	817
16.2.4	Pitting Corrosion	818
16.2.5	Intergranular Corrosion	818
16.2.6	Selective leaching	819
16.2.7	Erosion-Corrosion	819
16.2.8	Radiation Damage	819
16.2.9	Stress Corrosion	819
16.3	Oxidation of metals	819
16.4	Environmentally Assisted Fracture in Metals	820
16.4.1	Stress Corrosion Cracking (SCC)	820
16.4.2	Hydrogen Damage in Metals	824
16.4.3	Liquid and Solid Metal Embrittlement	830
16.5	Environmental Effects in Polymers	831
16.5.1	Chemical or Solvent Attack	832
16.5.2	Swelling	832
16.5.3	Oxidation	833
16.5.4	Radiation Damage	834
16.5.5	Environmental Cracking	835
16.5.6	Alleviating the Environmental Damage in Polymers	836
16.6	Environmental Effects in Ceramics	836
16.6.1	Oxidation of Ceramics	839
	Suggested Reading	840
	Exercises	840
	<i>Appendixes</i>	843
	<i>Index</i>	851

Preface to the First Edition

Courses in the mechanical behavior of materials are standard in both mechanical engineering and materials science/engineering curricula. These courses are taught, usually, at the junior or senior level. This book provides an introductory treatment of the mechanical behavior of materials with a balanced mechanics–materials approach, which makes it suitable for both mechanical and materials engineering students. The book covers metals, polymers, ceramics, and composites and contains more than sufficient information for a one-semester course. It therefore enables the instructor to choose the path most appropriate to the class level (junior- or senior-level undergraduate) and background (mechanical or materials engineering). The book is organized into 15 chapters, each corresponding, approximately, to one week of lectures. It is often the case that several theories have been developed to explain specific effects; this book presents only the principal ideas. At the undergraduate level the simple aspects should be emphasized, whereas graduate courses should introduce the different viewpoints to the students. Thus, we have often ignored active and important areas of research. Chapter 1 contains introductory information on materials that students with a previous course in the properties of materials should be familiar with. In addition, it enables those students unfamiliar with materials to “get up to speed.” The section on the theoretical strength of a crystal should be covered by all students. Chapter 2, on elasticity and viscoelasticity, contains an elementary treatment, tailored to the needs of undergraduate students. Most metals and ceramics are linearly elastic, whereas polymers often exhibit nonlinear elasticity with a strong viscous component. In Chapter 3, a broad treatment of plastic deformation and flow and fracture criteria is presented. Whereas mechanical engineering students should be fairly familiar with these concepts, (Section 3.2 can therefore be skipped), materials engineering students should be exposed to them. Two very common tests applied to materials, the uniaxial tension and compression tests, are also described. Chapters 4 through 9, on imperfections, fracture, and fracture toughness, are essential to the understanding of the mechanical behavior of materials and therefore constitute the core of the course. Point, line (Chapter 4), interfacial, and volumetric (Chapter 5) defects are discussed. The treatment is introductory and primarily descriptive. The mathematical treatment of defects is very complex and is not really essential to the understanding of the mechanical behavior of materials at an engineering level. In Chapter 6, we use the concept of dislocations to explain work-hardening; our understanding of this phenomenon, which dates from the 1930s, followed by contemporary developments, is presented. Chapters 7 and 8 deal with fracture from a macroscopic (primarily mechanical) and a microstructural viewpoint, respectively. In brittle materials, the fracture strength under

tension and compression can differ by a factor of 10, and this difference is discussed. The variation in strength from specimen to specimen is also significant and is analyzed in terms of Weibull statistics. In Chapter 9, the different ways in which the fracture resistance of materials can be tested is described. In Chapter 10, solid solution, precipitation, and dispersion strengthening, three very important mechanisms for strengthening metals, are presented. Martensitic transformation and toughening (Chapter 11) are very effective in metals and ceramics, respectively. Although this effect has been exploited for over 4,000 years, it is only in the second half of the 20th century that a true scientific understanding has been gained; as a result, numerous new applications have appeared, ranging from shape-memory alloys to maraging steels, that exhibit strengths higher than 2 GPa. Among novel materials with unique properties that have been developed for advanced applications are intermetallics, which often contain ordered structures. These are presented in Chapter 12. In Chapters 13 and 14, a detailed treatment of the fundamental mechanisms responsible for creep and fatigue, respectively, is presented. This is supplemented by a description of the principal testing and data analysis methods for these two phenomena. The last chapter of the book deals with composite materials. This important topic is, in some schools, the subject of a separate course. If this is the case, the chapter can be omitted.

This book is a spinoff of a volume titled *Mechanical Metallurgy* written by these authors and published in 1984 by Prentice-Hall. That book had considerable success in the United States and overseas, and was translated into Chinese. For the current volume, major changes and additions were made, in line with the rapid development of the field of materials in the 1980s and 1990s. Ceramics, polymers, composites, and intermetallics are nowadays important structural materials for advanced applications and are comprehensively covered in this book. Each chapter contains, at the end, a list of suggested reading; readers should consult these sources if they need to expand a specific point or if they want to broaden their knowledge in an area. Full acknowledgment is given in the text to all sources of tables and illustrations. We might have inadvertently forgotten to cite some of the sources in the final text; we sincerely apologize if we have failed to do so. All chapters contain solved examples and extensive lists of homework problems. These should be valuable tools in helping the student to grasp the concepts presented.

By their intelligent questions and valuable criticisms, our students provided the most important input to the book; we are very grateful for their contributions. We would like to thank our colleagues and fellow scientists who have, through painstaking effort and unselfish devotion, proposed the concepts, performed the critical experiments, and developed the theories that form the framework of an emerging quantitative understanding of the mechanical behavior of materials. In order to make the book easier to read, we have opted to minimize the use of references. In a few places, we have placed them

in the text. The patient and competent typing of the manuscript by Jennifer Natelli, drafting by Jessica McKinnis, and editorial help with text and problems by H. C. (Bryan) Chen and Elizabeth Kristofetz are gratefully acknowledged. Krishan Chawla would like to acknowledge research support, over the years, from the US Office of Naval Research, Oak Ridge National Laboratory, Los Alamos National Laboratory, and Sandia National Laboratories. He is also very thankful to his wife, Nivedita; son, Nikhilesh; and daughter, Kanika, for making it all worthwhile! Kanika's help in word processing is gratefully acknowledged. Marc Meyers acknowledges the continued support of the National Science Foundation (especially R. J. Reynik and B. MacDonald), the US Army Research Office (especially G. Mayer, A. Crowson, K. Iyer, and E. Chen), and the Office of Naval Research. The inspiration provided by his grandfather, Jean-Pierre Meyers, and father, Henri Meyers, both metallurgists who devoted their lives to the profession, has inspired Marc Meyers. The Institute for Mechanics and Materials of the University of California at San Diego generously supported the writing of the book during the 1993–96 period. The help provided by Professor R. Skalak, director of the institute, is greatly appreciated. The Institute for Mechanics and Materials is supported by the National Science Foundation. The authors are grateful for the hospitality of Professor B. Ilshner at the École Polytechnique Fédérale de Lausanne, Switzerland during the last part of the preparation of the book.

Marc André Meyers
La Jolla, California

Krishan Kumar Chawla
Birmingham, Alabama

Preface to the Second Edition

The second edition of *Mechanical Behavior of Materials* has revised and updated material in every chapter to reflect the changes occurring in the field. In view of the increasing importance of bioengineering, a special emphasis is given to the mechanical behavior of biological materials and biomaterials throughout this second edition. A new chapter on environmental effects has been added. Professors Fine and Voorhees¹ make a cogent case for integrating biological materials into materials science and engineering curricula. This trend is already in progress at many US and European universities. Our second edition takes due recognition of this important trend. We have resisted the temptation to make a separate chapter on biological and biomaterials. Instead, we treat these materials together with traditional materials, viz., metals, ceramics, polymers, etc. In addition, taking due cognizance of the importance of electronic materials, we have emphasized the distinctive features of these materials from a mechanical behavior point of view.

The underlying theme in the second edition is the same as in the first edition. The text connects the fundamental mechanisms to the wide range of mechanical properties of different materials under a variety of environments. This book is unique in that it presents, in a unified manner, important principles involved in the mechanical behavior of different materials: metals, polymers, ceramics, composites, electronic materials, and biomaterials. The unifying thread running throughout is that the nano/microstructure of a material controls its mechanical behavior. A wealth of micrographs and line diagrams are provided to clarify the concepts. Solved examples and chapter-end exercise problems are provided throughout the text.

This text is designed for use in mechanical engineering and materials science and engineering courses by upper division and graduate students. It is also a useful reference tool for the practicing engineers involved with mechanical behavior of materials. The book does not presuppose any extensive knowledge of materials and is mathematically simple. Indeed, Chapter 1 provides the background necessary. We invite the reader to consult this chapter off and on because it contains very general material.

In addition to the major changes discussed above, the mechanical behavior of cellular and electronic materials was incorporated. Major reorganization of material has been made in the following parts: elasticity; Mohr circle treatment; elastic constants of fiber reinforced composites; elastic properties of biological and of biomaterials; failure criteria of composite materials; nanoindentation technique and its use in extracting material properties; etc. New solved and

¹ M. E. Fine and P. Voorhees, "On the evolving curriculum in materials science & engineering," *Daedalus*, Spring 2005, 134.

chapter-end exercises are added. New micrographs and line diagrams are provided to clarify the concepts.

We are grateful to many faculty members who adopted the first edition for classroom use and were kind enough to provide us with very useful feedback. We also appreciate the feedback we received from a number of students. MAM would like to thank Kanika Chawla and Jennifer Ko for help in the biomaterials area. The help provided by Marc H. Meyers and M. Cristina Meyers in teaching him the rudiments of biology has been invaluable. KKC would like to thank K. B. Carlisle, N. Chawla, A. Goel, M. Koopman, R. Kulkarni, and B. R. Patterson for their help. KKC acknowledges the hospitality of Dr. P. D. Portella at Federal Institute for Materials Research and Testing (BAM), Berlin, Germany, where he spent a part of his sabbatical. As always, he is grateful to his family members, Anita, Kanika, Nikhil, and Nivi for their patience and understanding.

Marc André Meyers
University of California, San Diego

Krishan Kumar Chawla
University of Alabama at Birmingham

A Note to the Reader

Our goal in writing *Mechanical Behavior of Materials* has been to produce a book that will be the pre-eminent source of fundamental knowledge about the subject. We expect this to be a guide to the student beyond his or her college years. There is, of course, a lot more material than can be covered in a normal semester-long course. We make no apologies for that in addition to being a classroom text, we want this volume to act as a useful reference work on the subject for the practicing scientist, researcher, and engineer.

Specifically, we have an introductory chapter dwelling on the themes of the book: structure, mechanical properties, and performance. This section introduces some key terms and concepts that are covered in detail in later chapters. We advise the reader to use this chapter as a handy reference tool, and consult it as and when required. We strongly suggest that the instructor use this first chapter as a self-study resource. Of course, individual sections, examples, and exercises can be added to the subsequent material as and when desired.

Enjoy!

Materials: Structure, Properties, and Performance

I.1 Introduction

Everything that surrounds us is matter. The origin of the word matter is *mater* (Latin) or *matri* (Sanskrit), for *mother*. In this sense, human beings anthropomorphized that which made them possible – that which gave them nourishment. Every scientific discipline concerns itself with matter. Of all matter surrounding us, a portion comprises materials. What are materials? They have been variously defined. One acceptable definition is “matter that human beings use and/or process.” Another definition is “all matter used to produce manufactured or consumer goods.” In this sense, a rock is not a material, intrinsically; however, if it is used in aggregate (concrete) by humans, it becomes a material. The same applies to all matter found on earth: a tree becomes a material when it is processed and used by people, and a skin becomes a material once it is removed from its host and shaped into an artifact.

The successful utilization of materials requires that they satisfy a set of properties. These properties can be classified into thermal, optical, mechanical, physical, chemical, and nuclear, and they are intimately connected to the structure of materials. The structure, in its turn, is the result of synthesis and processing. A schematic framework that explains the complex relationships in the field of the mechanical behavior of materials, shown in Figure 1.1, is Thomas’s iterative tetrahedron, which contains four principal elements: mechanical properties, characterization, theory, and processing. These elements are related, and changes in one are inseparably linked to changes in the others. For example, changes may be introduced by the synthesis and processing of, for instance, steel. The most common metal, steel has a wide range of strengths and ductilities (*mechanical properties*), which makes it the material of choice for numerous applications. While low-carbon steel is used as reinforcing bars in concrete and in the body of automobiles, quenched and tempered high-carbon steel is used in more critical applications such as axles and gears. Cast iron, much more brittle, is used in a variety of applications, including automobile

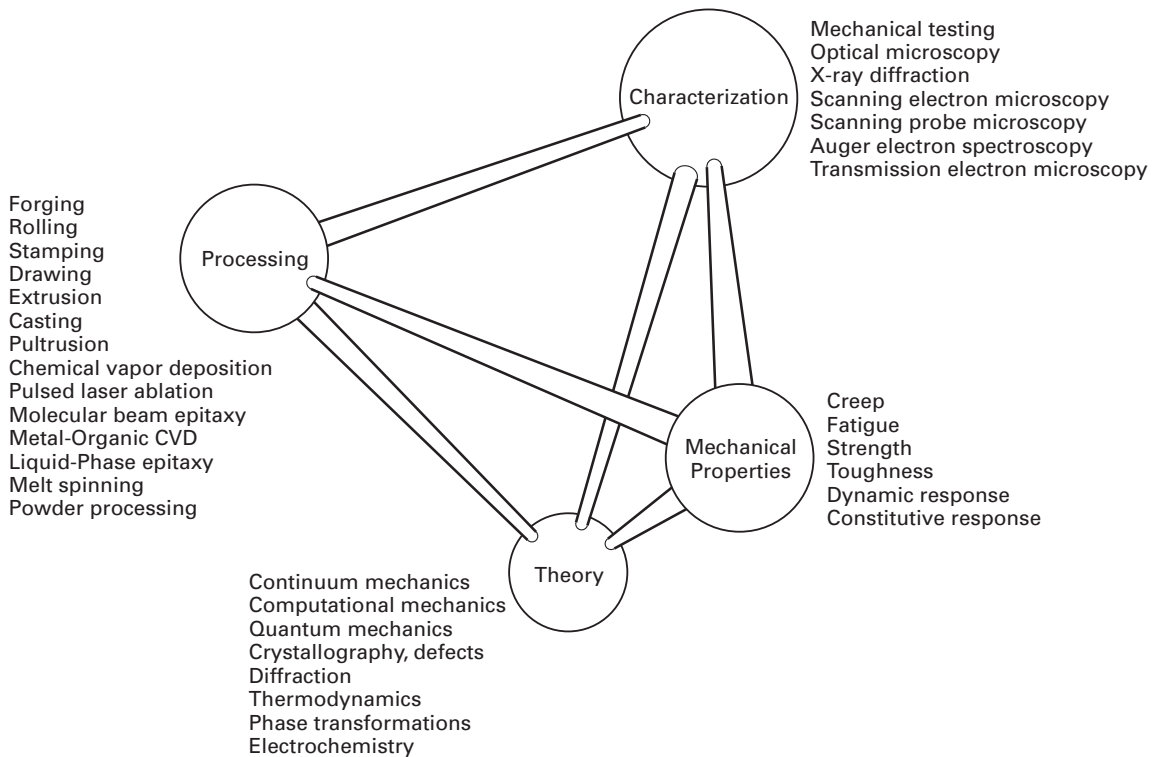


Fig. 1.1 Iterative materials tetrahedron applied to mechanical behavior of materials. (After G. Thomas.)

engine blocks. These different applications require, obviously, different mechanical properties of the material. The different properties of the three materials, resulting in differences in performance, are attributed to differences in the internal structure of the materials. The understanding of the structure comes from *theory*. The determination of the many aspects of the micro-, meso-, and macrostructure of materials is obtained by *characterization*. Low-carbon steel has a primarily ferritic structure (body-centered cubic; see Section 1.3.1), with some interspersed pearlite (a ferrite–cementite mixture). The high hardness of the quenched and tempered high-carbon steel is due to its martensitic structure (body-centered tetragonal). The relatively brittle cast iron has a structure resulting directly from solidification, without subsequent mechanical working such as hot rolling. How does one obtain low-carbon steel, quenched and tempered high-carbon steel, and cast iron? By different *synthesis* and *processing* routes. The low-carbon steel is processed from the melt by a sequence of mechanical working operations. The high-carbon steel is synthesized with a greater concentration of carbon ($>0.5\%$) than the low-carbon steel (0.1%). Additionally, after mechanical processing, the high-carbon steel is rapidly cooled from a temperature of approximately $1,000\text{ }^{\circ}\text{C}$ by throwing it into water or oil; it is then reheated to an intermediate temperature (tempering). The cast iron is synthesized with even higher carbon contents ($\sim 2\%$). It is poured directly into the molds and allowed to solidify in them. Thus, no mechanical working, except for some minor machining, is needed. These interrelationships among

structure, properties, and performance, and their modification by synthesis and processing, constitute the central theme of materials science and engineering. The tetrahedron of Figure 1.1 lists the principal processing methods, the most important theoretical approaches, and the most-used characterization techniques in materials science today.

The selection, processing, and utilization of materials have been part of human culture since its beginnings. Anthropologists refer to humans as “the toolmakers,” and this is indeed a very realistic description of a key aspect of human beings responsible for their ascent and domination over other animals. It is the ability of humans to manufacture and use tools, and the ability to produce manufactured goods, that has allowed technological, cultural, and artistic progress and that has led to civilization and its development. Materials were as important to a Neolithic tribe in the year 10,000 BC as they are to us today. The only difference is that today more complex synthetic materials are available in our society, while Neolithic tribes had only natural materials at their disposal: wood, minerals, bones, hides, and fibers from plants and animals. Although these naturally occurring materials are still used today, they are vastly inferior in properties to synthetic materials.

1.2 Monolithic, Composite, and Hierarchical Materials

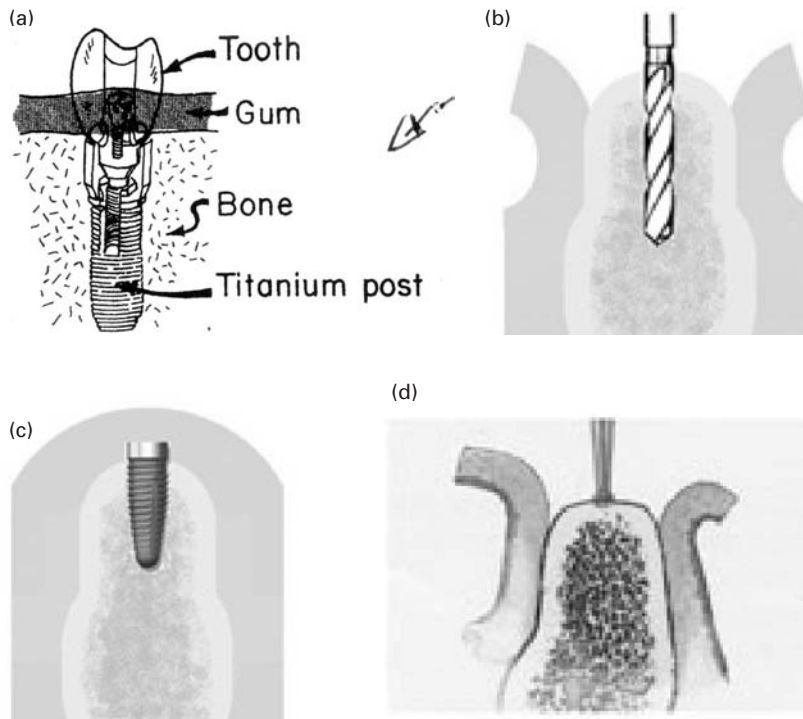
The early materials used by humans were natural, and their structure varied widely. Rocks are crystalline, pottery is a mixture of glassy and crystalline components, wood is a fibrous organic material with a cellular structure, and leather is a complex organic material. Human beings started to synthesize their own materials in the Neolithic period: ceramics first, then metals, and later, polymers. In the twentieth century, simple monolithic structures were used first. The term *monolithic* comes from the Greek *mono* (one) and *lithos* (stone). It means that the material has essentially uniform properties throughout. Microstructurally, monolithic materials can have two or more phases. Nevertheless, they have properties (electrical, mechanical, optical, and chemical) that are constant throughout. Table 1.1 presents some of the important properties of metals, ceramics, and polymers. Their detailed structures will be described in Section 1.3. The differences in their structure are responsible for differences in properties. Metals have densities ranging from 3 to 19 g/cm⁻³; iron, nickel, chromium, and niobium have densities ranging from 7 to 9 g/cm⁻³; aluminum has a density of 2.7 g/cm⁻³; and titanium has a density of 4.5 g/cm⁻³. Ceramics tend to have lower densities, ranging from 5 g/cm⁻³ (titanium carbide; TiC = 4.9) to 3 g/cm⁻³ (alumina; Al₂O₃ = 3.95; silicon carbide; SiC = 3.2). Polymers have the lowest densities, fluctuating around 1 g cm⁻³. Another marked difference among these

Table 1.1 Summary of Properties of Main Classes of Materials

Property	Metals	Ceramics	Polymers
Density (g/cm^3)	from 2 to 20	from 1 to 14	from 1 to 2.5
Electrical conductivity	high	low	low
Thermal conductivity	high	low	low
Ductility or strain-to-fracture (%)	4–40	<1	2–4
Tensile strength (MPa)	100–1,500	100–400	–
Compressive strength (MPa)	100–1,500	1,000–5,000	–
Fracture toughness ($\text{MNm}^{-3/2}$)	10–30	1–10	2–8
Maximum service temperature ($^{\circ}\text{C}$)	1,000	1,800	250
Corrosion resistance	low to medium	superior	medium
Bonding	metallic (free-electron cloud)	ionic or covalent	covalent
Structure	mostly crystalline (Face-centered cubic; FCC; Body-centered cubic; BCC; Hexagonal closed packed; HCP)	complex crystalline structure	amorphous or semicrystalline polymer

three classes of materials is their ductility (ability to undergo plastic deformation). At room temperature, metals can undergo significant plastic deformation. Thus, metals tend to be ductile, although there are a number of exceptions. Ceramics, on the other hand, are very brittle, and the most ductile ceramics will be more brittle than most metals. Polymers have a behavior ranging from brittle (at temperatures below their glass transition temperature) to very deformable (in a nonlinear elastic material, such as rubber). The fracture toughness is a good measure of the resistance of a material to failure and is generally quite high for metals and low for ceramics and polymers. Ceramics far outperform metals and polymers in high-temperature applications, since many ceramics do not oxidize even at very high temperatures (the oxide ceramics are already oxidized) and retain their strength to such temperatures. One can compare the mechanical, thermal, optical, electrical, and electronic properties of the different classes of materials and see that there is a very wide range of properties. Thus, monolithic structures built from primarily one class of material cannot provide all desired properties.

In the field of biomaterials (materials used in implants and life-support systems), developments also have had far-reaching effects. The mechanical performance of implants is critical in many applications, including hipbone implants, which are subjected to high stresses, and endosseous implants in the jaw designed to serve as the base for



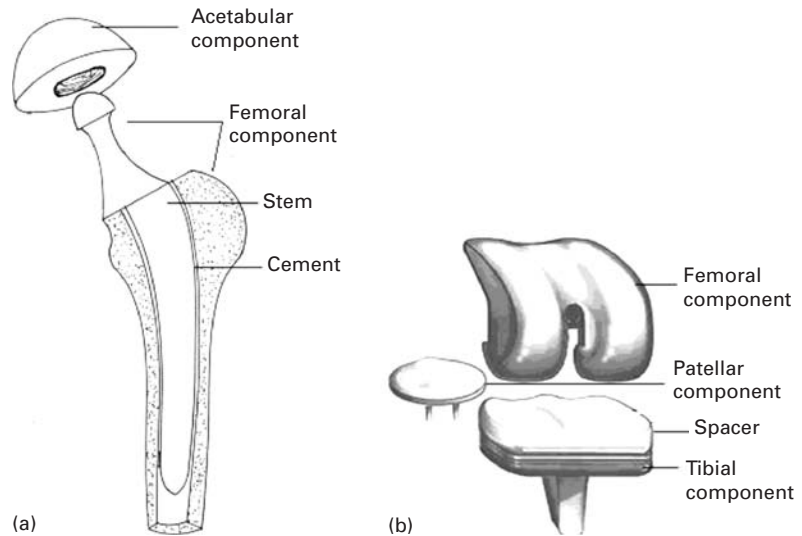
teeth. Figure 1.2 (a) shows the most successful design for endosseous implants in the jawbone. With this design, the tooth is fixed to the post and is effective. A titanium post is first screwed into the jawbone and allowed to heal. The tooth is then fixed to the post, and is effectively rooted into the jaw. The insertion of endosseous implants into the mandibles or maxillae, which was initiated in the 1980s, has been a revolution in dentistry. There is a little story associated with this discovery. Researchers were investigating the bone marrow of rabbits. They routinely used stainless steel hollow cylinders screwed into the bone. Through the hole, they could observe the bone marrow. It so happened that one of these cylinders was made of titanium. Since these cylinders were expensive, the researchers removed them periodically, in order to reuse them. When they tried to remove the titanium cylinder, it was tightly fused to the bone. This triggered the creative intuition of one of the researchers, who said "What if . . .?"

Figure 1.2(c) shows the procedure used to insert the titanium implant. The site is first marked with a small drill that penetrates the cortical bone. Then successive drills are used to create the orifice of desired diameter (Figure 1.2(d)). The implant is screwed into the bone and the tissue is closed (Figure 1.2(c)). This implant is allowed to heal and fuse with the bone for approximately six months. Chances are that most readers will have these devices installed sometime in their lives.

Hip- and knee-replacement surgery is becoming commonplace. In the USA alone between 250,000 and 300,000 of each procedure are carried out annually. The materials of the prostheses have an

Fig. 1.2 (a) Complete enclosures implant, (b) A hole is drilled and (c) a titanium post is screwed into jawbone. (d) Marking of site with small drill. (Courtesy of J. Mahooti.)

Fig. 1.3 (a) Total hip replacement prosthesis; (b) total knee replacement prosthesis.



important bearing on survival probability. Typical hip and knee prostheses are shown in Figure 1.3.

The hip prosthesis is made up of two parts: the acetabular component, or socket portion, which replaces the acetabulum; the femoral component, or stem portion, which replaces the femoral head.

The femoral component is made of a metal stem with a metal ball on the extremity. In some prostheses a ceramic ball is attached to the metal stem. The acetabular component is a metal shell with a plastic inner socket liner made of metal, ceramic, or a plastic called ultra-high-molecular-weight polyethylene (UHMWPE) that acts like a bearing. A *cemented* prosthesis is held in place by a type of epoxy cement that attaches the metal to the bone. An *uncemented* prosthesis has a fine mesh of holes on the surface area that touches the bone. The mesh allows the bone to grow into the mesh and become part of the bone. Biomaterial advances have allowed experimentation with new bearing surfaces, and there are now several different options when hip-replacement surgery is considered.

The metal has to be inert in the body environment. The preferred materials for the prostheses are Co-Cr alloys (Vitalium) and titanium alloys. However, there are problems that have not yet been resolved: the metallic components have elastic moduli that far surpass those of bone. Therefore, they “carry” a disproportionate fraction of the load, and the bone is therefore unloaded. Since the health and growth of bone is closely connected to the loads applied to it, this unloading tends to lead to bone loss.

The most common cause of joint replacement failure is wear of the implant surfaces. This is especially critical for the polymeric components of the prosthesis. This wear produces debris which leads to tissue irritation. Another important cause of failure is loosening of the implant due to weakening of the surrounding bone. A third source of failure is fatigue.

Biocompatibility is a major concern for all implants, and ceramics are especially attractive because of their (relative) chemical inertness. Metallic alloys such as Vitalium[®] (a cobalt-based alloy) and titanium alloys also have proved to be successful, as have polymers such as polyethylene. A titanium alloy with a solid core surrounded by a porous periphery (produced by sintering of powders) has shown considerable potential. The porous periphery allows bone to grow and affords very effective fixation. Two new classes of materials that appear to present the best biocompatibility with bones are the Bioglass[®] and calcium phosphate ceramics. Bones contain calcium and phosphorus, and Bioglass[®] is a glass in which the silicon has been replaced by those two elements. Thus, the bone “perceives” these materials as being another bone and actually bonds with it. Biomechanical properties are of great importance in bone implants, as are the elastic properties of materials. If the stiffness of a material is too high, then when implanted the material will carry more of the load placed on it than the adjacent bone. This could in turn lead to a weakening of the bone, since bone growth and strength depends on the stresses that the bone is subjected to. Thus, the elastic properties of bone and implant should be similar. Polymers reinforced with strong carbon fibers are also candidates for such applications. Metals, on the other hand, are stiffer than bones and tend to carry most of the load. With metals, the bones would be shielded from stress, which could lead to bone resorption and loosening of the implant.

Although new materials are being developed continuously, monolithic materials, with their uniform properties, cannot deliver the range of performance needed in many critical applications. *Composites* are a mixture of two classes of materials (metal–ceramic, metal–polymer, or polymer–ceramic). They have unique mechanical properties that are dependent on the amount and manner in which their constituents are arranged. Figure 1.4(a) shows schematically how different composites can be formed. Composites consist of a matrix and a reinforcing material. In making them, the modern materials engineer has at his or her disposal a very wide range of possibilities. However, the technological problems involved in producing some of them are immense, although there is a great deal of research addressing those problems. Figure 1.4(b) shows three principal kinds of reinforcement in composites: particles, continuous fibers, and discontinuous (short) fibers. The reinforcement usually has a higher strength than the matrix, which provides the ductility of the material. In ceramic-based composites, however, the matrix is brittle, and the fibers provide barriers to the propagating cracks, increasing the toughness of the material.

The alignment of the fibers is critical in determining the strength of a composite. The strength is highest along a direction parallel to the fibers and lowest along directions perpendicular to it. For the three kinds of composite shown in Figure 1.4(b), the polymer matrix plus (aramid, carbon, or glass) fiber is the most common combination if no high-temperature capability is needed.

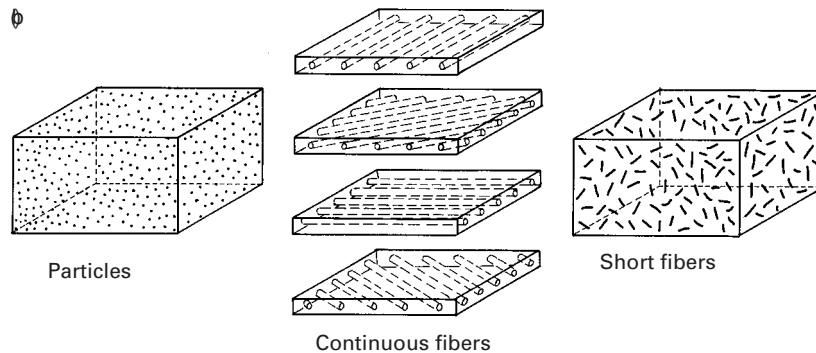
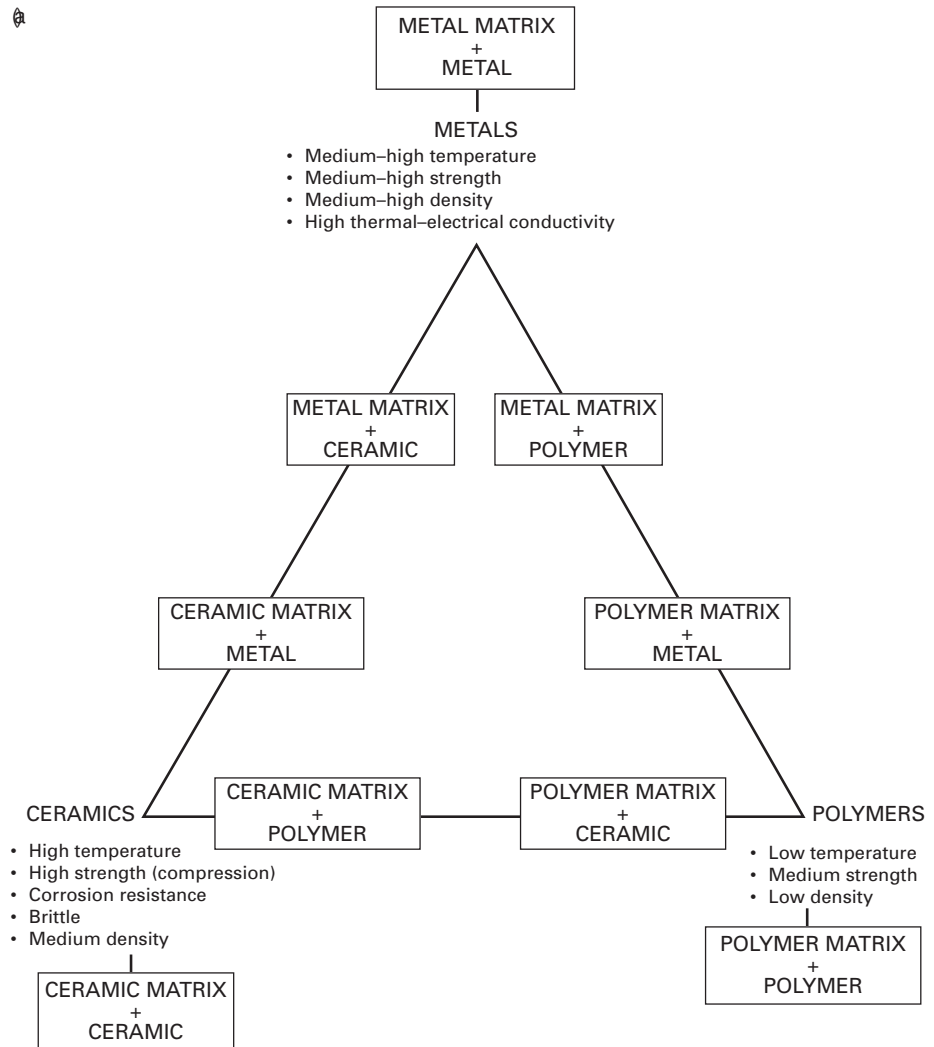


Fig. 1.4 (a) Schematic representations of different classes of composites. (b) Different kinds of reinforcement in composite materials. Composite with continuous fibers with four different orientations (shown separately for clarity).

Table 1.2 Specific Modulus and Strength of Materials Used in Aircraft

Material	Elastic Modulus	Tensile Strength
	Density ($GPa/g \cdot cm^{-3}$)	Density ($MPa/g \cdot cm^{-3}$)
Steel (AISI 4340)	25	230
Al (7075-T6)	25	180
Titanium (Ti-6Al-4V)	25	250
E Glass/Epoxy composite	21	490
S Glass/Epoxy composite	47	790
*Axamid/Epoxy composite	55	890
HS (High Tensile Strength) Carbon/Epoxy composite	92	780
HM (high modulus) Carbon/Epoxy composite	134	460

Composites are becoming a major material in the aircraft industry. Carbon/epoxy and aramid/epoxy composites are being introduced in a large number of aircraft parts. These composite parts reduce the weight of the aircraft, increasing its economy and payload. The major mechanical property advantages of advanced composites over metals are better stiffness-to-density and strength-to-density ratios and greater resistance to fatigue. The values given in Table 1.2 apply to a unidirectional composite along the fiber reinforcement orientation. The values along other directions are much lower, and therefore the design of a composite has to incorporate the anisotropy of the materials. It is clear from the table that composites have advantages over monolithic materials. In most applications, the fibers are arranged along different orientations in different layers. For the central composite of Figure 1.4(b), these orientations are 0° , 45° , 90° , and 135° to the tensile axis.

Can we look beyond composites in order to obtain even higher mechanical performance? Indeed, we can: Nature is infinitely imaginative.

Our body is a complex arrangement of parts, designed, as a whole, to perform all the tasks needed to keep us alive. Scientists are looking into the make-up of soft tissue (skin, tendon, intestine, etc.), which is a very complex structure with different units active at different levels complementing each other. The structure of soft tissue has been called a *hierarchical* structure, because there seems to be a relationship between the ways in which it operates at different levels. Figure 1.5 shows the structure of a tendon. This structure begins with the tropocollagen molecule, a triple helix of polymeric protein chains. The tropocollagen molecule has a diameter of approximately

Fig. 1.5 A model of a hierarchical structure occurring in the human body. (Adapted from E. Baer, *Sci. Am.* 254, No. 10 (1986) 179.)

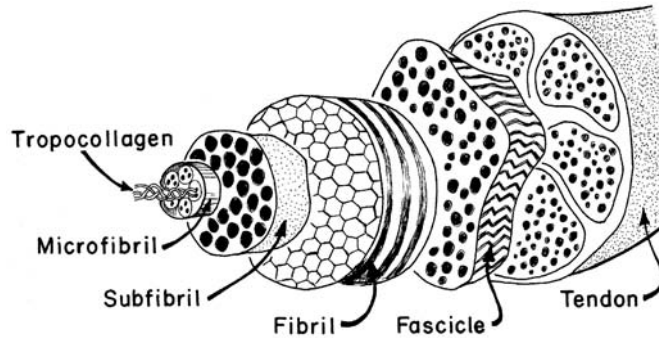
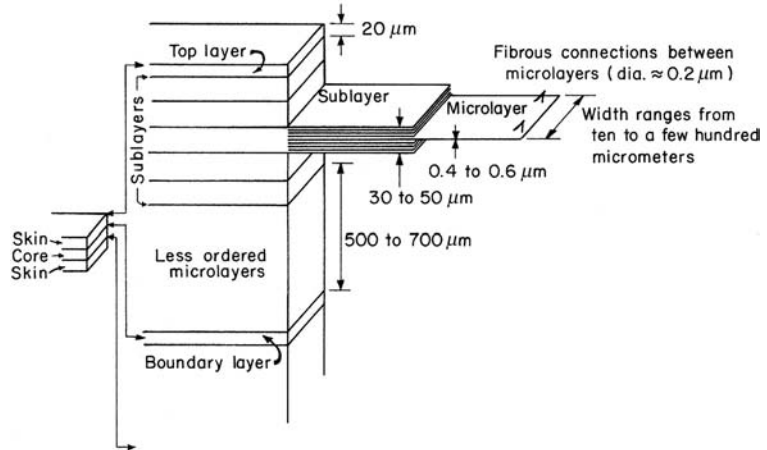


Fig. 1.6 Schematic illustration of a proposed hierarchical model for a composite (not drawn to scale). (Courtesy of E. Baer.)



1.5 mm. The tropocollagen organizes itself into microfibrils, subfibrils, and fibrils. The fibrils, a critical component of the structure, are crimped when there is no stress on them. When stressed, they stretch out and then transfer their load to the fascicles, which compose the tendon. The fascicles have a diameter of approximately 150–300 μm and constitute the basic unit of the tendon. The hierarchical organization of the tendon is responsible for its toughness. Separate structural units can fail independently and thus absorb energy locally, without causing the failure of the entire tendon. Both experimental and analytical studies have been done, modeling the tendon as a composite of elastic, wavy fibers in a viscoelastic matrix. Local failures, absorbing energy, will prevent catastrophic failure of the entire tendon until enormous damage is produced.

Materials engineers are beginning to look beyond simple two-component composites, imitating nature in organizing different levels of materials in a hierarchical manner. Baer¹ suggests that the study of biological materials could lead to new hierarchical designs for composites. One such example is shown in Figure 1.6, a layered structure of liquid-crystalline polymers consisting of alternating core and skin layers. Each layer is composed of sublayers which, in their

¹ E. Baer, *Sci. Am.* 254, No. 10 (1986) 179.

turn, are composed of microlayers. The molecules are arranged in different arrays in different layers. The lesson that can be learned from this arrangement is that we appear to be moving toward composites of increasing complexity.

Example 1.1 | (Design problem)

Discuss advanced materials used in bicycle frames.

This is a good case study, and the instructor can “pop” similar questions on an exam, using different products. For our specific example here, we recommend the insightful article by M. F. Ashby, *Met. and Mat. Trans.*, A 26A (1995) 3057. Ashby states that “*Materials and processes underpin all engineering design.*”



Fig. E1.1 Bending moments (M_1 and M_2) and torsional torques (T_1 and T_2) generated in bicycle frame by forces F_1 and F_2 applied to pedals.

Figure E1.1 shows a bicycle, with forces F_1 and F_2 applied to the frame by the pedals. These forces produce bending moments and torsions in the frame tubes. In bicycle frames, *weight* and *stiffness* are the two primary requirements. Stiffness is important because excessive flexing of the bicycle upon pedaling absorbs energy that should be used

to propel the bicycle forward. This requires the definition of new properties, because just the strength or endurance limit (the stress below which no failure due to fatigue occurs) and Young's modulus (defined in Chapter 2) are not sufficient. In conversations, we always say that aluminum bicycles are "stiffer" than steel bicycles, whereas steel provides a more "cushioned" ride. An aluminum bicycle may indeed be stiffer than a steel bicycle, although E_{st} ($= 210$ GPa) $\approx 3 E_{Al}$ ($= 70$ GPa). We will see shortly how this can happen and what is necessary for it to occur. The forces F_1 and F_2 cause bending moments (M_1 and M_2), respectively. The bending stresses in a hollow tube of radius r and thickness t are²

$$\sigma = \frac{Mr}{I},$$

where I is the moment of inertia, M the bending moment, and r the radius of the tube. Setting $\sigma = \sigma_e$, the endurance limit, and substituting the expression for the moment of inertia $I = \pi r^3 t$, we obtain the thickness of the tube, t , from:

$$M = \frac{\sigma_e \pi^3 t}{r}.$$

From strength considerations, the mass per unit length of the bicycle frame is

$$\frac{m}{L} = 2\pi r t \rho = \frac{2M}{r} \left(\frac{\rho}{\sigma_e} \right), \quad (\text{E1.1.1})$$

where ρ is the density of the frame. Now, the radius of curvature ρ' of a circular beam under bending is given by the Bernoulli-Euler equation,

$$\frac{1}{\rho'} = \frac{d^2 v}{dx^2} = \frac{M}{EI},$$

where v is the deflection of the beam. Substituting for I , we obtain

$$\frac{1}{\rho'} = \frac{M}{E \pi r^3 t}, \text{ or } \pi r t = \frac{M \rho'}{r^2 E}.$$

From bending considerations, the mass per unit length is

$$\frac{m}{L} = 2\pi r t \rho = \frac{2M \rho'}{r^2} \left(\frac{\rho}{E} \right) \quad (\text{E1.1.2})$$

A similar expression can be developed for the torsion, which is important in pedaling. The torsion is shown in Figure E1.2 as T_1 and T_2 . Since M , the applied moment, is given by the weight of cyclist, it is constant for each frame. Likewise, the maximum curvature $1/\rho'$ can be fixed. The quantity m/L has to be minimized for both strength and stiffness considerations. Ashby accomplished this by plotting (σ_e/ρ) and (E/ρ) , whose reciprocals appear in Equations (E1.1.1) and (E1.1.2), respectively. (See Figure E1.2.) The computations assume a constant r , but

² Students should consult their notes on the mechanics of materials or examine a book such as *Engineering Mechanics of Solids*, by E. P. Popov (Englewood Cliffs, NJ: Prentice Hall, 1990).

varying tube thickness t . The most common candidate metals (steels, titanium, and aluminum alloys) are closely situated in the figure. The expanded window in this region shows a clearer separation of the various alloys. Continuous carbon fiber reinforced composites (CFRPs) are the best materials, and polymers and glass/fiber reinforced polymer composites (GFRPs) have insufficient stiffness. By relaxing the requirement of constant r and allowing different tube radii, the results are changed considerably. This example illustrates how material properties enter into the design of a product and how compound properties (E/ρ , σ/ρ) need to be defined for a specific application. It can be seen from Equations (E1.1.1) and (E1.1.2) that strength scales with r and stiffness with r^2 . By varying r , it is possible to obtain aluminum bicycle frames that are stiffer than steel. Now the student is prepared to go on a bike ride!

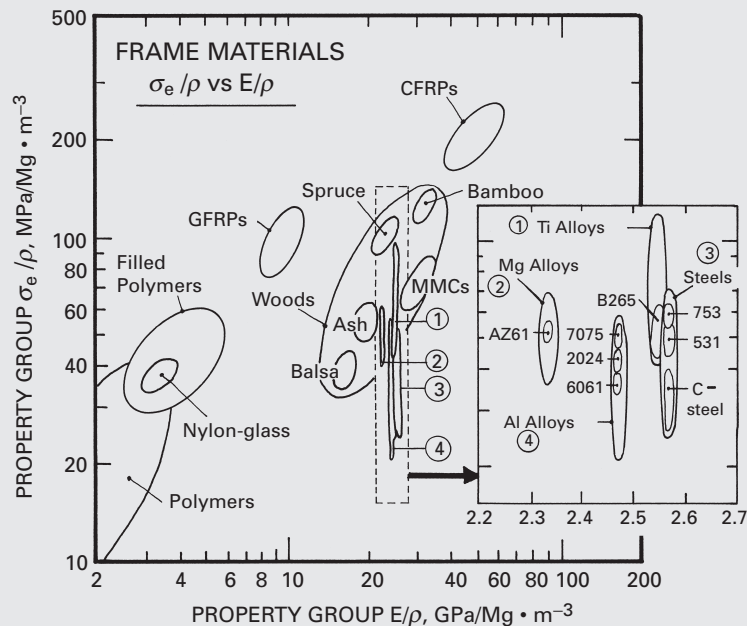


Fig. E1.2 Normalized strength (σ_e/ρ) versus normalized Young's modulus (E/ρ) for potential bicycle frames. (Adapted from M. F. Ashby, *Met. and Mat. Trans.*, **A26** (1995) 3057.)

Example 1.2

Suppose you are a design engineer for the ISAACS bicycle company. This company traditionally manufactures chromium-molybdenum (Cr-Mo) steel frames. The racing team is complaining that the bicycles are too "soft" and that stiffer bicycles would give them a competitive edge. Additionally, the team claims that competing teams have aluminum bikes which are considerably lighter. You are asked to

redesign the bikes, using a precipitation hardenable aluminum alloy (7075 H4).

- Calculate the ratio of the stiffness of the two bikes if the tube diameters are the same.
- What would you do to increase the stiffness of the two bikes?
- If the steel frame weighs 4 kg, what would the aluminum frame weigh? State your assumptions.

Given:

	σ_e (MPa)	ρ (kg/m ³)	E (GPa)	G (GPa)
7075 Al	500	2700	70	27
4340 Steel	1350	7800	210	83

Steel tube diameter, $2r = 25$ mm

Wall thickness, $t = 1.25$ mm

Solution: The mass per unit length, from strength considerations, is

$$\frac{m}{L} = 2\pi r t \rho = \frac{2M}{r} \left(\frac{\rho}{\sigma_e} \right).$$

The mass per unit length, from bending considerations, is

$$\frac{m}{L} = 2\pi r t \rho = \frac{2M\rho'}{r^2} \left(\frac{\rho}{E} \right).$$

where ρ' is the radius of curvature and M is the bending moment applied by cyclist.

The radius of curvature ρ' is a good measure of the stiffness; the larger ρ' , the higher is the stiffness, for a fixed M .

$$(a) \quad r_{Al} = r_{St} = 12.5 \text{ mm.}$$

For the two metals, we have:

	Steel	Aluminum
ρ/σ_e	5.77	5.4
ρ/E	37.14	38.57

The mass-to-length ratios are

$$\frac{\left(\frac{m}{L}\right)_{St}}{\left(\frac{m}{L}\right)_{Al}} = \frac{\frac{2M}{r} \left(\frac{\rho}{\sigma_e}\right)_{St}}{\frac{2M}{r} \left(\frac{\rho}{\sigma_e}\right)_{Al}} = 1.06.$$

For the same weight, we calculate the ratio of the radii of curvature from bending:

$$1.06 \frac{\rho'_{Al}}{\rho'_{St}} = \frac{\left(\frac{\rho}{E}\right)_{St}}{\left(\frac{\rho}{E}\right)_{Al}} = 0.96,$$

$$\frac{\rho'_{Al}}{\rho'_{St}} = \frac{0.96}{1.06} = 0.91.$$

Thus, the stiffness is approximately the same for each metal.

(b) We increase diameter of the tubes. This is possible because the wall thickness of aluminum bikes is approximately three times the wall thickness of steel bikes.³ For instance, we can increase the diameter to 50 mm!⁴

(c) Let us assume that, for aluminum, $2r_{Al} = 50$ mm. Then

$$\frac{\left(\frac{m}{L}\right)_{St}}{\left(\frac{m}{L}\right)_{Al}} = x = \frac{\frac{2M\rho'_{St}}{r_{St}^2} \left(\frac{\rho}{E}\right)_{St}}{\frac{2M\rho'_{Al}}{r_{Al}^2} \left(\frac{\rho}{E}\right)_{Al}},$$

$$x \frac{\rho'_{Al} r_{St}^2}{\rho'_{St} r_{Al}^2} = \left(\frac{\rho}{E}\right)_{St}.$$

Going back to the strength equation, we obtain

$$x = \frac{\left(\frac{m}{L}\right)_{St}}{\left(\frac{m}{L}\right)_{Al}} = \frac{\frac{2M}{r_{St}} \left(\frac{\rho}{\sigma_c}\right)_{St}}{\frac{2M}{r_{Al}} \left(\frac{\rho}{\sigma_c}\right)_{Al}} = 2 \frac{5.77}{5.4} = 2.14.$$

If the total weight of the steel frame is 4 kg, then

$$\frac{w_{Al}}{w_{St}} = \frac{\left(\frac{m}{L}\right)_{Al}}{\left(\frac{m}{L}\right)_{St}} \cdot w_{St} = \frac{4}{2.14} = 1.86.$$

The stiffness ratio will be

$$\frac{\rho'_{Al}}{\rho'_{St}} = \frac{1}{x} \frac{r_{Al}^2 \left(\frac{\rho}{E}\right)_{St}}{r_{St}^2 \left(\frac{\rho}{E}\right)_{Al}} = \frac{4}{2.14} \frac{37.14}{38.54} = 1.80,$$

or

$$\rho'_{Al} = 1.8\rho'_{St}.$$

The aluminum bike is almost twice as stiff!

1.3 Structure of Materials

The *crystallinity*, or periodicity, of a structure, does not exist in gases or liquids. Among solids, the metals, ceramics, and polymers may or may not exhibit it, depending on a series of processing and composition parameters. Metals are normally crystalline. However, a metal cooled at a superfast rate from its liquid state – called *splat cooled* – can have an amorphous structure. (This subject is treated in greater detail in Section 1.3.4.) Silicon dioxide (SiO_2) can exist as amorphous (fused silica) or as crystal (cristoballite or tridymite). Polymers consisting of molecular chains can exist in various degrees of crystallinity.

Readers not familiar with structures, lattices, crystal systems, and Miller indices should study these subjects before proceeding with

³ Since the wall thickness is larger, we can produce larger tube diameters without danger of collapse by buckling.

⁴ A 50-mm steel tube would have walls that would be exceedingly thin; indeed, it could be dented by pressing it with the fingers.

the text. Most books on materials science, physical metallurgy, or X-rays treat the subjects completely. A brief introduction is presented next.

1.3.1 Crystal Structures

To date, seven crystal structures describe all the crystals that have been found. By translating the unit cell along the three crystallographic orientations, it is possible to construct a three-dimensional array. The translation of each unit cell along the three principal directions by distances that are multiples of the corresponding unit cell size produces the crystalline lattice.

Up to this point, we have not talked about atoms or molecules; we are just dealing with the mathematical operations of filling space with different shapes of blocks. We now introduce atoms and molecules, or “repeatable structural units.” The unit cell is the smallest repetitive unit that will, by translation, produce the atomic or molecular arrangement. Bravais established that there are 14 space lattices. These lattices are based on the seven crystal structures. The points shown in Figure 1.7 correspond to atoms or groups of atoms. The 14 Bravais lattices can represent the unit cells for all crystals. Figure 1.8 shows the indices used for directions in the cubic system. The same symbols are employed for different structures. We simply use the vector passing through the origin and a point (m, n, o) :

$$\mathbf{V} = m\mathbf{i} + n\mathbf{j} + o\mathbf{k}.$$

When the direction does not pass through the origin, and we have the head of the vector at (m, n, o) and the tail at (p, q, r) , the vector \mathbf{V} is given by:

$$\mathbf{V} = (m - p)\mathbf{i} + (n - q)\mathbf{j} + (o - r)\mathbf{k}.$$

The notation used for a direction is

$$[m \ n \ o].$$

When we deal with a family of directions, we use the symbol $\langle m \ n \ o \rangle$.

The following family encompasses all equivalent directions:

$$\begin{aligned} \langle m \ n \ o \rangle \Rightarrow [m \ n \ o], [m \ o \ n], [o \ m \ n], [o \ n \ m], [n \ m \ o], [m \ \bar{n} \ o], \\ [m \ o \ \bar{n}], [o \ m \ \bar{n}], [o \ \bar{n} \ m], [\bar{n} \ m \ o], \dots \end{aligned}$$

A direction not passing through the origin can be represented by

$$[(m - p)(n - q)(o - r)].$$

Note that for the negative, we use a bar on top. For planes, we use the Miller indices, obtained from the intersection of a plane with the coordinate axes. Figure 1.9 shows a plane and its intercepts. We take the inverse of the intercepts and multiply them by their common

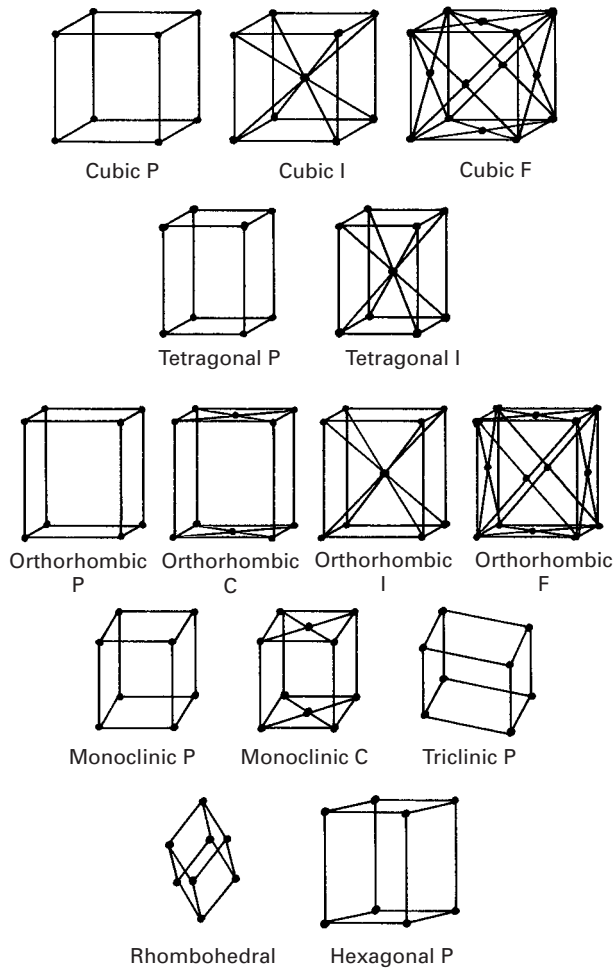


Fig. 1.7 The 14 Bravais space lattices (P = primitive or simple; I = body-centered cubic; F = face-centered cubic; C = base-centered cubic).

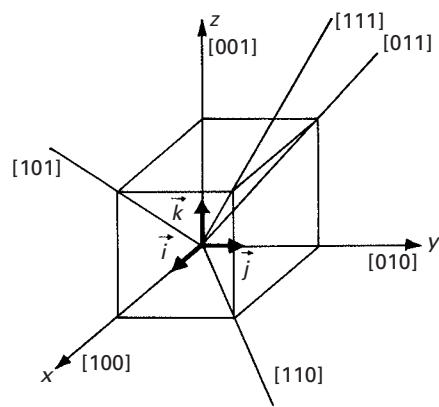


Fig. 1.8 Directions in a cubic unit cell.

Fig. 1.9 Indexing of planes by Miller rules in the cubic unit cell.

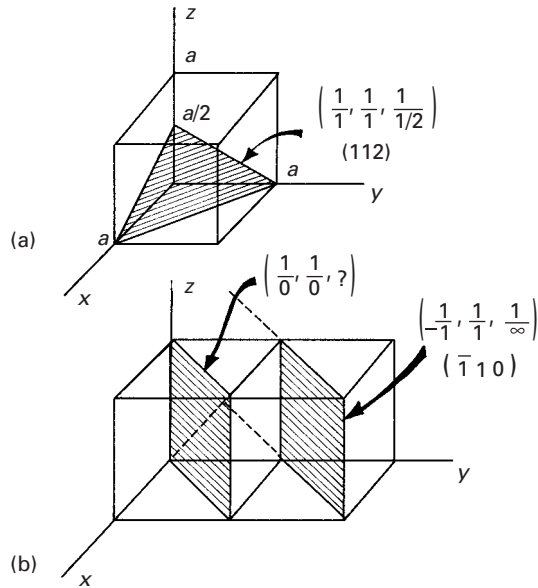
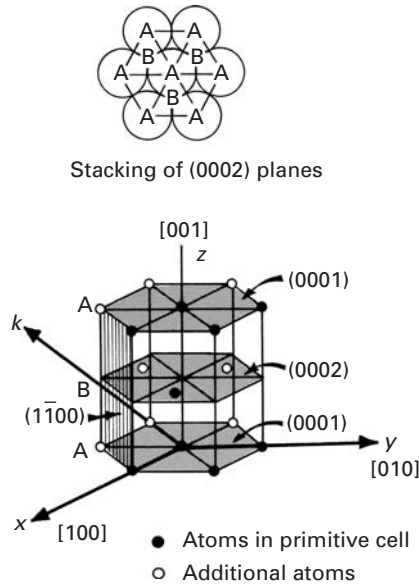


Fig. 1.10 Hexagonal structure consisting of a three-unit cell.



denominator so that we end up with integers. In Figure 1.9 (a), we have

$$\frac{1}{1}, \frac{1}{1}, \frac{1}{1/2} \Rightarrow (112).$$

Figure 1.9(b) shows an indeterminate situation. Thus, we have to translate the plane to the next cell, or else translate the origin. The indeterminate situation arises because the plane passes through the origin. After translation, we obtain intercepts $(-1, 1, \infty)$. By inverting them, we get $(\bar{1} 10)$. The symbol for a family of planes is $\{m n o\}$.

For hexagonal structures, we have a slightly more complicated situation. We represent the hexagonal structure by the arrangement shown in Figure 1.10. The atomic arrangement in the basal plane is shown in the top portion of the figure. Often, we use four axes (x, y, k, z) with unit vectors ($\vec{i}, \vec{j}, \vec{k}, \vec{l}$) to represent the structure. This is mathematically unnecessary, because three indices are sufficient to represent a direction in space from a known origin. Still, the redundancy is found by some people to have its advantages and is described here. We use the intercepts to designate the planes. The hatched plane (prism plane) has indices

$$\frac{1}{1}, \frac{1}{-1}, \frac{1}{\infty}, \frac{1}{\infty}.$$

After determining the indices of many planes, we learn that one always has

$$h + k = -i.$$

Thus, we do not have to determine the index for the third horizontal axis. If we use only three indices, we can use a dot to designate the fourth index, as follows:

$$(1\bar{1} \cdot 0).$$

For the directions, we can use either the three-index notation or a four-index notation. However, with four indices, the $h + k = -i$ rule will not apply in general, and one has to use special “tricks” to make the vector coordinates obey the rule.

If the indices in the three-index notation are h' , k' , and ℓ' , the four index notation of directions can be obtained by the following simple equations;

$$h = \frac{1}{3}(2h' - k')$$

$$k = \frac{1}{3}(2k' - h')$$

$$i = -\frac{1}{3}(h' + k')$$

$$\ell = \ell'$$

It can be easily verified that $h + k = -i$. Thus, the student is equipped to express the directions in the four-index notation.

1.3.2 Metals

The metallic bond can be visualized, in a very simplified way, as an array of positive ions held together by a “glue” consisting of electrons. These positive ions, which repel each other, are attracted to the “glue,” which is known as an electron gas. Ionic and covalent bonding, on the other hand, can be visualized as direct attractions between atoms. Hence, these types of bonding – especially covalent

Example I.3

Write the indices for the directions and planes marked in Figure E1.3.

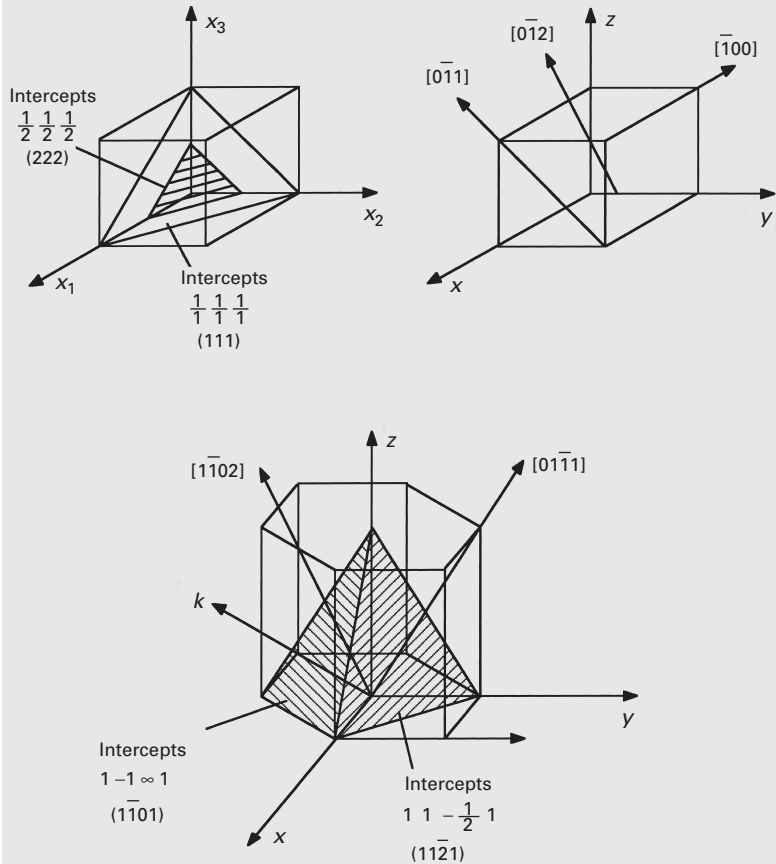


Fig. E1.3

bonding – are strongly directional and determine the number of neighbors that one atom will have, as well as their positions.

The bonding – and the sizes of the atoms in turn – determines the type of structure a metal has. Often, the structure is very complicated for ionic and covalent bonding. On the other hand, the directionality of bonding is not very important for metals, and atoms pack into the simplest and most compact forms; indeed, they can be visualized as spheres. The structures favored by metals are the face-centered cubic (FCC), body-centered cubic (BCC), and hexagonal close-packed (HCP) structures. In the periodic table, of the 81 elements to the left of the Zintl line, 53 have either the FCC or the HCP structure, and 21 have the BCC structure; the remaining 8 have other structures. The Zintl line defines the boundary of the elements with metallic character in the table. Some of them have several structures, depending on temperature. Perhaps the most

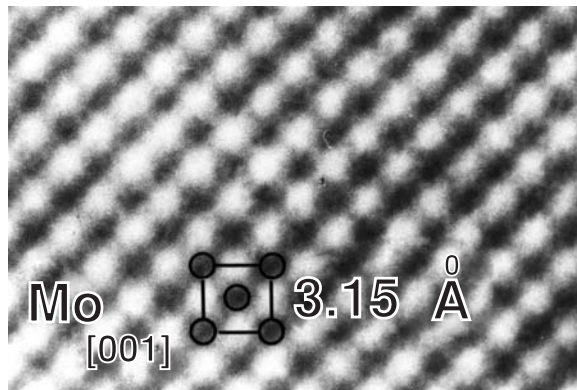


Fig. 1.11 Transmission electron micrograph of atomic resolution of (001) plane in molybdenum showing body-centered cubic arrangement of atoms. (Courtesy of R. Gronsky.)

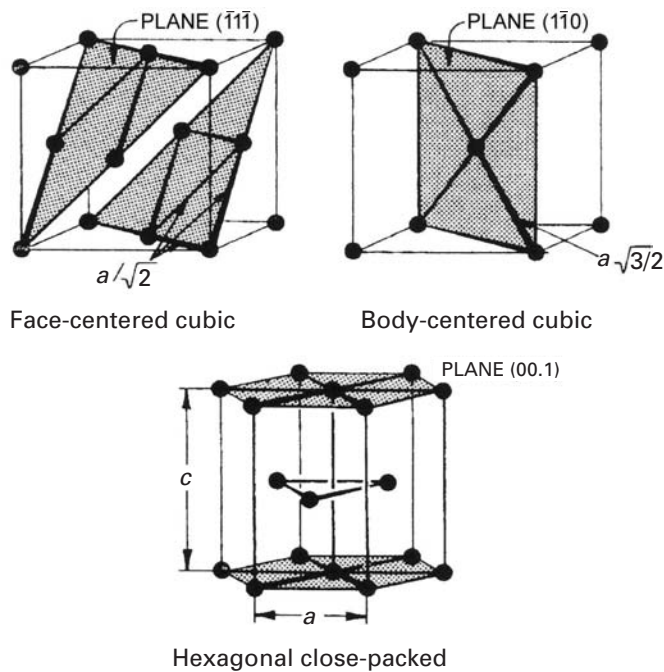


Fig. 1.12 Most closely packed planes in (a) FCC; (b) BCC; (c) HCP.

complex of the metals is plutonium, which undergoes six polymorphic transformations.

Transmission electron microscopy can reveal the positions of the individual atoms of a metal, as shown in Figure 1.11 for molybdenum. The regular atomic array along a [001] plane can be seen. Molybdenum has a BCC structure.

Figure 1.12 shows the three main metallic structures. The positions of the atoms are marked by small spheres and the atomic planes by dark sections. The small spheres do not correspond to the scaled-up size of the atoms, which would almost completely fill the available space, touching each other. For the FCC and HCP structures, the coordination number (the number of nearest neighbors of an atom) is 12. For the BCC structure, it is 8.

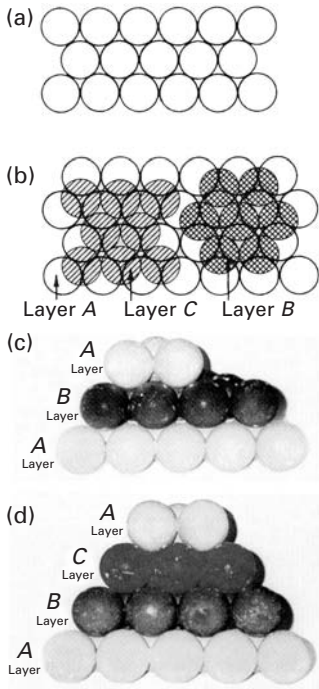


Fig. 1.13 (a) Layer of most closely packed atoms corresponding to (111) in FCC and (00.1) in HCP. (b) Packing sequence of most densely packed planes in AB and AC sequence. (c) Photograph of ball model showing the ABAB sequence of the HCP structure. (d) Photograph of ball model showing the ABCABC sequence of the FCC structure.

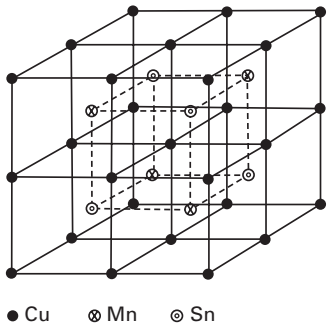


Fig. 1.14 β -ordered phase in Heusler alloys (Cu_2MnSn). (Reprinted with permission from M. A. Meyers, C. O. Ruud, and C. S. Barrett, *J. Appl. Cryst.*, 6 (1973) 39.)

The planes with the densest packing are indicated in the figure. They are $(1\bar{1}1)$, $(1\bar{1}0)$, and (00.1) for the FCC, BCC, and HCP structures, respectively. These planes have an important effect on the directionality of deformation of the metal, as will be seen in chapters 4 and 6. The distances between the nearest neighbors are also indicated in the figure. The reader should try to calculate them as an exercise. These distances are $a\sqrt{2}$, $(a\sqrt{3}/2)$, and a for the FCC, BCC, and HCP structures, respectively.

The similarity between the FCC and HCP structures is much greater than might be expected from looking at the unit cells. Planes (111) and (00.1) have the same packing, as may be seen in Figure 1.13. This packing, the densest possible of coplanar spheres, is shown in Figure 1.13(a). The packing of a second plane similar to, and on top of, the first one (called A) can be made in two different ways; Figure 1.13(b) indicates these two planes by the letters B and C. Hence, either alternative can be used. A third plane, when placed on top of plane B, would have two options: A or C. If the second plane is C, the third plane can be either A or B. If only the first and second layers are considered, the FCC and HCP structures are identical. If the position of the third layer coincides with that of the first (the ABA or ACA sequence), we have the HCP structure. Since this packing has to be systematically maintained in the lattice, one would have ABABAB . . . or ACACAC . . . In case the third plane does not coincide with the first, we have one of the two alternatives ABC or ACB. Since this sequence has to be systematically maintained, we have ABCAB-CABC . . . or ACBACBACB . . . This stacking sequence corresponds to the FCC structure. We thus conclude that the only difference between the FCC and HCP structures (the latter with a theoretical c/a ratio of 1.633) is the stacking sequence of the most densely packed planes. The difference resides in the next neighbors and in the greater symmetry of the FCC structure.

Figures 1.13(c) and (d) show photographs of ideal ball stackings. The ABA . . . sequence of layers, characteristic of HCP structure (Figure 1.13(c)) is compared with the ABCA . . . sequence for the FCC structure (Figure 1.13(d)).

In addition to the metallic elements, intermediate phases and intermetallic compounds exist in great numbers, with a variety of structures. For instance, the beta phase in the copper-manganese-tin (Cu-Mn-Sn) system exhibits a special ordering for the composition Cu_2MnSn . The unit cell (BCC) is shown in Figure 1.14. However, the ordering of the Cu, Mn, and Sn atoms creates a superlattice composed of four BCC cells. This superlattice is FCC; hence, the unit cell for the ordered phase is FCC, whereas that for the disordered phase has a BCC unit cell. This ordering has important effects on the mechanical properties and is discussed in Chapter 11.

Table 1.3 lists some of the most important intermetallic compounds and their structures. Intermetallic compounds have a bonding that is somewhat intermediate between metallic and ionic/covalent bonding, and have properties that are most desirable for high-temperature applications. Nickel and titanium aluminides are

Table 1.3 | Some Important Intermetallic Compounds and Their Structure

Compound	Melting Point (°C)	Type of Structure
Ni ₃ Al	1,390	L1 ₂ (ordered FCC)
Ti ₃ Al	1,600	DO ₁₉ (ordered hexagonal)
TiAl	1,460	L1 ₀ (ordered tetragonal)
Ni–Ti	1,310	CsCl
Cu ₃ Au	1,640	B ₂ (ordered BCC)
FeAl	1,250–1,400	B ₂ (ordered BCC)
NiAl	1,380–1,638	B ₂ (ordered BCC)
MoSi ₂	2,025	C1 I _b (tetragonal)
Al ₃ Ti	1,300	DO ₂₂ (tetragonal)
Nb ₃ Sn	2,134	A15
Nb ₅ Si ₃	2,500	(tetragonal)

candidates for high-temperature applications in jet turbines and aircraft applications.

Example 1.4

Determine the ideal c/a ratio for the hexagonal structure.

Solution: The atoms in the basal A plane form a closely packed array, as do the atoms in the B plane going through the mid plane. If we take three atoms in the basal plane, with an atom in the B plane resting among them, we have constructed a tetrahedron. The sides of the tetrahedron are $2r = a$, where r is the atomic radius. The height of this tetrahedron is $c/2$, since the distance between planes is c . Hence, the problem is now reduced to finding the height, $c/2$, of a regular tetrahedron. In Figure E1.4, we have

$$DF = \frac{c}{2},$$

$$AB = AC = BC = AD = DB = DC = a.$$

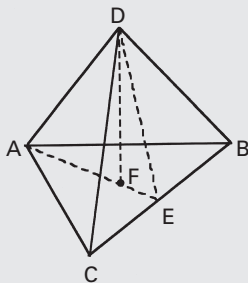


Fig. E1.4

For triangle AEC ,

$$AE^2 + EC^2 = AC^2,$$

$$AE = \sqrt{a^2 - \frac{a^2}{4}} = \frac{a}{2}\sqrt{3}.$$

For triangle DFE ,

$$EF^2 = DF^2 = DE^2.$$

But

$$EF = \frac{1}{3}AE = \frac{a}{6}\sqrt{3},$$

$$DE = AE = \frac{a}{2}\sqrt{3},$$

$$DF = \left(\frac{3a^2}{4} - \frac{3a^2}{36}\right)^{1/2},$$

$$\frac{c}{2} = a\left(\frac{2}{3}\right)^{1/2},$$

$$\frac{c}{a} = 2\left(\frac{2}{3}\right)^{1/2}.$$

Thus,

$\frac{c}{a} = 1.633.$

Example 1.5

If the copper atoms have a radius of 0.128 nm, determine the density in FCC and BCC structures.

(i) In FCC structures, $4r = \sqrt{2}a_0$

$$a_0 = \frac{4}{\sqrt{2}}r = \frac{4}{\sqrt{2}} \times 0.128 \text{ nm}$$

$$a_0 = 0.362 \text{ nm}$$

There are 4 atoms per unit cell in FCC. Atomic mass (or weight) of copper is 63.54 g/g.mol. So, density of copper (ρ) in FCC structures is

$$\rho = \frac{63.54 \times 4}{(0.362 \times 10^{-7})^3 \times (6.02 \times 10^{23})} = 8.89 \text{ g/cm}^3$$

\uparrow
 Avogadro's number

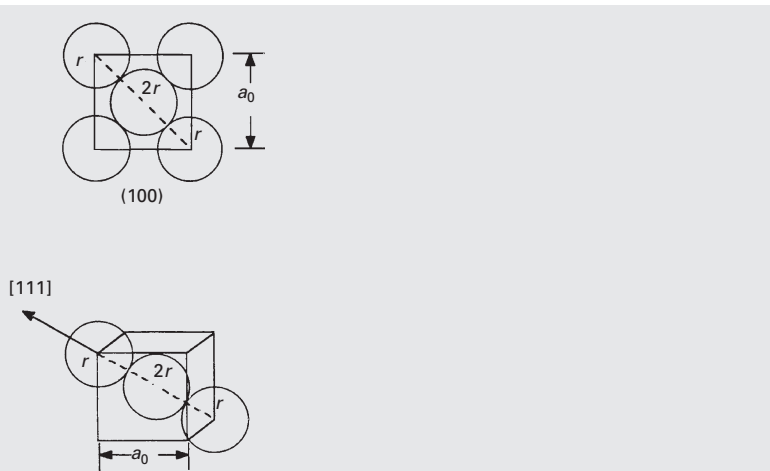
(ii) In BCC structures, $4r = \sqrt{3}a_0$

$$a_0 = \frac{4}{\sqrt{3}}r = \frac{4}{\sqrt{3}} \times 0.128 \text{ nm}$$

$$a_0 = 0.296 \text{ nm}$$

There are 2 atoms per unit cell in BCC structures.

$$\rho = \frac{63.54 \times 2}{(0.296 \times 10^{-7})^3 \times (6.02 \times 10^{23})} = 8.14 \text{ g/cm}^3$$

**Fig. E1.5**

The stable form of Cu is FCC. Only under unique conditions, such as Cu precipitates in iron, is the BCC form stable (because of the constraints of surrounding material).

1.3.3 Ceramics

The name ceramic comes from the Greek KERAMOS (pottery). The production of pottery made of clay dates from 6500 BC. The production of silicate glass in Egypt dates from 1500 BC. The main ingredient of pottery is a hydrous aluminum silicate that becomes plastic when mixed, in fine powder form, with water. Thus, the early utilization of ceramics included both crystalline and glassy materials. Portland cement is also a silicate ceramic; by far the largest tonnage production of ceramics today – glasses, clay products (brick, etc.), cement – are silicate-based.

However, there have been dramatic changes since the 1970s and a wide range of new ceramics has been developed. These new ceramics are finding applications in computer memories (due to their unique magnetic applications), in nuclear power stations (UO_2 fuel rods), in rocket nose cones and throats, in submarine sonar units (piezoelectric barium titanate), in jet engines (as coatings to metal turbine blades) as electronic packaging components (Al_2O_3 , SiC substrates), as electro-optical devices (lithium niobate, capable of transforming optical into electrical information and vice versa), as optically transparent materials (ruby and yttrium garnet in lasers, optical fibers), as cutting tools (boron nitride, synthetic diamond, tungsten carbide), as refractories, as military armor (Al_2O_3 , SiC, B_4C), and in a variety of structural applications.

The structure of ceramics is dependent on the character of the bond (ionic, covalent, or partly metallic), on the sizes of the atoms, and on the processing method. We will first discuss the crystalline

Example 1.6

Sketch the 12 members of the $\langle 110 \rangle$ family for a cubic crystal. Indicate the four $\{111\}$ planes. You may use several sketches.

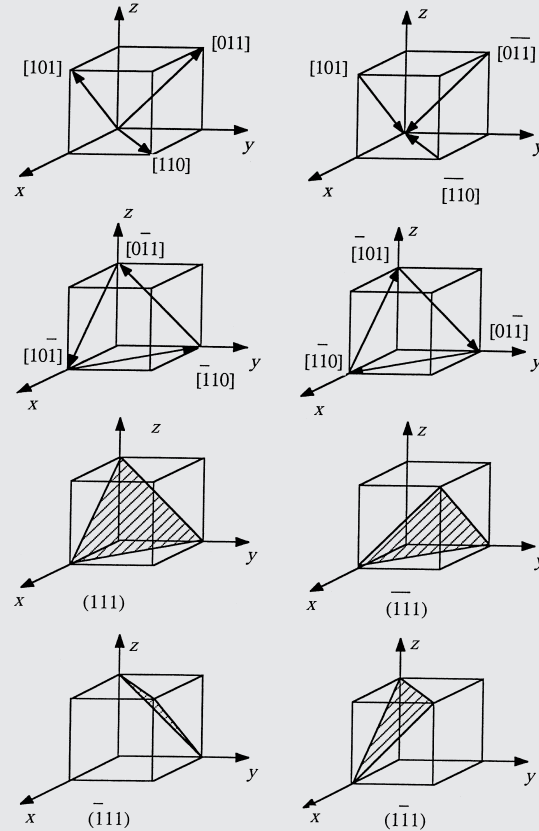


Fig. E1.6

ceramics. Transmission electron microscopy has reached the point of development where we can actually image individual atoms, and Figure 1.15 shows a beautiful picture of the zirconium atoms in ZrO_2 . The much lighter oxygen atoms cannot be seen but their positions are marked in the electron micrograph. By measuring the atomic distances along two orthogonal directions, one can see that the structure is not cubic, but tetragonal. The greater complexity of ceramics, in comparison to metallic structures, is evident from Figure 1.15. Atoms of different sizes have to be accommodated by a structure, and bonding (especially covalent) is highly directional. We will first establish the difference between ionic and covalent bonding.

The electronegativity value is a measure of an atom's ability to attract electrons. Compounds in which the atoms have a large difference in electronegativity are principally ionic, while compounds with the same electronegativity are covalent. In ionic bonding one

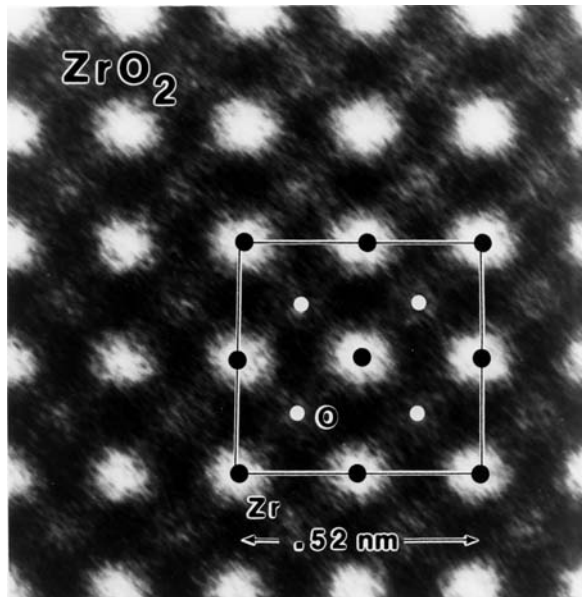


Fig. 1.15 Transmission electron micrograph of ZrO_2 at high resolution, showing individual Zr atoms and oxygen sites. (Courtesy of R. Gronsky.)

atom loses electrons and is therefore positively charged (cation). The atom that receives the electrons becomes negatively charged (anion). The bonding is provided by the attraction between positive and negative charges, compensated by the repulsion between charges of equal signs. In covalent bonding the electrons are shared between the neighboring atoms. The quintessential example of covalent bonding is diamond. It has four electrons in the outer shell, which combine with four neighboring carbon atoms, forming a tridimensional regular diamond structure, which is a complex cubic structure. Figure 1.16 shows the diamond structure. The bond angles are fixed and equal to $70^\circ 32'$. The covalent bond is the strongest bond, and diamond has the highest hardness of all materials. Another material that has covalent bonding is SiC.

As the difference of electronegativity is increased, the bonding character changes from pure covalent to covalent-ionic, to purely ionic. Ionic crystals have a structure determined largely by opposite charge surrounding an ion. These structures are therefore established by the maximum packing density of ions. Compounds of metals with oxygen (MgO , Al_2O_3 , ZrO_2 , etc.) and with group VII elements (NaCl , LiF , etc.) are largely ionic. The most common structures of ionic crystals are presented in Figure 1.17. Evidently, one has more complex structures in ceramics than in metals because the combinations possible between the elements are so vast.

Ceramics also exist in the glassy state. Silica in this state has the unique optical property of being transparent to light, which is used technologically to great advantage. The building blocks of silica in crystalline and amorphous forms are the silica tetrahedra. Silicon bonds to four oxygen atoms, forming a tetrahedron. The oxygen atoms bond to just two silicon atoms. Numerous structures are possible, with

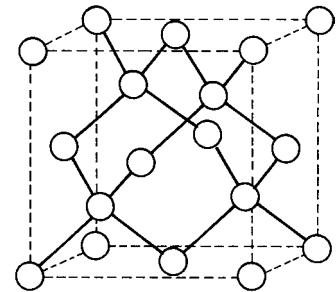
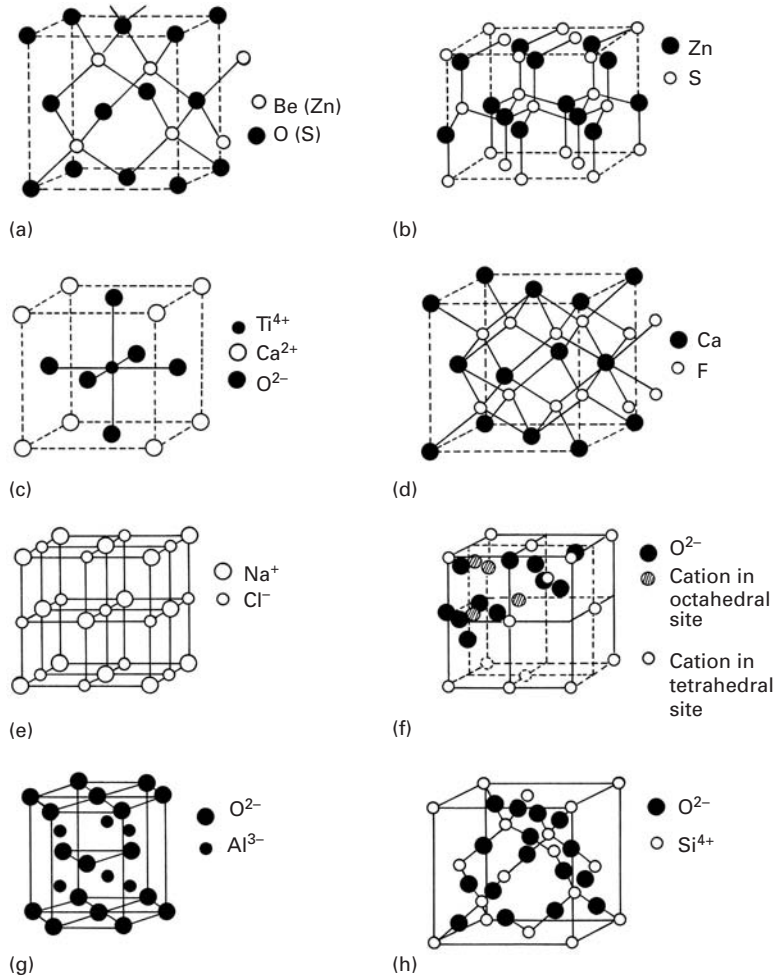


Fig. 1.16 Crystal structure of diamond.

Fig. 1.17 Most common structures for ceramics. (a) Zinc blende (ZnS, BeO, SiC). (b) Wurtzite (ZnS, ZnO, SiC, BN). (c) Perovskite (CoTiO₃, BaTiO₃, YCu₂Ba₃O_{7-x}). (d) Fluorite (ThO₂, UO₂, CeO₂, ZrO₂, PuO₂). (e) NaCl (KCl, LiF, KBr, MgO, CaO, VO, MnO, NiO). (f) Spinel (FeAl₂O₄, ZnAl₂O₄, MoAl₂O₄). (g) Corundum (Al₂O₃, Fe₂O₃, Cr₂O₃, Ti₂O₃, V₂O₃). (h) Crystobalite (SiO₂ – quartz). The CsCl structure, which has one Cs⁺ surrounded by four Cl⁻ ions in cube edges, is not shown.



different arrangements of the tetrahedra. Pure silica crystallizes into quartz, cristobalite, and tridymite. Because of these bonding requirements, the structure of silica is fairly open and, consequently, gives the mineral a low density. Quartz has a density of 2.65 g/cm^{-3} , compared with 3.59 g/cm^{-3} and 3.92 g/cm^{-3} , for MgO and Al₂O₃, respectively. The structure of cristobalite (Figure 1.17 (h)) shows clearly that each Si atom (open circle) is surrounded by four oxygen atoms (filled circles), while each oxygen atom binds two Si atoms. A complex cubic structure results. However, an amorphous structure in silica is more common when the mineral is cooled from the liquid state. Condensation of vapor on a cold substrate is another method by means of which thin, glassy films are made. One can also obtain glassy materials by electro-deposition, as well as by chemical reaction. Chapter 3 describes glassy metals in greater detail. Figure 1.18 provides a schematic representation of silica in its crystalline and glassy forms in an idealized two-dimensional pattern. The glassy state lacks long-range ordering; the three-dimensional silica tetrahedra arrays lack both symmetry and periodicity.

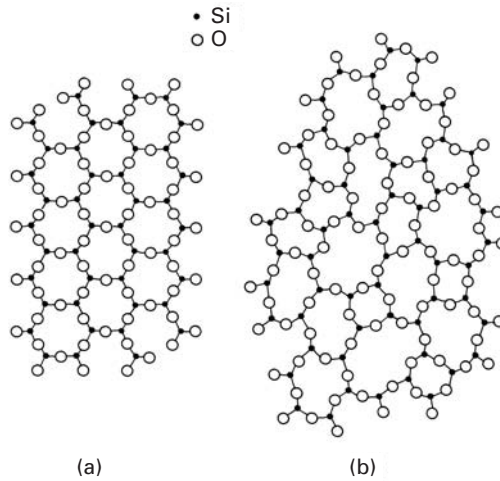


Fig. 1.18 Schematic representation of (a) ordered crystalline and (b) random-network glassy form of silica.

Example 1.7

Determine the C-C-C-bonding angle in polyethylene.

The easiest manner to visualize the bonding angle is to assume that one C atom is in the center of a cube and that it is connected to four other C atoms at the edges of the cube. (See Figure E1.7.) Suppose all angles are equal to α .

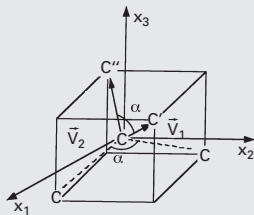


Fig. E1.7

The problem is best solved vectorially. We set the origin of the axes at the center of the carbon atom and have

$$\vec{V}_1 = \frac{1}{2}\vec{i} + \frac{1}{2}\vec{j} + \frac{1}{2}\vec{k},$$

$$\vec{V}_2 = \frac{1}{2}\vec{i} + \frac{1}{2}\vec{j} - \frac{1}{2}\vec{k}.$$

The angle between two vectors is (see Chapter 6 or any calculus text)

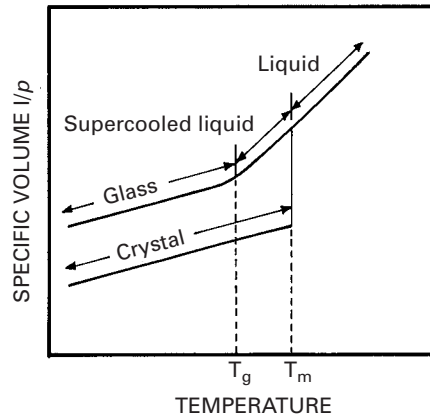
$$\cos \alpha = \frac{\frac{1}{2}\left(-\frac{1}{2}\right) + \frac{1}{2}\left(-\frac{1}{2}\right) + \frac{1}{2} \cdot \frac{1}{2}}{\sqrt{\frac{1}{4} + \frac{1}{4} + \frac{1}{4}} \cdot \sqrt{\frac{1}{4} + \frac{1}{4} + \frac{1}{4}}} = -\frac{1}{3}.$$

so

$$\alpha = 109.47^\circ.$$

(Note: When we have double bonds, the angle is changed.)

Fig. 1.19 Specific volume (inverse of density) as a function of temperature for glassy and crystalline form of a material.



1.3.4 Glasses

As described earlier, glasses are characterized by a structure in which no long-range ordering exists. There can be short-range ordering, as indicated in the individual tetrahedral arrays of SiO_4^{-4} in Figure 1.18, which shows both the crystalline and glassy forms of silica. Over distances of several atomic spacings, the ordering disappears, leading to the glassy state. It is possible to have glassy ceramics, glassy metals, and glassy polymers.

The structure of glass has been successfully described by the *Zachariasen* model. The *Bernal* model is also a successful one. It consists of drawing lines connecting the centers of adjacent atoms and forming polyhedra. These polyhedra represent the glassy structure of glass. Glassy structures represent a less efficient packing of atoms or molecules than the equivalent crystalline structures. This is very easily understood with the “suitcase” analog. We all know that by throwing clothes randomly into a suitcase, the end result is often a major job of sitting on the suitcase to close it. Neat packing of the same clothes occupies less volume. The same happens in glasses. If we plot the inverse of the density (called *specific volume*) versus temperature, we obtain the plot shown in Figure 1.19. Contraction occurs as the temperature is lowered. If the material crystallizes, there is a discontinuity in the specific volume at the melting temperature T_m . If insufficient time is allowed for crystallization, the material becomes a supercooled liquid, and contraction follows the liquid line. At a temperature T_g , called the *glass transition temperature*, the supercooled liquid is essentially solid, with very high viscosity. It is then called a glass. This difference in specific volume between the two forms is often referred to as *excess volume*.

In ceramics, reasonably low cooling rates can produce glassy structures. The regular arrangement of the silica tetrahedra of Figure 1.18(a) requires a significant amount of time. The same is true for polymeric chains, which need to arrange themselves into regular

crystalline arrangements. For metals, this is more difficult. Only under extreme conditions it is possible to obtain solid metals in a noncrystalline structure. Figure 1.20 shows a crystalline and a glassy alloy with the same composition. The liquid state is frozen in, and the structure resembles that of glasses. It is possible to arrive at these special structures by cooling the alloy at such a rate that virtually no reorganization of the atoms into periodic arrays can take place. The required cooling rate is usually on the order of 10^6 to 10^8 K/s⁻¹. It is also possible to arrive at the glassy state by means of solid-state processing (very heavy deformation and reaction) and from the vapor.

The original technique for obtaining metallic glasses was called splat cooling and was pioneered by Duwez and students.⁵ An alloy in which the atomic sizes are quite dissimilar, such as Fe-B, is ideal for retaining the “glassy” state upon cooling. This technique consisted of propelling a drop of liquid metal with a high velocity against a heat-conducting surface such as copper. The interest in these alloys was mainly academic at the time. However, the unusual magnetic properties and high strength exhibited by the alloys triggered worldwide interest, and subsequent research has resulted in thousands of papers. The splat-cooling technique has been refined to the point where 0.07- to 0.12-mm-thick wires can be ejected from an orifice. Production rates as high as 1,800 m/min can be obtained. Sheets and ribbons can be manufactured by the same technique. An alternative technique consists of vapor deposition on a substrate (sputtering). This seems a most promising approach, and samples with a thickness of several millimeters have been successfully produced.

1.3.5 Polymers

From a microstructural point of view, polymers are much more complex than metals and ceramics. On the other hand, they are cheap and easily processed. Polymers have lower strengths and moduli and lower temperature-use limits than do metals or ceramics. Because of their predominantly covalent bonding, polymers are generally poor conductors of heat and electricity. Polymers are generally more resistant to chemicals than are metals, but prolonged exposure to ultraviolet light and some solvents can cause degradation of a polymer's properties.

Chemical Structure

Polymers are giant chainlike molecules (hence, the name *macromolecules*), with covalently bonded carbon atoms forming the backbone of the chain. Polymerization is the process of joining together many monomers, the basic building blocks of polymers, to form the

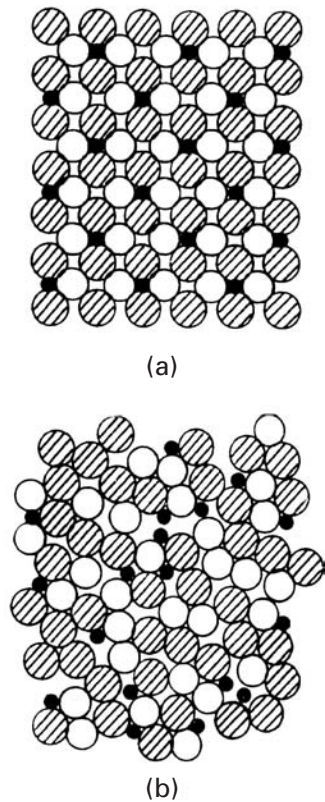
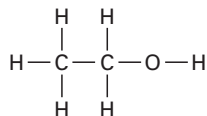


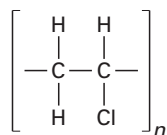
Fig. 1.20 Atomic arrangements in crystalline and glassy metals. (a) Crystalline metal section. (b) Glassy metal section. (Courtesy of L. E. Murr.)

⁵ W. Klement, R. H. Willens, and P. Duwez, *Nature*, 187 (1960) 869.

chains. For example, the ethyl alcohol monomer has the chemical formula



The monomer vinyl chloride has the chemical formula $\text{C}_2\text{H}_3\text{Cl}$, which, on polymerization, becomes polyvinyl chloride (PVC). The structural formula of polyvinyl chloride is represented by



where n is the degree of polymerization.

Types of Polymers

The difference in the behavior of polymers stems from their molecular structure and shape, molecular size and weight, and amount and type of bond (covalent or van der Waals). The different chain configurations are shown in Figure 1.21. A *linear polymer* consists of a long chain of atoms with attached side groups (Figure 1.21(a)). Examples include polyethylene, polyvinyl chloride, and polymethyl methacrylate. Note the coiling and bending of the chain. *Branched polymers* have branches attached to the main chain (Figure 1.21(b)). Branching can occur with linear, cross-linked, or any other types of polymers. A *crossed-linked polymer* has molecules of one chain bonded with those of another (Figure 1.21(c)). Cross-linking of molecular chains results in a three-dimensional network. It is easy to see that cross-linking makes sliding of molecules past one another difficult, resulting in strong and rigid polymers. *Ladder polymers* have two linear polymers linked in a regular manner (Figure 1.21(d)). Not unexpectedly, ladder polymers are more rigid than linear polymers.

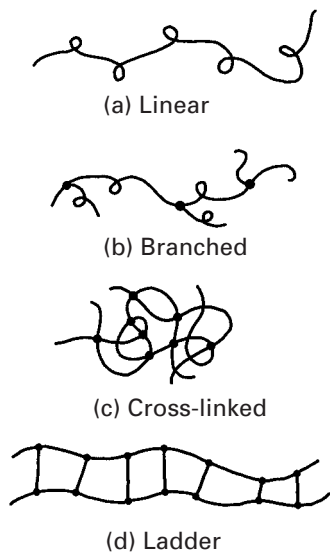


Fig. 1.21 Different types of molecular chain configurations.

Yet another classification of polymers is based on the type of the repeating unit (see Figure 1.22.) When we have one type of repeating unit – for example, A – forming the polymer chain, we call it a *homopolymer*. *Copolymers*, on the other hand, are polymer chains having two different monomers. If the two different monomers, A and B , are distributed randomly along the chain, then we have a *regular*, or *random*, *copolymer*. If, however, a long sequence of one monomer A is followed by a long sequence of another monomer B , we have a *block copolymer*. If we have a chain of one type of monomer A and branches of another type B , then we have a *graft copolymer*.

Tacticity has to do with the order of placement of side groups on a main chain. It can provide variety in polymers. Consider a polymeric

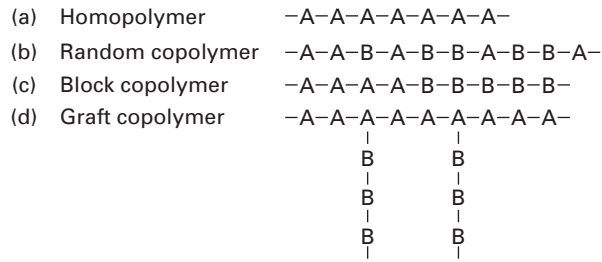


Fig. 1.22 (a) Homopolymer: one type of repeating unit. (b) Random copolymer: two monomers, A and B, distributed randomly. (c) Block copolymer: a sequence of monomer A, followed by a sequence of monomer B. (d) Graft copolymer: Monomer A forms the main chain, while monomer B forms the branched chains.

backbone chain having side groups. For example, a methyl group (CH_3) can be attached to every second carbon atom in the polypropylene chain. By means of certain catalysts, it is possible to place the methyl groups all on one side of the chain or alternately on the two sides, or to randomly distribute them in the chain. Figure 1.23 shows tacticity in polypropylene. When we have all the side groups on one side of the main chain, we have an *isotactic* polymer. If the side groups alternate from one side to another, we have a *syndiotactic* polymer. When the side groups are attached to the main chain in a random fashion, we get an *atactic* polymer.

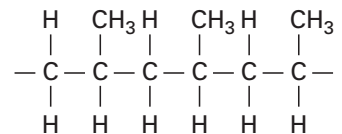
Thermosetting Polymers and Thermoplastics

Based on their behavior upon heating, polymers can be divided into two broad categories:

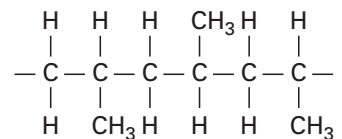
- (i) thermosetting polymers,
- (ii) thermoplastics.

When the molecules in a polymer are cross-linked in the form of a network, they do not soften on heating. We call these cross-linked polymers *thermosetting* polymers. Thermosetting polymers decompose upon heating. Cross-linking makes sliding of molecules past one another difficult, which produces a strong and rigid polymer. A typical example is rubber cross-linked with sulfur, i.e., vulcanized rubber. Vulcanized rubber has 10 times the strength of natural rubber. Common examples of thermosetting polymers include phenolic, polyester, polyurethane, and silicone. Polymers that soften or melt upon heating are called *thermoplastics*. Suitable for liquid flow processing, they are mostly linear polymers – for example, low- and high-density polyethylene and polymethyl methacrylate (PMMA).

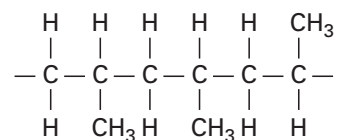
Polymers can have an amorphous or partially crystalline structure. When the structure is amorphous, the molecular chains are arranged randomly, i.e., without any apparent order. Thermosetting polymers, such as epoxy, phenolic, and unsaturated polyester, have an amorphous structure. Semicrystalline polymers can be obtained by using special processing conditions. For example, by precipitating a polymer from an appropriate dilute solution, we can obtain small, platelike crystalline lamellae, or crystallites. Such solution-grown polymer crystals are characteristically small. Figure 1.24 shows a transmission electron micrograph of a lamellar crystal of poly



Isotactic polypropylene



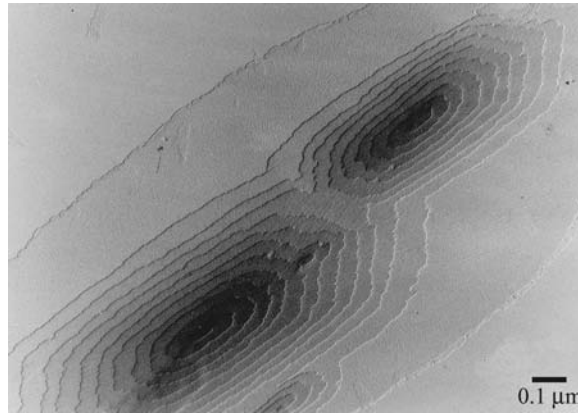
Syndiotactic polypropylene



Atactic polypropylene

Fig. 1.23 Tacticity, or the order of placement of side groups.

Fig. 1.24 Electron micrograph of a lamellar crystal showing growth spirals around screw dislocations. (Courtesy of H. D. Keith.)



(ϵ -caprolactone). Note the formation of new layers of growth spirals around screw dislocations. The screw dislocations responsible for crystal growth are perpendicular to the plane of the micrograph. Polymeric crystals involve molecular chain packing, rather than the atomic packing characteristic of metals. Molecular chain packing requires a sufficiently stereographic regular chemical structure. Solution-grown polymeric crystals generally have a lamellar form, and the long molecular chains crystallize by folding back and forth in a regular manner. Lamellar polymeric crystals have straight segments of molecules oriented normal to the lamellar panes. Figure 1.25 depicts some important chain configurations in a schematic manner. The flexible, coiled structure is shown in Figure 1.25(a), while the chain-folding configuration that results in crystalline polymers is shown in Figure 1.25(b). Under certain circumstances, one can obtain an extended and aligned chain structure, shown in Figure 1.25(c). Such a structure, typically obtained in fibrous form, has very high strength and stiffness. A semicrystalline configuration called a fringed micelle structure is shown in Figure 1.25(d). Almost all so-called semicrystalline polymers are, in reality, mixtures of crystalline and amorphous regions. Only by using very special techniques, such as solid-state polymerization, is it possible to prepare a 100% crystalline polymer. Polydiacetylene single crystals in the form of lozenges and fibers have been prepared by solid-state polymerization.

Partially crystallized, or semicrystalline, polymers can also be obtained from melts. Generally, because of molecular chain entanglement, the melt-formed crystals are more irregular than those obtained from dilute solutions. A characteristic feature of melt-formed polymers is the formation of *spherulites*. When seen under cross-polarized light in an optical microscope, the classical spherulitic structure shows a Maltese cross pattern. (See Figure 1.26(a).) Figure 1.26(b) presents a schematic representation of a spherulite whose diameter can vary between a few tens to a few hundreds of micrometers. Spherulites can nucleate at a variety of points, as, for

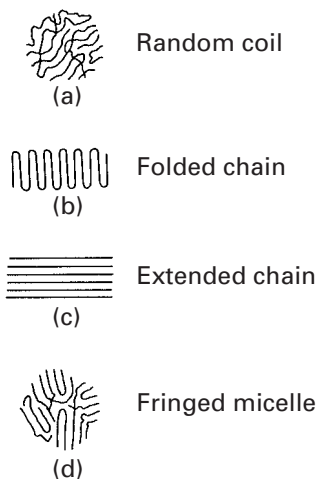


Fig. 1.25 Some important chain configurations. (a) A flexible, coiled chain structure. (b) A folding chain structure. (c) An extended and aligned chain structure. (d) A fringed micelle chain structure.

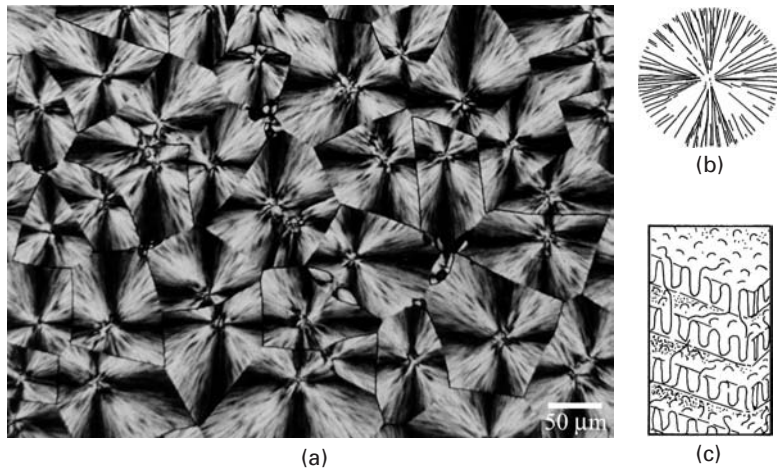


Fig. 1.26 Spherulitic structures. (a) A typical spherulitic structure in a melt-formed polymer film. (Courtesy of H. D. Keith.) (b) Schematic of a spherulite. Each spherulite consists of an assembly of radially arranged narrow crystalline lamellae. (c) Each lamella has tightly packed polymer chains folding back and forth. Amorphous regions fill the spaces between the crystalline lamellae.

example, with dust or catalyst particles, in a quiescent melt and then grow as spheres. Their growth stops when the neighboring spherulites impinge upon each other. Superficially, the spherulites look like grains in a metal. There are, however, differences between the two. Each grain in a metal is a single crystal, whereas each spherulite in a polymer is an assembly of radially arranged, narrow crystalline lamellae. The fine-scale structure of these lamellae, consisting of tightly packed chains folding back and forth, is shown in Figure 1.26(c). Amorphous regions containing tangled masses of molecules fill the spaces between the crystalline lamellae.

Degree of Crystallinity

The *degree of crystallinity* of a material can be defined as the fraction of the material that is fully crystalline. This is an important parameter for semicrystalline polymers. Depending on their degree of crystallinity, such polymers can show a range of densities, melting points, etc. It is worth repeating that a 100% crystalline polymer is very difficult to obtain in practice. The reason for the difficulty is the long chain structure of polymers: some twisted and entangled segments of chains that get trapped between crystalline regions never undergo the conformational reorganization necessary to achieve a fully crystalline state. Molecular architecture also has an important bearing on a polymer's crystallization behavior. Linear molecules with small or no side groups crystallize easily. Branched chain molecules with bulky side groups do not crystallize as easily. For example, linear, high-density polyethylene can be crystallized to 90%, while branched polyethylene can be crystallized only to about 65%. Generally, the stiffness and strength of a polymer increase with the degree of crystallinity.

Like crystalline metals, crystalline polymers have imperfections. It is, however, not easy to analyze these defects, because the topological connectivity of polymer chains leads to large amounts and

numerous types of disorder. Polymers are also very sensitive to damage by the electron beam in TEM, making it difficult to image them. Generally, polymer crystals are highly anisotropic. Because of covalent bonding along the backbone chain, polymeric crystals show low-symmetry structures, such as orthorhombic, monoclinic, or triclinic. Deformation processes such as slipping and twinning, as well as phase transformations that take place in monomeric crystalline solids, may also occur in polymeric crystals.

Molecular Weight and Distribution

Molecular weight is a very important attribute of polymers, especially because it is not so important in the treatment of nonpolymeric materials. Many mechanical properties increase with molecular weight. In particular, resistance to deformation does so. Of course, concomitant with increasing molecular weight, the processing of polymers becomes more difficult.

The molecular weight of a polymer is given by the product of the molecular weight of the repeat unit (the “mer”) and the number of repeat units. The molecular weight of the ethylene repeat unit ($-\text{CH}_2-\text{CH}_2-$) is 28. We write the chemical formula: $\text{H}(-\text{CH}_2-\text{CH}_2-)_n\text{H}$. If n , the number of repeat units, is 10,000, the high-density polyethylene will have a molecular weight of 280,002. In almost all polymers, the chain lengths are not equal, but rather, there is a distribution of chain lengths. In addition, there may be more than one species of chain in the polymer. This makes for different parameters describing the molecular weight.

The number-averaged molecular weight (M_n) of a polymer is the total weight of all of the polymer’s chains divided by the total number of chains:

$$M_n = \sum N_i M_i / \sum N_i,$$

where N_i is the number of chains of molecular weight M_i .

The weight-averaged molecular weight (M_w) is the sum of the square of the total molecular weight divided by the total molecular weight. Thus,

$$M_w = \sum N_i M_i^2 / \sum M_i N_i.$$

Two other molecular weight parameters are

$$M_z = \sum N_i M_i^3 / \sum N_i M_i^2,$$

and

$$M_v = \left[\sum N_i M_i^{(1+a)} / \sum N_i M_i \right]^{1/a},$$

where a has a value between 0.5 and 0.8.

Typically, $M_n : M_w : M_z = 1 : 2 : 3$. Figure 1.27 shows a schematic molecular weight distribution curve with various molecular weight parameters indicated. Molecular weight distributions of the same polymer

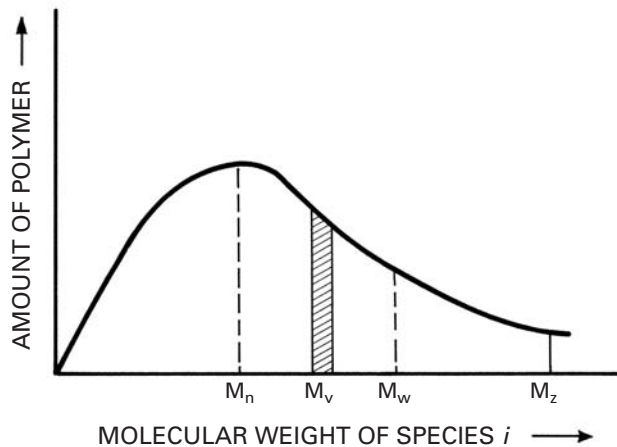


Fig. I.27 A schematic molecular weight distribution curve. Various molecular weight parameters are indicated.

obtained from two different sources can be very different. Also, molecular weight distributions are not necessarily single peaked. For single-peaked distributions, M_n is generally near the peak – that is, the most probable molecular weight. The weight-averaged molecular weight, M_w , is always larger than M_n . The molecular weight characterization of a polymer is very important. The existence of a very high-molecular-weight tail can make processing very difficult because of the enormous contribution of the tail to the melt viscosity of a polymer. The low end of the molecular weight distribution, however, can be used as a plasticizer.

It is instructive to compare some monomers with low- and high-molecular-weight polymers. A very common monomer is a molecule of water, H_2O , with a molecular weight of 18. Benzene, on the other hand, is a low-molecular-weight organic solvent; its molecular weight is 78. By contrast, natural rubber has a molecular weight of about 10^4 , and polyethylene, a common synthetic polymer, can have a molecular weights greater than this. Polymers having such large molecular weights are sometimes called *high polymers*. Their molecular size is also very great.

Example I.8

A polymer has three species of molecular weights: 3×10^6 , 4×10^6 , and 5×10^6 . Compute its number-averaged molecular weight M_n and weight-averaged molecular weight M_w .

Solution: For the number-averaged molecular weight, we have

$$\begin{aligned} M_n &= \frac{\sum N_i M_i}{\sum N_i} \\ &= \frac{3 \times 10^6 + 4 \times 10^6 + 5 \times 10^6}{3} = 4 \times 10^6. \end{aligned}$$

The weight-averaged molecular weight is

$$\begin{aligned} M_w &= \frac{\sum N_i M_i^2}{\sum N_i M_i} \\ &= \frac{(3 \times 10^6)^2 + (4 \times 10^6)^2 + (5 \times 10^6)^2}{3 \times 10^6 + 4 \times 10^6 + 5 \times 10^6} \\ &= \frac{50 \times 10^{12}}{12 \times 10^6} = 4.17 \times 10^6. \end{aligned}$$

Example 1.9

Estimate the molecular weight of polyvinyl chloride with degree of polymerization, n , equal to 800.

Solution: The molecular weight of each *mer* of polyvinyl chloride (C_2H_3Cl) is

$$2(12) + 3(1) + 35.5 = 62.5.$$

For $n = 800$, the molecular weight is $800 \times 62.5 = 50,000$ g/mol.

Example 1.10

Discuss how a polymer's density changes as crystallization proceeds from the melt.

Answer: The density increases and the volume decreases as crystallization proceeds. This is because the molecular chains are more tightly packed in the crystal than in the molten or noncrystalline polymer. This phenomenon is, in fact, exploited in the so-called *density* method to determine the degree of crystallinity.

Quasi Crystals

Quasi crystals represent a new state of solid matter. In a crystal, the unit cells are identical, and a single unit cell is repeated in a periodic manner to form the crystalline structure. Thus, the atomic arrangement in crystals has positional and orientational order. Orientational order is characterized by a rotational symmetry; that is, certain rotations leave the orientations of the unit cell unchanged. The theory of crystallography holds that crystals can have twofold, threefold, fourfold, or sixfold axes of rotational symmetry; a fivefold rotational symmetry is not allowed. A two-dimensional analogy of this is that one can tile a bathroom wall using a single shape of tile *if and only if* the tiles are rectangles (or squares), triangles, or hexagons, but not if the tiles are pentagons. One may obtain a glassy structure by rapidly cooling a vapor or liquid well below its melting point, until the disordered atomic arrangement characteristic of the vapor or liquid state gets frozen in. The atomic packing in the glassy state is

dense but random. This can be likened to a mosaic formed by taking an infinite number of different shapes of tile and randomly joining them together. Clearly, the concept of a unit cell will not be valid in such a case. The atomic structure in the glassy state will have neither positional nor orientational order.

Quasi crystals are not perfectly periodic, but they do follow the rigorous theorems of crystallography. They can have any rotational symmetry axes which are prohibited in crystals. It is worth reminding the reader that a glassy structure shows an electron diffraction pattern consisting of diffuse rings for all orientations. A crystalline structure has an electron diffraction pattern that depends on the crystal symmetry.

Schectman et al. discovered that a rapidly solidified (melt-spun) aluminum-manganese alloy showed fivefold symmetry axis.⁶ They observed a metastable phase that showed a sharp electron diffraction pattern with a perfect icosahedral symmetry. (Remember that sharp electron diffraction patterns are associated with the orderly atomic arrangement in crystals and icosahedral symmetry is forbidden in crystals.) At first, this was thought to be a paradox. However, some very careful and sophisticated electron microscopy work showed conclusively that it was indeed an icosahedral (twentyfold) symmetry. Al-Mn alloys containing 18 to 25.3 weight percent Mn examined by transmission electron microscopy showed the same anomalous diffraction. In particular, Al-25.3 wt% Mn alloy consisted almost entirely of one phase which has a composition close to Al_6Mn . The selected area diffraction pattern of Al_6Mn showed a fivefold symmetry. This new kind of structure is neither amorphous nor crystalline; rather, the new phase in this alloy had a three-dimensional icosahedral symmetry.

Perhaps, it would be in order for us to digress a bit and explain this icosahedral symmetry. *Icosahedral* means twenty faces. An icosahedron has twenty triangular faces, thirty edges, and twelve vertices. Consider the two-dimensional case. As pointed out earlier, one can tile a bathroom wall without leaving an open space (a *crack*) by hexagons. Three hexagons can be tightly packed without leaving a crack. Three pentagons, however, cannot be tightly packed. The reader may try this out. In three dimensions, four spheres pack tightly to form a tetrahedron. Twenty tetrahedrons can, with small distortions, fit tightly into an icosahedron. Icosahedrons have fivefold symmetry (five triangular faces meet at each vertex) and they *cannot* fit together tightly, i.e., complete space filling is not possible with them. An icosahedron, therefore, cannot serve as a unit cell for a crystalline structure. Therefore, structures, are known as quasi crystals.

1.3.6 Liquid Crystals

A liquid crystal is a state of matter that shares some properties of liquids and crystals. Like all liquids, liquid crystals are fluids; however, unlike ordinary liquids, which are isotropic, liquid crystals can be anisotropic. Liquid crystals are also called *mesophases*. The liquid

⁶ D. Schectman, I. A. Blech, D. Gratias, and J. W. Cahn, *Phys. Rev. Lett.*, 53 (1984) 1951.

crystalline state exists in a specific temperature range, below which the solid crystalline state prevails and above which the isotropic liquid state prevails. That is, the liquid crystal has an order between that of a liquid and a crystalline solid. In a crystalline solid, the atoms, ions, or molecules are arranged in an orderly manner. This very regular three-dimensional order is best described in terms of a crystal lattice. Because of a different periodic arrangement in different directions, most crystals are anisotropic. Now consider a crystal lattice with rod-shaped molecules at the lattice points. In this case, we now have, in addition to a positional order, an orientational order. An analogy that is used to qualitatively describe the order in a liquid crystal is as follows: If a random pile of pencils is subjected to an external force, it will undergo an ordering process very much akin to that seen in liquid crystals. The pencils, long and rigid, tend to align themselves, with their long axes approximately parallel. By far the most important characteristic of liquid crystals is that their long molecules tend to organize according to certain patterns. The order of orientation is described by a directed line segment called the *director*. This order is the source of the rather large anisotropic effect in liquid crystals, a characteristic that is exploited in electrooptical displays or the so-called liquid-crystal displays. Another important application of liquid crystals is the production of strong and stiff organic fibers such as aramid fiber, in which a rigid, rodlike molecular arrangement is provided by an appropriate polymer solution in the liquid crystalline state.⁷ When a polymer manifests the liquid crystalline order in a solution, we call it a *lyotropic* liquid crystal, and when the polymer shows the liquid crystalline state in the melt, it is called a *thermotropic* liquid crystal. The three types of order in the liquid crystalline state are nematic, smectic, and cholesteric, shown schematically in Figure 1.28. A nematic order is an approximately parallel array of polymer chains that remains disordered with regard to end groups or chain units; that is, there is no positional order along the molecular axis. Figure 1.28(a) shows this type of order, with the director vector n as indicated. In smectic order, we have one-dimensional, long-range positional order. Figure 1.28(b) shows smectic-A order, which has a layered structure with long-range order in the direction perpendicular to the layers. In this case, the director is perpendicular to the layer. Other more complex smectics are B, C, D, F, and G. The director in these may not be perpendicular to the layer, or there may exist some positional order as well. Cholesteric-type liquid crystals, shown in Figure 1.28(c), have nematic order with a superimposed spiral arrangement of nematic layers; that is, the director n , pointed along the molecular axis, has a helical twist.

1.3.7 Biological Materials and Biomaterials

The mechanical properties of biological materials are, of course, of great importance, and the design of all living organisms is optimized

⁷ See K. K. Chawla, *Fibrous Materials* (Cambridge, U.K.: Cambridge University Press, 1998).

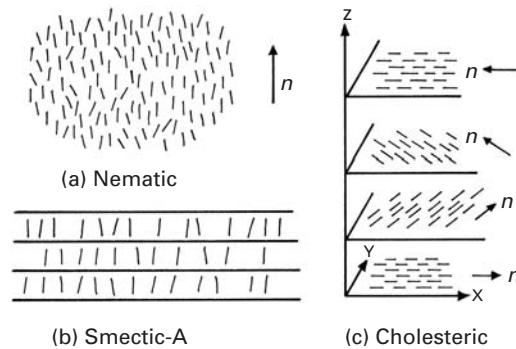
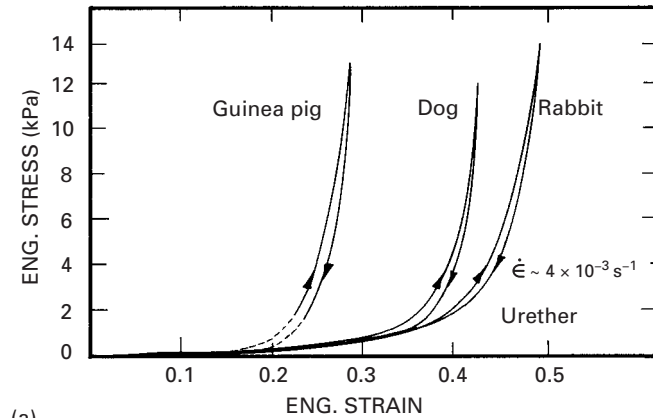


Fig. 1.28 Different types of order in the liquid crystalline state.

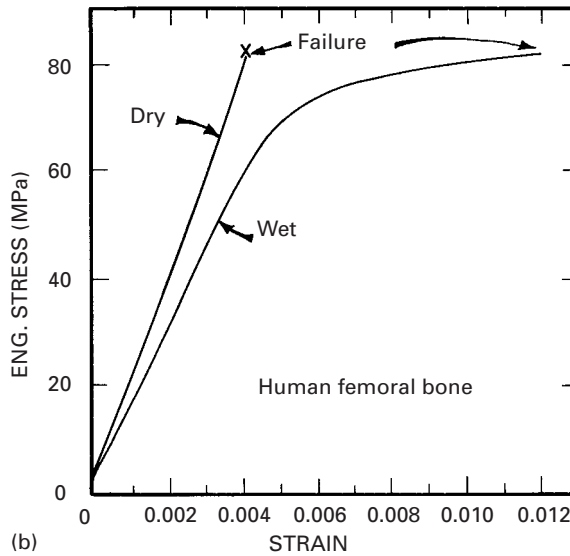
for the use of these properties. Biological materials cover a very broad range of structures. The common feature is the hierarchical organization of the structure, so that failure at one level does not generate catastrophic fracture: The other levels in the hierarchy “take up” the load. Figure 1.29 demonstrates this fact. Figure 1.29(a) shows the response of the urether of three animals: guinea pig, dog, and rabbit. This muscle is a thick-walled cylindrical tube that has the ability to contract until the closure of the inner hole is complete. With a nonlinear elastic mechanical response, the urether is not unlike other soft tissues in that regard: its stiffness increases with loading, and the muscle becomes very stiff after a certain strain is reached. The unloading and loading responses are different, as shown in the figure, and this causes a hysteresis. Increases in length of 50% can be produced. Bone, on the other hand, is a material with drastically different properties: its strength and stiffness are much higher, and its maximum elongation is much lower. The structure of bones is quite complex, and they can be considered composite materials. Figure 1.29(b) illustrates the strength (in tension) of dry and wet bone. The maximum tensile strength is approximately 80 MPa, and Young’s modulus is about 20 GPa.

The abalone shell and the shells of bivalve molluscs are often used as examples of a naturally occurring laminated composite material. These shells are composed of layers of calcium carbonate, glued together by a viscoplastic organic material. The calcium carbonate is hard and brittle. The effect of the viscoplastic glue is to provide a crack-deflection layer so that cracks have difficulty propagating through the composite. Figure 1.30 shows cracks that are deflected at each soft layer. The toughness of this laminated composite is vastly superior to that of a monolithic material, in which the crack would be able to propagate freely, without barriers. The effect is shown at two scales: the mesoscale and the microscale. At the mesoscale, layers of calcium carbonate have a thickness of approximately 500 μm . At the microscale, each calcium carbonate layer is made up of small brick-shaped units (about $0.5 \times 7.5 \mu\text{m}$ longitudinal section), glued together with the organic matter. The formation of this laminated composite results in a fracture toughness and strength

Fig. 1.29 Stress–strain curves for biological materials. (a) Urether. (After F. C. P. Yin and Y. C. Fung, *Am. J. Physiol.* 221 (1971), 1484.) (b) Human femur bone. (After F. G. Evans, *Artificial Limbs*, 13 (1969) 37.)



(a)



(b)

(about $4 \text{ MPa/m}^{1/2}$ and approximately 150 MPa , respectively) that are much superior to those of the monolithic CaCO_3 . The composite also exhibits a hierarchical structure; that is, the layers of CaCO_3 and organic glue exist at more than one level (at the micro- and mesolevels). This naturally occurring composite has served as inspiration for the synthesis of B_4C -Al laminate composites, which exhibit a superior fracture toughness.⁸ In these synthetic composites, there is a 40% increase in both fracture toughness and strength over monolithic B_4C -Al cermets. *Biomimetics* is the field of materials science in which inspiration is sought from biological systems for the design of novel materials.

Another area of biomaterials in which mechanical properties have great importance is bioimplants. Complex interactions between the

⁸ M. Sarikaya, K. E. Gunnison, M. Yasrebi, and I. A. Aksay, *Mater. Soc. Symp. Proc.*, 174 (1990) 109.

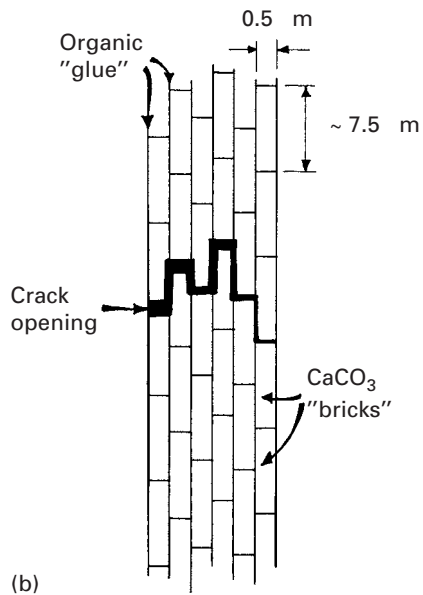
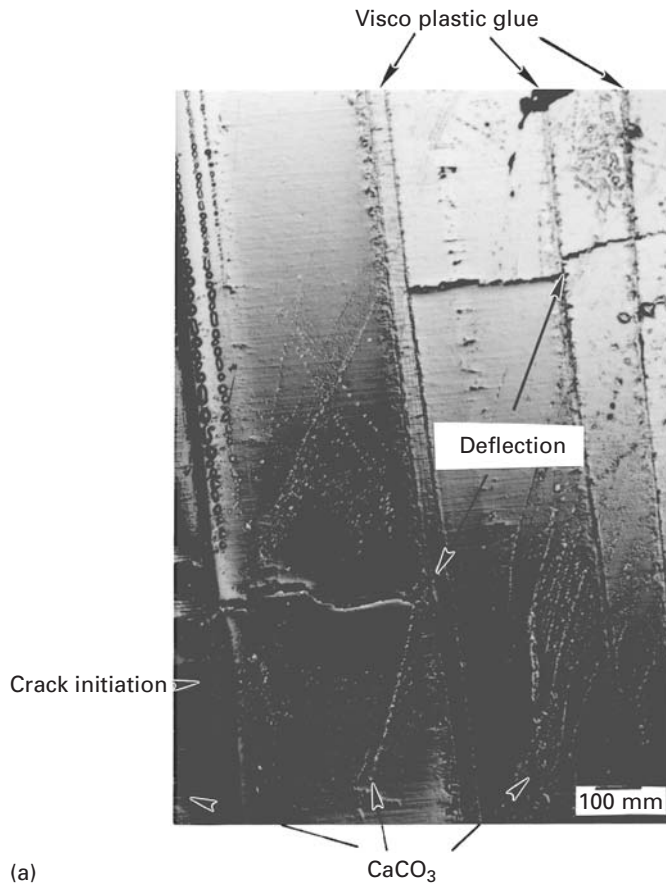


Fig. I.30 (a) Cross section of abalone shell showing how a crack, starting at left, is deflected by viscoplastic layer between calcium carbonate lamellae (mesoscale). (b) Schematic drawing showing arrangement of calcium carbonate in nacre, forming a miniature "brick and mortar" structure (microscale).

musculoskeletal system and these implants occur in applications where metals and ceramics are used as replacements for hips, knees, teeth, tendons, and ligaments. The matching of material and bone stiffness is important, as are the mechanisms of bonding tissue to these materials. The number of scientific and technological issues is immense, and the field of bioengineering focuses on these.

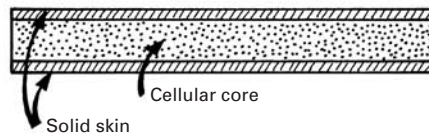
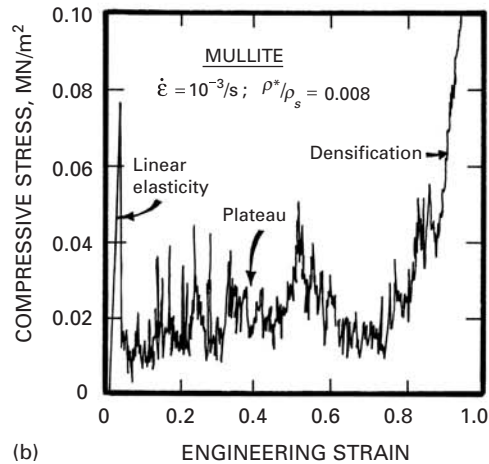
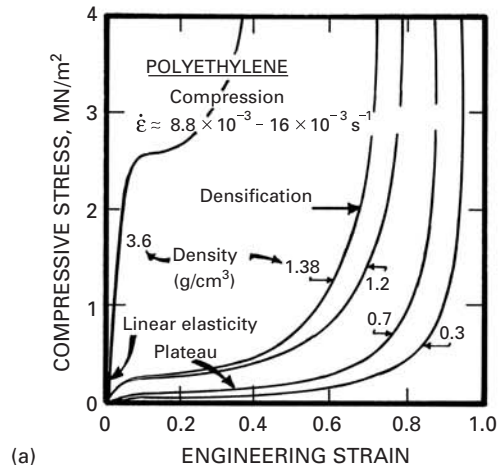
1.3.8 Porous and Cellular Materials

Wood, cancellous bone, styrofoam, cork, and insulating tiles of the Space Shuttle are examples of materials that are not compact; their structure has air as a major component. The great advantage of cellular structures is their low density. Techniques for making foam metals, ceramics, and polymers have been developed, and these cellular materials have found a wide range of applications, in insulation, in cushioning, as energy-absorbing elements, in sandwich panels for aircraft, as marine buoyancy components, in skis, and more.

The mechanical response of cellular materials is quite different from that of bulk materials. The elastic loading region is usually followed by a plateau that corresponds to the collapse of the pores, either by elastic, plastic buckling of the membranes or by their fracture. The third stage is an increase in the slope, corresponding to final densification. Figure 1.31(a) shows representative curves for polyethylene with different initial densities. The plateau occurs at different stress levels and extends to different strains for different initial densities. The bulk (fully dense) polyethylene is shown for comparison purposes. Cellular mullite, an alumina-silica solid solution, exhibits a plateau marked by numerous spikes, corresponding to the breakup of the individual cells (Figure 1.31(b)). Materials with initial densities as low as 5% of the bulk density are available as foams. Figure 1.31(c) shows a very important use of foams: Sandwich structures, composed of end sheets of solid material in which a foam forms the core region, have numerous applications in the aerospace industry. The foam between the two panels makes them more rigid; this is accomplished without a significant increase in weight.

There are many biological examples of sandwich structures. The toucan beak (Figure 1.32(a)) is a structure with very low density (0.04 g cm^{-3}) that consists of an external layer of compact keratin. Figure 1.32(b) shows the keratin layer. It is composed of superimposed scales. The inside of the toucan beak is a cellular material with extremely low density, Figure 1.33(b). The function of the cellular material is to provide structural rigidity to the system. In the absence of this foam, the external shell would buckle easily. Hence the toucan can fly without taking a nose dive.

As examples of foams in synthetic and naturally occurring materials, we show in Figure 1.33 two structures. Figure 1.33(a) shows an open-celled aluminum foam. We sectioned the beak of the toucan and observed that the inside is composed of a foam with similar length scale. Nature uses foams for the same purposes we do: to provide



(c) Sandwich structure

Fig. 1.31 Compressive stress–strain curves for foams. (a) Polyethylene with different initial densities. (b) Mullite with relative density $\rho^*/\rho_s = 0.08$. (Adapted from L. J. Gibson and M. F. Ashby, *Cellular Solids: Structure and Properties* (Oxford, U.K.: Pergamon Press, 1988), pp. 124, 125.) (c) Schematic of a sandwich structure.

rigidity to structures with the addition of minimal weight. In Chapter 12 we give a detailed analysis of stresses involved in foams.

1.3.9 Nano- and Microstructure of Biological Materials

Biological materials are more complex than synthetic materials. They form complex arrays, hierarchical structures, and are often multifunctional, i.e., one material has more than one function. For

Fig. I.32 (a) Toucan beak; (b) external shell made of keratin scales. (Courtesy of Y. Seki.)

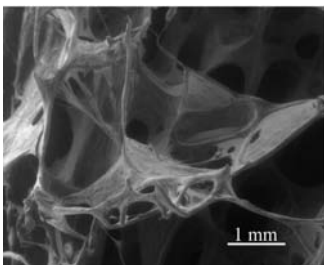
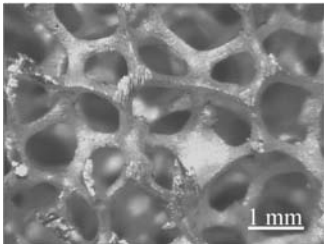
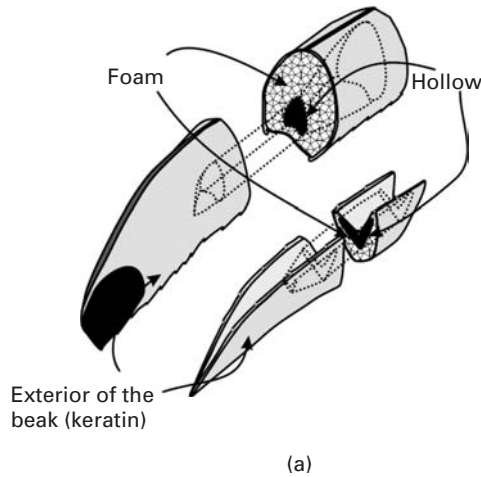
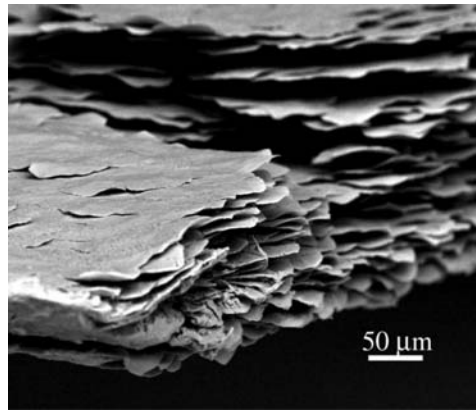


Fig. I.33 Cellular materials: (a) synthetic aluminium foam; (b) foam found in the inside of toucan beak. (Courtesy of M. S. Schneider and K. S. Vecchio.)



example, bone has a structural function and serves as a producer of red blood cells (in marrow). We classify biological materials, from the mechanical property viewpoint, into soft and hard. Hard materials provide the skeleton, teeth, and nails in vertebrates and the exoskeleton in arthropods. Soft biological materials build skin, muscle, internal organs, etc. Table 1.4 provides the distribution (on a weight percentage) of different constituents of the body.

Here are some examples of “hard” biological materials:

- Calcium phosphate (hydroxyapatite- $\text{Ca}_{10}(\text{PO}_4)_6(\text{OH})_2$): teeth, bone
- Chitin: nails
- Keratin: bird beaks, horn, hair
- Calcium carbonate (aragonite): mollusc shells, some reptile eggs (calcite): bird’s eggs, crustaceans, molluscs
- Amorphous silica ($\text{SiO}_2(\text{H}_2\text{O})_n$): spicules in sponges
- Iron oxide (Magnetite - Fe_3O_4): teeth in chitons (a weird-looking marine worm), bacteria.

Table 1.4 Occurrence of Different Biological Materials in the Body

Biological Material	Weight Percentage in Human Body
Proteins	17
Lipids	15
Carbohydrates	1
Minerals	7
DNA, RNA	2
Water	58

Of the above, iron oxide, calcium phosphate, silica, and iron oxide are minerals. Chitin and keratin are proteins.

Figure 1.34(a) shows the atomic arrangement of the calcium, phosphorus, and oxygen atoms in hydroxyapatite. The unit cell is quite complex and consists of four primitive hexagonal cells juxtaposed. We should remember that the hexagonal cell is composed of three primitive cells, brought together at their 120° angles ($3 \times 120 = 360$). In the case of the hydroxyapatite unit cell, there are four unit cells: two at the 60° angle and two at the 120° ($2 \times 60 + 2 \times 120 = 360$).

Figure 1.34(b) shows the aragonitic form of calcium carbonate. Aragonite has the orthorhombic structure. However, it is important to recognize that the minerals do not occur in isolation in living organisms. They are invariably intimately connected with organic materials, forming complex hierarchically structured composites. The resulting composite has mechanical properties that far surpass those of the monolithic minerals. Although we think of bone as a cellular mineral, it is actually composed of 60% collagen (on a volume percentage basis) and 30–40% hydroxyapatite (on a weight basis). If the mineral is dissolved away, the entire collagen framework is retained.

The principal organic building blocks in living organisms are the proteins. The word comes from Greek (*Proteios*) which means “of first rank” and indeed proteins play a key role in most physiological processes. The soft tissues in the body are made of proteins. As seen above, they are also an important component of biominerals. In order to fully understand proteins, we have to start at the atomic/molecular level, as we did for polymers.

Actually, proteins can be conceived of as polymers with a greater level of complexity. We start with amino acids, which are compounds containing both an amine ($-\text{NH}_2$) and a carboxyl ($-\text{COOH}$) group. Most of them have the following structure, where R stands for a radical:

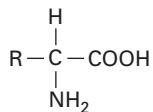


Fig. 1.34 Atomic structure of hydroxyapatite: (a) small white atoms (P), large gray atoms (O), black atoms (Ca). (b) Atomic structure of aragonite: large dark atoms (Ca), small gray atoms (C), large white atoms (O).

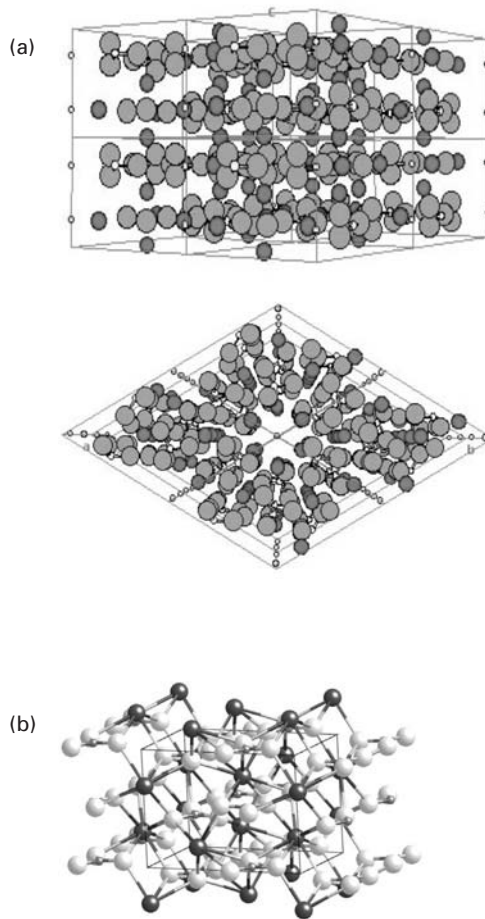


Table 1.5 shows eight main amino acids. There are currently 20 amino acids in proteins. In addition to these eight, we have the following: aspartic acid, glycine, methionine, asparagine, glutamine, arginine, threonine, valine, tyrosine, isoleucine, phenylalaline, and tryptophan.

In DNA, the four amino acids present are designated by the letters ACTG: adenine, cytosine, thymine, and guanine. In both DNA and proteins, these amino acids combine themselves by forming links between the carboxyl group of one amino acid and the amino group of another. These linear chains, similar to polymer chains, are called polypeptide chains. The polypeptide chains acquire special configurations because of the formation of bonds (hydrogen, van der Waals, and covalent bonds) between amino acids on the same or different chains. The two most common configurations are the alpha helix and the beta sheet. Figure 1.35(a) shows how an alpha helix is formed. The NH and CO groups form hydrogen bonds between them in a regular pattern, and this creates the particular conformation of the chain that is of helical shape. One such bond is shown in Figure 1.35(a). In

Table I.5 Eight Amino Acids Found in Proteins

Name	Chemical Formula
Alanine	$\begin{array}{c} \text{H} \quad \text{O} \\ \quad \\ \text{CH}_3 - \text{C} - \text{C} - \text{OH} \\ \\ \text{NH}_2 \end{array}$
Leucine	$\begin{array}{c} \text{CH}_3 \quad \quad \quad \text{O} \\ \diagdown \quad \diagup \quad \quad \\ \text{CH} - \text{CH}_2 - \text{C} - \text{COOH} \\ \diagup \quad \quad \quad \\ \text{CH}_3 \quad \quad \quad \text{NH}_2 \end{array}$
Phenylalanine	$\begin{array}{c} \text{CH}=\text{CH} \quad \quad \quad \text{H} \\ \diagdown \quad \diagup \quad \quad \quad \\ \text{CH} \quad \quad \quad \text{C} - \text{CH}_2 - \text{C} - \text{COOH} \\ \diagup \quad \quad \quad \\ \text{CH}-\text{CH} \quad \quad \quad \text{NH}_2 \end{array}$
Proline	$\begin{array}{c} \text{H} \\ \\ \text{CH}_2 - \text{CH}_2 - \text{C} - \text{COOH} \\ \quad \quad \quad \\ \text{CH}_2 \quad \quad \quad \text{N} - \text{H} \end{array}$
Serine	$\begin{array}{c} \text{H} \\ \\ \text{H} - \text{O} - \text{CH}_2 - \text{C} - \text{COOH} \\ \\ \text{NH}_2 \end{array}$
Cysteine	$\begin{array}{c} \text{H} \\ \\ \text{H} - \text{S} - \text{CH}_2 - \text{C} - \text{COOH} \\ \\ \text{NH}_2 \end{array}$
Glutamate	$\begin{array}{c} \text{O} \quad \quad \quad \text{H} \\ \quad \quad \quad \\ \text{O} - \text{C} - \text{CH}_2 - \text{CH}_2 - \text{C} - \text{COOH} \\ \quad \quad \quad \\ \quad \quad \quad \text{NH}_2 \end{array}$
Lysine	$\begin{array}{c} \text{H} \\ \\ \text{NH}_3 - \text{CH}_2 - \text{CH}_2 - \text{CH}_2 - \text{CH}_2 - \text{C} - \text{COOH} \\ \\ \text{NH}_2 \end{array}$

Figure 1.35(b) several hydrogen bonds are shown, causing the polypeptide chain to fold. The radicals stick out. This is shown in a clear fashion in Figure 1.36(a). The hydrogen bonds are also shown.

Another common conformation of polypeptide chains is the beta sheet. In this conformation, separate chains are bonded. Figure 1.36(b) shows two anti-parallel chains that are connected by hydrogen bonds. We can see that the radicals (large grey balls) of two adjacent chains stick out of the sheet plane on opposite sides. Successive chains can bond in such a fashion, creating pleated sheets.

Fig. 1.35 (a) Structure of alpha helix; dotted double lines indicate hydrogen bonds. (b) Structure of beta sheet with two anti-parallel polypeptide chains connected by hydrogen bonds (double-dotted lines).

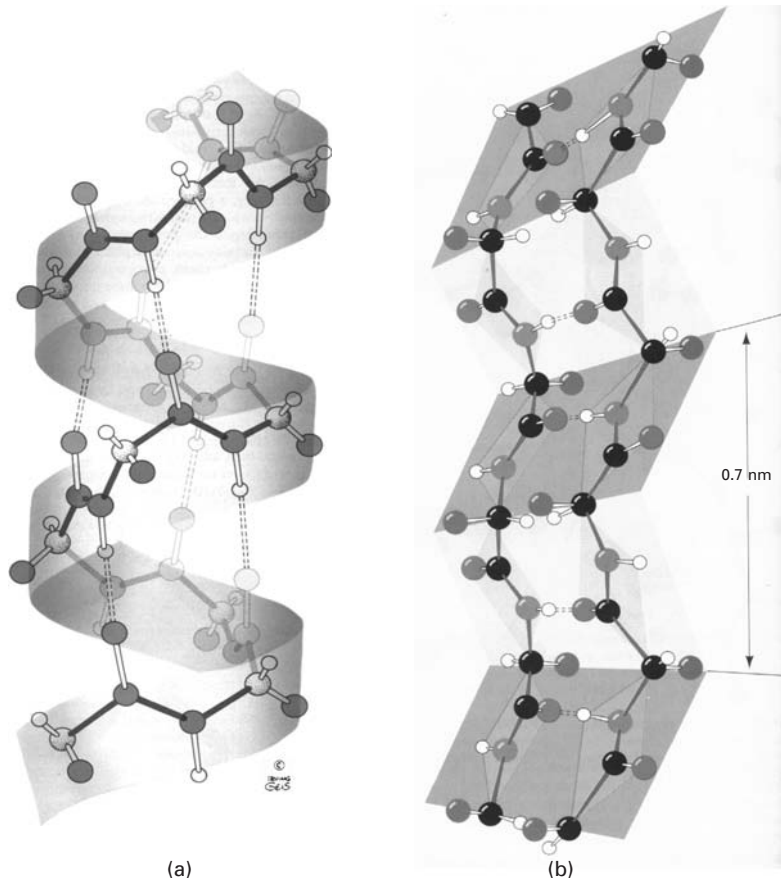
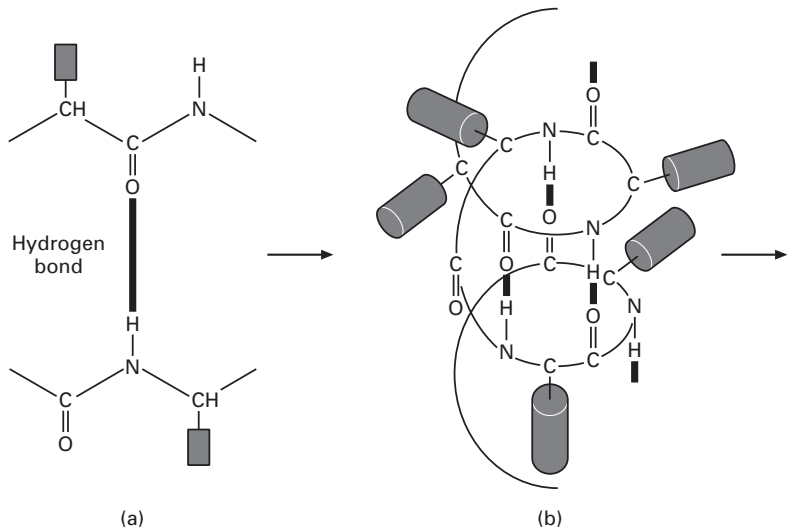


Fig. 1.36 (a) Hydrogen bond connecting a CO to an NH group in a polypeptide. (b) Successive hydrogen bonds on same polypeptide chain leading to formation of a helical arrangement. (Adapted from A. Vander, J. Sherman, D. Luciano, *Human Physiology*, 8th ed. (New York: McGraw Hill, 2001).)



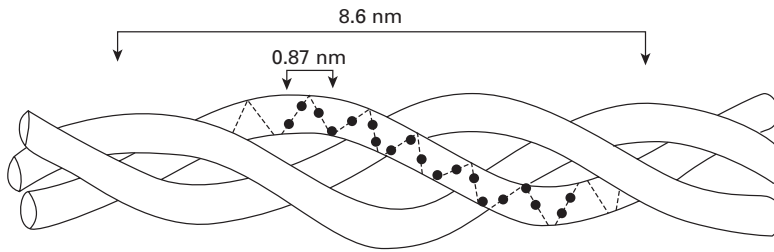


Fig. 1.37 Triple helix structure of collagen. (Adapted from Y. C. Fung, *Biomechanics: Mechanical Properties of Living Tissues* (Berlin: Springer, 1993).)

We describe below the most important proteins: collagen, actin, myosin, elastin, resilin and abductin, keratin, cellulose and chitin.

Collagen

Collagen is a rather stiff and hard protein. It is a basic structural material for soft and hard bodies; it is present in different organs and tissues and provides structural integrity. Fung⁹ compares it to steel, which is the principal load-carrying component in structures. In living organisms, collagen plays the same role: it is the main load-carrying component of blood vessels, tendons, bone, muscle, etc. In rats, 20% of the proteins are collagen. Humans are similar to rats in physiology and behavior, and the same proportion should apply. Figure 1.37 shows the structure of collagen. It is a triple helix, each strand being made up of sequences of amino acids. Each strand is itself a left-handed helix with approximately 0.87 nm per turn. The triple helix has a right-handed twist with a period of 8.6 nm. The dots shown in a strand in Figure 1.37 represent glycine and different amino acids. There are over 10 types of collagen, called Type I, II, X, etc. Fiber-forming collagens organize themselves into fibrils, Figure 1.38. Figure 1.38(c) is a transmission electron micrograph of tendon fibrils. Each fibril has transverse striations, which are spaced approximately 68 nm apart. These striations are caused by the staggering of the individual collagen molecules. This staggering is represented in a schematic manner in Figure 1.38(b). The length of each collagen molecule is 4.4 times the distance of stagger, 68 nm. This is equal to 300 nm. The diameter of the fibrils varies between 20 and 40 nm.

Fibrils, in turn, arrange themselves into fibers. Fibers are bundles of fibrils with diameters between 0.2 and 12 μm . In tendons, these fibers can be as long as the entire tendon. In tendons and ligaments, the collagen fibers form primarily one-dimensional networks. In skin, blood vessels, intestinal mucosa and the female vaginal tract, the fibers organize themselves into more complex patterns leading to two- and three-dimensional networks.

The hierarchical organization of a tendon starts with tropocollagen (a form of collagen), and moves up, in length scale, to fascicles. There is a crimped, or wavy structure shown in the fascicles that

⁹ Y. C. Fung, *Biomechanics: Mechanical Properties of Living Tissues* (Berlin, Springer, 1993)

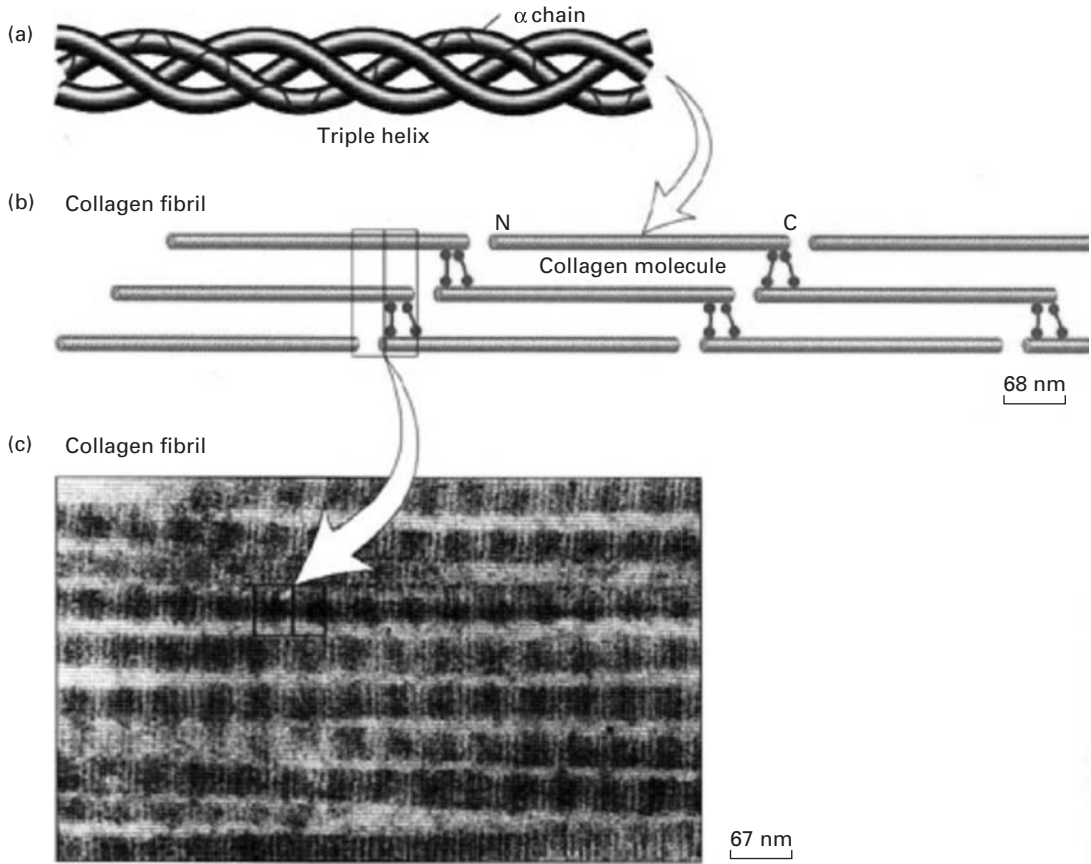


Fig. 1.38 Hierarchical organization of collagen, starting with triple helix, and going to fibrils. (From H. Lodish et al., *Molecular Cell Biology*, 4th ed. (New York, W.H. Freeman & Company, 1999).)

has an important bearing on the mechanical properties. Figure 1.39 shows an idealized representation of a wavy fiber. Two parameters define it: the wavelength $2l_0$ and the angle θ_0 . Typical values for the Achilles tendon of a mature human are $l_0 = 20\text{--}50\ \mu\text{m}$ and $\theta_0 = 6\text{--}8^\circ$. These bent collagen fibers stretch out in tension. When the load is removed, the waviness returns. When the tendon is stretched beyond the straightening of the waviness, damage starts to occur. Figure 1.40 shows a schematic stress–strain curve for tendons. The tendon was stretched until rupture. There are essentially three stages:

- Region I: toe part, in which the slope rises rapidly. This is the physiological range in which the tendon operates under normal conditions.
- Region II: linear part, with a constant slope.
- Region III: slope decreases with strain and leads to failure.

The elastic modulus of collagen is approximately 1 GPa and the maximum strain is in the 10–20% range. Cross-linking increases with age, and collagen becomes less flexible.

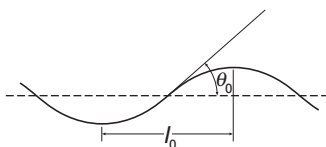


Fig. 1.39 Idealized configuration of a wavy collagen fiber.

Actin and Myosin

These are the principal proteins of muscles, leukocytes (white blood cells), and endothelial cells. Muscles contract and stretch

through the controlled gliding/grabbing of the myosin with respect to the actin fibers. Figure 1.41(a) shows an actin fiber. It is composed of two polypeptides in a helical arrangement. Figure 1.41(b) shows the myosin protein. It has little heart-shaped “grapplers” called cross-bridges. The tip of the cross-bridges bind and unbind to the actin filaments. Figure 1.41(c) shows the myosin and actin filaments, and the cross-bridges at different positions. The cross-bridges are hinged to the myosin and can attach themselves to different positions along the actin filaments as the actin is displaced to the left. Thus, the muscles operate by a micro-telescoping action of these two proteins.

Figure 1.42 shows how the filaments organize themselves into myofibrils. Bundles of myofibrils form a muscle fiber. The Z line represents the periodicity in the myosin–actin units (that are called sarcomeres) and is approximately equal to 3 μm in the stretched configuration. It shortens when the muscle is contracted. This gives the muscle a striated pattern when observed at high magnification. They resemble a coral snake in the microscope. Myofibrils have a diameter of approximately 1–2 μm .

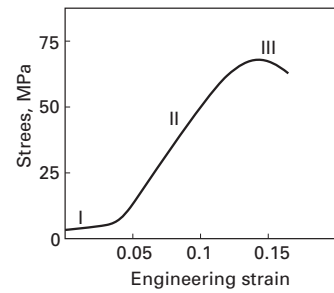


Fig. 1.40 Stress–strain curve of collagen with three characteristic stages.

Elastin

Elastin is found in skin, walls of arteries and veins, and lung tissue. A prominent place is in the “*ligamentum nuchae*,” a long ligament that runs along the top of the neck in horses and is constantly under tension. Other vertebrates have it too, but it is less pronounced. In this manner, the horse can keep the head up without using muscles. The “*ligamentum nuchae*” plays a role similar to the cables in a suspension bridge. It is a rather robust cylinder.

Resilin and Abductin

They are found in arthropods. They have properties similar to those of elastin, but occur in totally different animals and have a different structure.

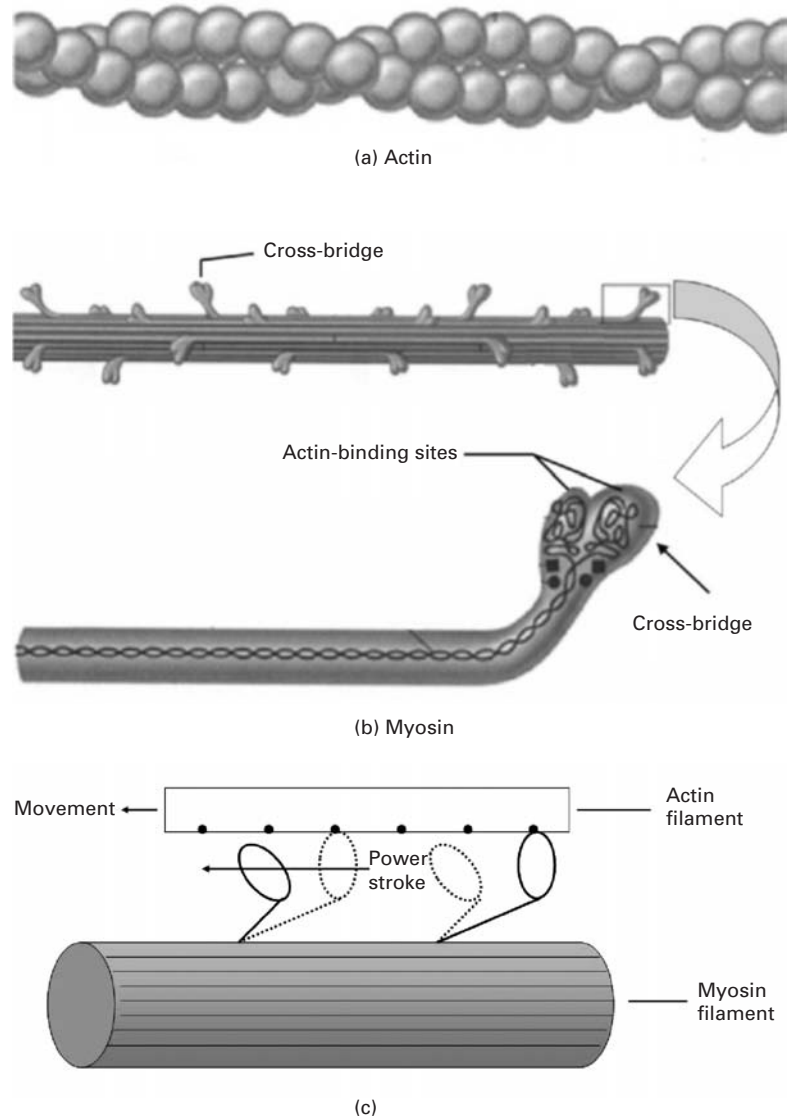
Keratin

Keratin is found in hair, horn, bird beaks and feathers, and whale baleen. The toucan beak presented in Section 1.3.8 is made of keratin. It has a structure similar to collagen (three interwoven helices). These helices combine themselves to form microfibrils with a diameter of 8 nm. Interestingly, it undergoes a phase transformation under tensile load, which increases its elongation.

Cellulose

Cellulose is the most abundant biological structural material, and is present in wood (which is a composite of cellulose and lignin) and cotton (almost pure cellulose). Cellulose is a cross-linked crystalline polymer. Its basic building block is a fibril with 3.5 nm diameter and 4 nm periodicity.

Fig. 1.41 Molecular structure of (a) actin and (b) myosin; (c) action of cross-bridges when actin filament is moved to left with respect to myosin filament; notice how cross-bridges detach themselves, then reattach themselves to actin.



Chitin

Chitin is a polysaccharide found in many invertebrates. The exoskeleton of insects is made of chitin.

Silk

Silk is composed of two proteins: fibroin (tough strands) and sericin, a gummy glue. The mechanical properties (strength and maximum elongation) can vary widely, depending on the application intended by the animal. For instance, among the silks produced by spiders are: dragline and spiral. Dragline, used in the radial components of the web, is the structural component, and has high tensile strength (600 MPa) and a strain at failure of about 6%. The spiral tangential

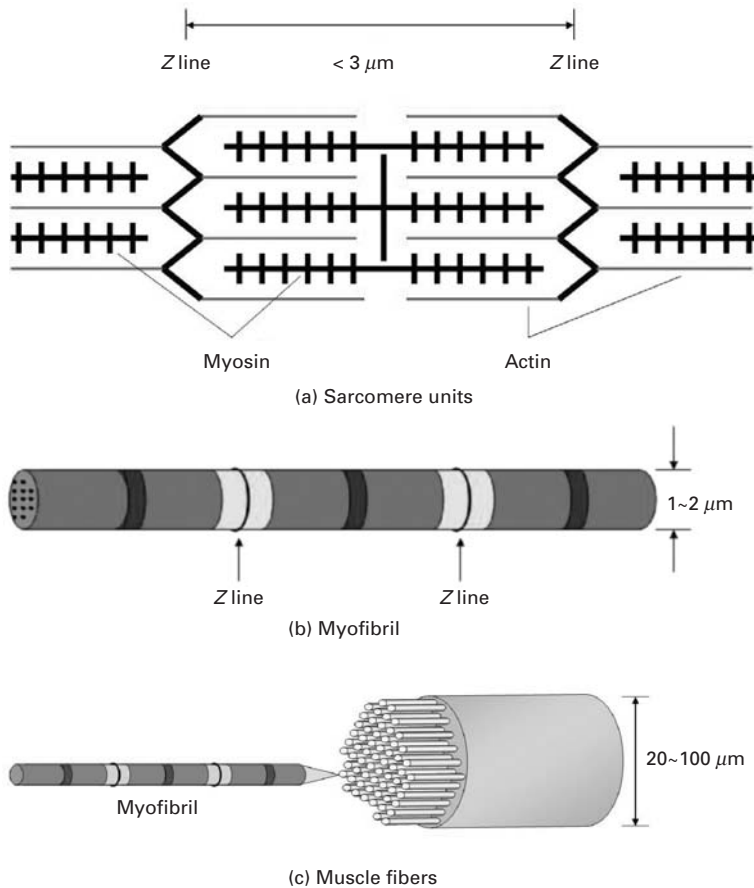


Fig. I.42 Structure of muscle, from (a) the sarcomere units, to (b) myofibril, and finally to (c) fibers.

components are intended to capture prey, and are “soft” and “sticky.” The strain at failure in this case can exceed 16, i.e. 1,600%.

Example I.11

Determine the maximum strain that the collagen fibers can experience without damage if their shape is as given in Figure 1.39 with a ratio between amplitude and wavelength of 0.2

We can assume a sine function of the form:

$$y = k \sin 2\pi x/\lambda.$$

The maximum of y is reached when $x = \pi/4$.

Hence:

$$y_{\max} = k = \lambda/5.$$

We can integrate over the length of the sine wave from 0 to 2π . However, this will lead to an elliptical integral of difficult solution. A simple approximation is to consider the shape of the wavy protein as an ellipse with major axis $2a$ and minor axis $2b$. The circumference is given by the

approximate expression (students should consult a mathematics text to obtain this expression):

$$L \approx \pi \left[\frac{3}{2}(a+b) - (ab)^{1/2} \right].$$

In the sine function, we have two arms, one positive and one negative. Their sum corresponds, in an approximate manner, to the circumference of the ellipse. The strain is equal to:

$$\varepsilon = \frac{L - 4a}{4a} = \frac{\pi \left[\frac{3}{2}(a+b) - (ab)^{1/2} \right] - 4a}{4a}.$$

Thus:

$$\varepsilon = \frac{\pi}{4} \left[\frac{3}{2} \left(1 + \frac{b}{a} \right) - \left(\frac{b}{a} \right)^{1/2} \right] - 1.$$

The following ratio is given:

$$\frac{b}{2a} = 0.2 \quad \text{and} \quad \frac{b}{a} = 0.4.$$

The corresponding strain is:

$$\varepsilon = 0.53.$$

Beyond this strain, the collagen will break.

1.3.10 The Sponge Spicule: An Example of a Biological Material

Marine sponges have long tentacles that are called spicules. These spicules act as antennas, which are subjected to marine currents and other stresses. These long silica rods have properties that dramatically exceed the strength of synthetic silica. Figure 1.43 shows the flexure strength of both spicule and synthetic silica. The difference in flexure strength between sponge spicule and synthetic silica is remarkable. The synthetic silica fractures at a relatively low stress of 200 MPa compared to the yield stress of the spicule at 870 MPa. The area under the stress-strain curve gives a reasonable idea of the toughness. Clearly the toughness of the spicule is many times higher than that of synthetic silica. As evidenced by Figure 1.43, failure does not occur catastrophically in the spicule. Instead, the spicule fails “gracefully,” which is a considerable advantage.

Figure 1.44 shows the microstructure of a fracture surface. The spicule consists of many concentric layers. This onion-like structure is responsible for the strengthening effect observed. When stress is applied to a silica rod, a crack will initiate at the weakest point in the material and propagate through the silica rod in a catastrophic manner. In contrast, crack propagation in the spicule will be arrested at each interface. This type of “graceful” failure is extremely useful. We can truly learn and apply this lesson from nature to modern material applications.

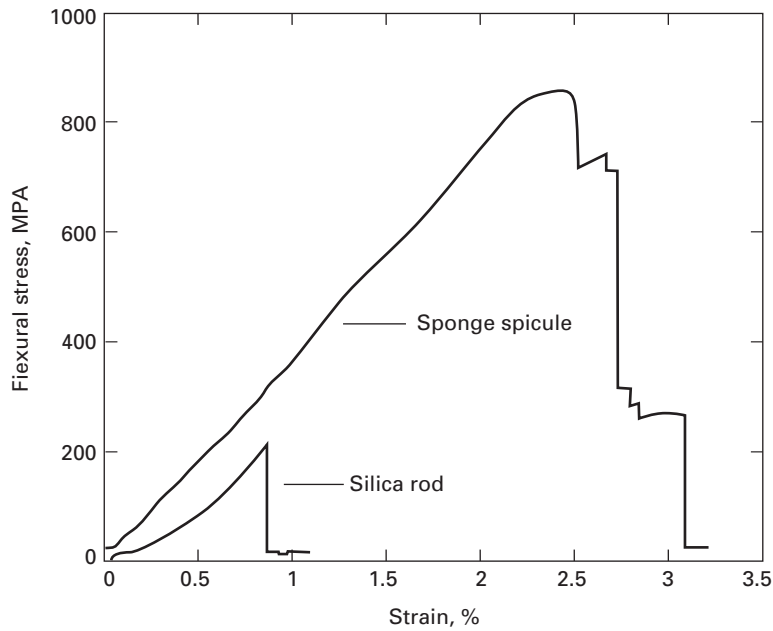


Fig. I.43 Stress-deflection responses of synthetic silica rod and sponge spicule in flexure testing. (Courtesy of M. Sarikaya and G. Mayer.)

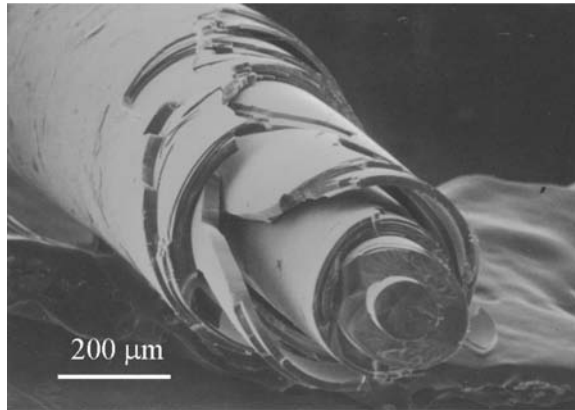


Fig. I.44 SEM of fractured sponge spicule showing two-dimensional concentric layers. (Courtesy of G. Mayer and M. Sarikaya.)

I.3.11 Active (or Smart) Materials

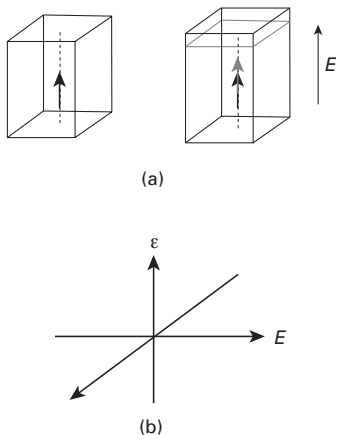
Technology puts greater and greater demand on materials and there is a constant push to develop materials with enhanced capabilities. The term *multifunctional materials* has been coined to describe materials with more than one capability. This is inspired by nature, where materials often have more than one function. For example, the trunk of a tree is at the same time a structural component and a carrier for the sap. Bones have a structural as well as a red-blood-producing function.

Another category of advanced materials are *active materials*. They are also called “smart” materials. Active materials have responses that can be used in all kinds of devices. Given below are the main classes of active materials.

- Shape memory alloys: The most common is a NiTi alloy known as Nitinol. It can undergo strains of 1–5% through a martensitic transformation that is reversible. A detailed description of these alloys is given in Chapter 11. There are numerous applications through two effects: the shape memory effect and the superelastic (or pseudo-elastic) effect: dental braces, stents, etc. They are presented in Chapter 11.
- Magnetorheological materials: These materials exhibit a viscosity that depends on an externally applied magnetic field. The suspension system of a US-made luxury automobile uses this material. The stiffness can be adjusted by varying the magnetic field.
- Piezoelectric ceramics and ferroelectricity:¹⁰ These materials generate an electric field when strained. Conversely, if an electric current is passed through them, they change their dimension. Barium titanate, lead zirconate titanate ($\text{Pb}(\text{Zr}, \text{Ti})\text{O}_3$) are examples. They have the perovskite structure with composition ABO_3 , where A and B are metals. They are characterized by a linear strain–electric field response. The maximum strain is on the order of 0.2%. Applications include vibration control, micropositioning devices, ultrasonics, and non-destructive evaluation.

It is a property of ferroelectrics to exhibit polarization in the absence of an electric field. Polarization is defined as dipole moment per unit volume or charge per unit area on the surface. The material is divided into domains, which are regions with uniformly oriented polarization. Ferroelectrics are characterized by a linear relationship between stress σ and polarization P :

$$P = d\sigma.$$



There is a converse relationship between strain ϵ and electric field, E :

$$\epsilon = dE,$$

where d is called the polarizability tensor. Figure 1.45(a) shows how the application of an externally applied electric field E results in a change in length of the specimen. Figure 1.45(b) shows the linear relationship between the strain and the field. This is a property of ferroelectric crystals, certain noncentrosymmetric crystals (e.g. quartz, ZnO), textured polycrystals, and polycrystals with a net spontaneous polarization. Applications include adaptive optics, active rotors and control surfaces, robotics, and MEMS/NEMS (microelectromechanical systems/nanoelectromechanical systems) actuators.

1.3.12 Electronic Materials

Electronic materials are composed, for the most part, of thin films arranged in several layers and deposited on a substrate. The most

Fig. 1.45 (a) Effect of applied field E on dimension of ferroelectric material. (b) Linear relationship between strain and electric field. (Courtesy of G. Ravichandran.)

¹⁰ K. Bhattacharya and G. Ravichandran, *Acta Mater.*, 51 (2003) 5941.

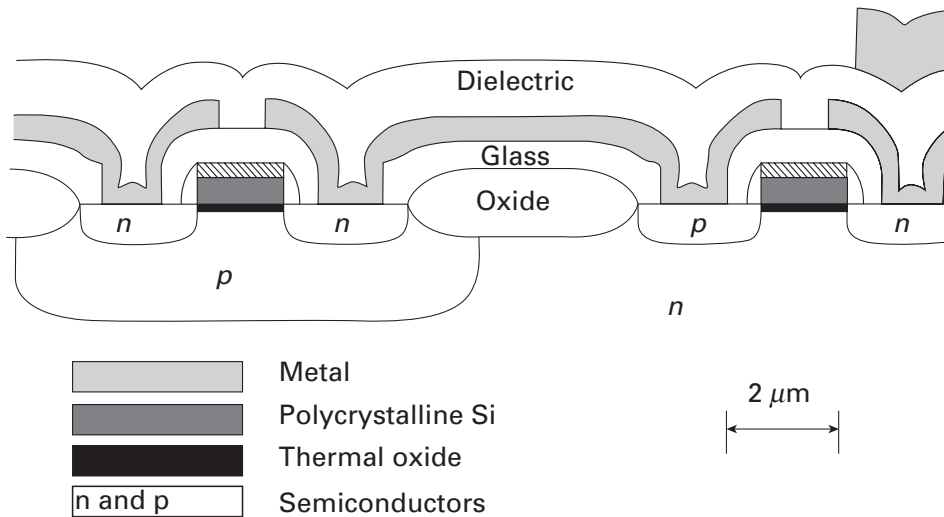


Fig. 1.46 Cross section of a complementary metal-oxide semiconductor (CMOS). (Adapted from W. D. Nix, *Met. Trans.*, 20A (1989) 2217.)

common substrate is monocrystalline silicon (the silicon wafer). Integrated circuits form the heart of modern computers and the silicon chip is a primary example. Figure 1.46 shows a schematic of the materials and structure used in a CMOS (complementary metal oxide semiconductor) transistor device. The *pn* junctions form transistors. The substrate is silicon, which in this case is *n* doped. The thin film layers are vapor deposited and there are a number of mechanical aspects that are of considerable importance. In Figure 1.46, we have monocrystalline and polycrystalline silicon, oxide, glass, metal, and a dielectric passivation layer.

The thin films deposited on the substrate have dimensions of a few nanometers to a few micrometers. These films may be under residual stresses as high as 500 MPa. These stresses are due to:

- Thermal expansion coefficient effects. When the film cools it contracts. The thermal expansion coefficients of the different layers can be different, creating internal stresses.
- Phase transformations. The phases in thin films are often non-equilibrium phases.

There are a number of mechanical problems associated with these stresses. Dislocations at the interface between substrate and thin film, cracking of the passivation layer, bending of the substrate/thin film system are a few examples. We will briefly describe these effects in chapters 2, 6, 9, and 13.

Magnetic hard disks are also made of thin films. The aluminum disk, upon which a thin layer of magnetic material is deposited, rotates at surface velocities approaching 80 km per hour, while the “head” flies aerodynamically over it. The distance between head and disk is as low as 0.3 μm. Some of the mechanical problems are friction, wear, and the unavoidable collisions between disk and head.

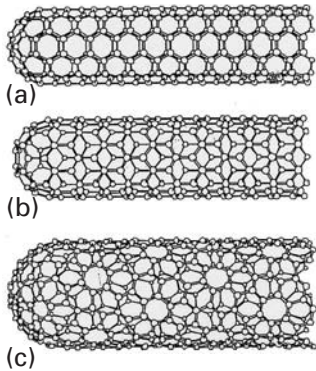


Fig. 1.47 Three configurations for single wall carbon nanotubes: (a) armchair; (b) “zig-zag”; (c) chiral. (Adapted from M. S. Dresselhaus, G. Dresselhaus, and R. Saito, *Carbon*, 33 (1995) 883.)

1.3.13 Nanotechnology^{11,12}

Nanotechnology refers to the structure and properties of materials and devices at the nanometer level. Developments in synthesis and characterization methods have resulted in materials that are designed from the “bottom up,” rather than from the “top down.” These terms were first used by the famous physicist Richard Feynman. The traditional method used in the design of new materials is to develop synthesis and processing techniques at the macro-scale, and then to carry out detailed characterization at the micrometer and nanometer scale. The new approach is to start with atoms, then assemble them into small arrays and characterize their structure and properties at that level. This approach was led by the semiconductor revolution. As the sizes of devices become smaller, we approach atomic dimensions. At that level, it is being found that many materials possess unique properties. Many biological processes also use the bottom-up approach. Atoms aggregate themselves into molecules and complex arrays through genetic messages. The atoms come together and self-organize themselves into complex arrays of amino acids, which in their turn form proteins. It is hoped that we will be able to fully harness this approach in the future. There are already applications of nanotechnology in the marketplace.

A material that is showing great potential because of unique characteristics is the carbon nanotube. The first nanotube was produced in Japan by S. Iijima. One can envisage a carbon nanotube by rolling a single layer of carbon atoms into a hollow cylinder. The ends can be semi-spherical caps (one half of a “Bucky-ball”). There are three morphologies for carbon nanotubes, shown in Figure 1.47: armchair, zig-zag, and chiral. They differ in the following:

- Armchair: the hexagons have the “pointy” side perpendicular to cylinder axis.
- Zig-Zag: the hexagons have the pointy side aligned with the cylinder axis.
- Chiral: The hexagons are inclined with respect to the cylinder axis, and the carbon sheet wraps itself helically around cylinder.

These carbon nanotubes have typically a diameter between 5 and 20 nm and length between 1 and 100 μm . They have outstanding mechanical properties, since they are based on the C-C bond, the strongest in nature. There are varying estimates of their strength, and values between 45 and 200 GPa are quoted. This would make them the strongest material known, ranking with diamond. Although the nanotubes are very short, one can envisage a day where continuous

¹¹ C. P. Poole and F. J. Owens, *Introduction to Nanotechnology* (Hoboken, NJ, Wiley-Interscience, 2003).

¹² M. Ratner and D. Ratner, *Nanotechnology* (Englewood Cliffs, NJ, Prentice Hall, 2003).

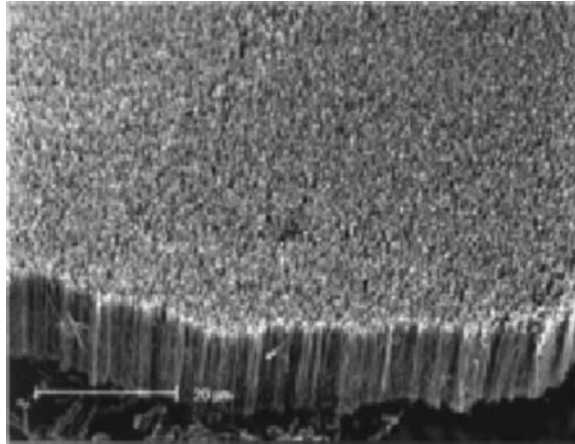


Fig. 1.48 Array of parallel carbon nanotubes grown as a forest. (From R. H. Baughman, A. A. Zakhidov and W. A. de Heer, *Science*, 297 (2002) 787.)

nanotubes are manufactured. Their incorporation as reinforcements in composites presents a bright prospect.

Figure 1.48 shows how arrays of parallel carbon nanotubes can be produced. The individual nanotubes, approximately $10\ \mu\text{m}$ in length, form a dense forest. The carbon nanotube is only one example of nanotechnology. The mechanical properties of metals are significantly increased when their grain size is reduced to the nanometer range. This topic, nanostructured materials, is treated in Chapter 5.

1.4 | Strength of Real Materials

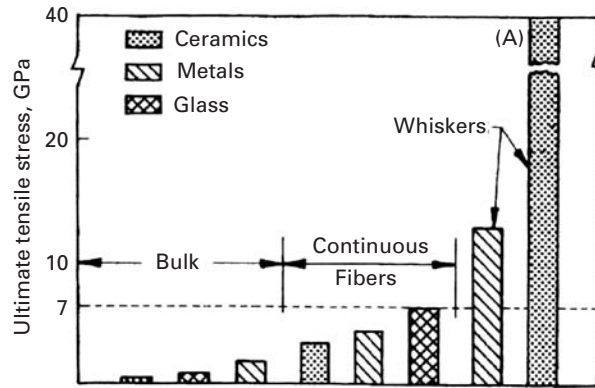
Materials deform and fail through defects. These defects (cracks, point defects, dislocations, twins, martensitic phase transformations, etc.) are discussed in chapters 4 through 8. The two principal mechanisms are crack growth and dislocations and plastic flow.

Crack growth: Real materials can have small internal cracks, at whose extremities high-stress concentrations are set up. Hence, the theoretical cleavage strength can be achieved at the tip of the crack at applied loads that are only a fraction of that stress. Griffith's theory (see Chapter 7) explains this situation very clearly. These stress concentrations are much lower in ductile materials, since plastic flow can take place at the tip of a crack, blunting the crack's tendency to grow.

Dislocations and plastic flow: Before the theoretical shear stress is reached, dislocations are generated and move in the material; if they are already present, they start moving and multiply. These dislocations are elementary carriers of plastic deformation and can move at stresses that are a small fraction of the theoretical shear stress. They will be discussed in detail in Chapter 4.

In sum, cracks prevent brittle materials from obtaining their theoretical cleavage stress, while dislocations prevent ductile materials from obtaining their theoretical shear stress.

Fig. 1.49 Theoretical strength of tridimensional materials, continuous fibers, and whiskers. The strength of the SiC whisker produced by the Philips Eindhoven Laboratory is indicated by (A).



To achieve the theoretical strength of a crystalline lattice, there are two possible methods: (1) eliminating all defects and (2) creating so many defects, that their interactions render them inoperative. The first approach has yielded some materials with extremely high strength. Unfortunately, this has been possible only in special configurations called “whiskers.” The second approach is the one more commonly pursued, because of the obvious dimensional limitations of the first; the strength levels achieved in bulk metals have steadily increased by an ingenious combination of strengthening mechanisms, but are still much lower than the theoretical strength. Maraging steels with useful strengths up to 2 GPa have been produced, as have patented steel wires with strengths of up to 4.2 GPa; the latter are the highest strength steels.

Figure 1.49 compares the ambient-temperature strength of tridimensional, filamentary, and whisker materials. The whiskers have a cross-sectional diameter of only a few micrometers and are usually monocrystalline (although polycrystalline whiskers have also been developed). Whiskers are one of the strongest materials developed by human beings. The dramatic effect of the elimination of two dimensions is shown clearly in Figure 1.49. The strongest whiskers are ceramics. Table 1.5 provides some illustrative examples. Iron whiskers with a strength of 12.6 GPa have been produced, compared with 2 GPa for the strongest bulk steels. The value 12.6 GPa is essentially identical to the theoretical shear stress, because the normal stress is twice the shear stress. In general, FCC whiskers tend to be much weaker than BCC whiskers and ceramics. For instance, Cu whiskers have a strength of about 2 GPa. This is consistent with the much lower theoretical shear strength exhibited by copper whiskers. It turns out that silver, gold, and copper have τ_{\max}/G ratios of 0.039 (see chapter 4). Hence, they are not good whisker materials. Figure 1.50 shows a stress-strain curve for a copper whisker. The specimen had a length between 2 and 3 mm and a cross-sectional diameter of 6.8 μm . The stress drops vertically after the yield point, with a subsequent plateau corresponding to the propagation of a Lüders band.

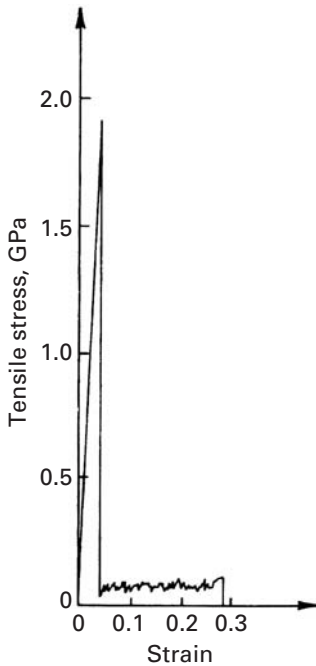


Fig. 1.50 Stress-strain curve of a copper whisker with a fiber direction $\langle 100 \rangle$. The whisker diameter is 6.8 μm . (Adapted with permission from K. Yoshida, Y. Goto, and M. Yamamoto, *J. Phys. Soc. Japan*, 21 (1966) 825.)

Table I.6 Tensile Strength of Whiskers at Room Temperature*

Material	Maximum Tensile Strength (GPa)	Young's Modulus (GPa)
Graphite	19.6	686
Al ₂ O ₃	15.4	532
Iron	12.6	196
SiC	20–40	700
Si	7	182
AlN	7	350
Cu	2	192

*Adapted with permission from A. Kelly, *Strong Solids* (Oxford, U.K.: Clarendon Press, 1973), p. 263.

In the elastic range, the curve deviates slightly from Hooke's law and exhibits some temporary inflections and drops (not shown in the figure). In many cases, for both metals and nonmetals, failure occurs at the elastic line, without appreciable plastic strain. When plastic deformation occurs, as, for example, in copper and zinc, a very large yield drop is observed. Although the strength of whiskers is not completely understood, it is connected to the absence of dislocations. It is impossible to produce a material virtually free of dislocations – in other words, perfect. However, for whiskers, dislocations can easily escape out of the material during elastic loading. Their density and mean free path are such that they will not interact and produce other sources of dislocation. Hence, the yield point is the stress required to generate dislocations from surface sources. The irregularities observed in the elastic range indicate that existing dislocations move and escape out of the whisker. At a certain stress, the whisker becomes essentially free of dislocations. When the stress required to activate surface sources is reached, the material yields plastically, or fails.

Example I.12

Calculate the stresses generated in a turbine blade if its cross-sectional area is 10 cm² and the mass of each blade is 0.2 kg.

This is an example of a rather severe environment where the material properties must be predicted with considerable detail. For example, the blade may be in a jet engine. Figure E1.12 shows a section of the compressor stage of a jet. The individual blades are fixed by a dovetail arrangement to the turbine vanes. Assume a rotational velocity $\omega = 10,000$ rpm and a mean radius $R = 0.5$ m. The centripetal acceleration in the bottom of each turbine blade is

$$a_c = \omega^2 R = \left[10,000 \times \frac{1}{60} \times 2\pi \right]^2 \times 0.5 = 5.4 \times 10^5 \text{ m/s}^2.$$

The stress that is generated is

$$\sigma = \frac{F}{A} = \frac{ma_c}{A} = \frac{0.2 \times 5.4 \times 10^5}{10 \times 10^{-4}} = 100 \text{ MPa,}$$

where F is the centripetal force and A is the cross-sectional area. This stress of 100 MPa is significantly below the flow stress of nickel-based superalloys at room temperature, but can be quite significant at higher temperatures.

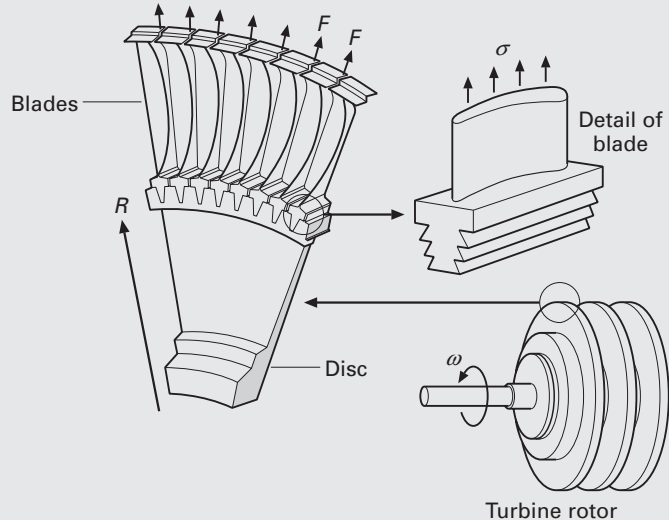


Fig. E1.12 Turbine blade subjected to centripetal force during operation.

Suggested Reading

Materials in General

- J. F. Shackelford. *Introduction to Materials Science for Engineers*, 4th ed. Upper Saddle River, NJ: Prentice Hall, 1996.
- W. F. Smith. *Principles of Materials Science and Engineering*, 3rd ed. New York, NY: McGraw Hill, 1996.
- D. R. Askeland and P. Phule. *The Science and Engineering of Materials*, 4th ed. Pacific Grove, CA: Thomson, 2003.
- W. D. Callister, Jr. *Materials Science and Engineering*, 4th ed. New York, NY: Wiley, 2003.

Metals

- C. S. Barrett and T. B. Massalski. *Structure of Metals*, 3rd rev. ed. Oxford: Pergamon, 1980.
- M. A. Meyers and K. K. Chawla. *Mechanical Metallurgy*. Englewood Cliffs, NJ: Prentice-Hall, 1984.

Ceramics

- W. D. Kingery, H. K. Bowen, and D. R. Uhlmann. *Introduction to Ceramics*, 2nd ed. New York, NY, J. Wiley, 1976.
- Y.-M. Chiang, D. Birnie III, and W. D. Kingery, *Physical Ceramics*, New York, NY: J. Wiley, 1997.

Polymers

- D. C. Bassett. *Principles of Polymer Morphology*. Cambridge, U.K.: Cambridge University Press, 1981.
- A. Hiltner (ed.). *Structure-Property Relationships of Polymeric Solids*. New York, NY: Plenum Press, 1983.
- R. J. Young. *Introduction to Polymers*. London: Chapman & Hall, 1986.
- B. Wunderlich. *Macromolecular Physics, Vol. 1: Crystal Structure*. New York, NY: Academic Press, 1973.
- B. Wunderlich. *Macromolecular Physics, Vol. 2: Crystal Nucleation*. New York, NY: Academic Press, 1976.

Composite Materials

- K. K. Chawla. *Composite Materials: Science & Engineering*. 2nd ed. New York, NY: Springer, 1998.
- K. K. Chawla. *Ceramic Matrix Composites*, 2nd ed. Boston, MA: Kluwer, 2003
- N. Chawla and K. K. Chawla. *Metal Matrix Composites*, New York, NY: Springer, 2006.

Liquid Crystals

- A. Ciferri, W. R. Krigbaum, and R. B. Meyer, eds. *Polymer Liquid Crystals*. New York, NY: Academic Press, 1982.

Biomaterials

- M. Elices (ed.). *Structural Biological Materials*, Amsterdam: Pergamon, 2000.
- J. F. V. Vincent. *Structural Biomaterials*. Princeton, NJ: Princeton University Press, 1991.
- Y. C. Fung. *Biomechanics: Mechanical Properties of Living Tissues*. New York, NY: Springer, 1981.

Cellular Materials

- L. J. Gibson and M. F. Ashby. *Cellular Solids: Structure and Properties*. Oxford, U.K.: Pergamon Press, 1988.

Electronic Materials

- W. D. Nix. Mechanical Properties of Thin Films, *Met. Trans.*, 20A (1989) 2217.
- L. B. Freund and S. Suresh. *Thin Film Materials: Stress, Defect Formation and Surface Evolution*. Cambridge, U.K.: Cambridge University Press, 2003

Exercises

1.1 A jet turbine rotates at a velocity of 7,500 rpm. Calculate the stress acting on the turbine blades if the turbine disc radius is 70 cm and the cross-sectional area is 15 cm². Take the length to be 10 cm and the alloy density to be 8.5 g/cm³.

1.2 The material of the jet turbine blade in Problem 1.1, Superalloy IN 718, has a room-temperature yield strength equal to 1.2 GPa; it decreases with temperature as

$$\sigma = \sigma_0 \left(1 - \frac{T - T_0}{T_m - T_0} \right),$$

where T_0 is the room temperature and T_m is the melting temperature in K ($T_m = 1,700$ K). At what temperature will the turbine flow plastically under the influence of centripetal forces?

1.3

- (a) Describe the mechanical properties that are desired in a tennis racket, and recommend different materials for the different parts of the racket.
- (b) Describe the mechanical properties that are desired in a golf club, and recommend different materials for the different parts of the club.

1.4 On eight cubes that have one common vertex, corresponding to the origin of axes, draw the family of $\{111\}$ planes. Show that they form an octahedron and indicate all $\langle 110 \rangle$ directions.

1.5 The frequency of loading is an important parameter in fatigue. Estimate the frequency of loading (in cycles per second, or Hz) of an automobile tire in the radial direction when the car speed is 100 km/h and the wheel diameter is 0.5 m.

1.6 Indicate, by their indices and in a drawing, six directions of the $\langle 112 \rangle$ family.

1.7 The density of Cu is 8.9 g/cm³ and its atomic weight (or mass) is 63.546. It has the FCC structure. Determine the lattice parameter and the radius of atoms.

1.8 The lattice parameter for W(BCC) is $a = 0.32$ nm. Calculate the density, knowing that the atomic weight (or mass) of W is 183.85.

1.9 Consider the unit cell of the CsCl which has NaCl structure. The radius of Cs⁺ is 0.169 nm and that of Cl is 0.181 nm. (a) Determine the packing factor of the structure, assuming that Cs⁺ and Cl⁻ ions touch each other along the diagonals of the cube. (b) Determine the density of CsCl if the atomic weight of Cs is 132.905 and of Cl is 35.453.

1.10 MgO has the same structure as NaCl. If the radii of O²⁻ and Mg²⁺ ions are 0.14 nm and 0.070 nm, respectively, determine (a) the packing factor and (b) the density of the material. The atomic weight of O₂ is 16 and that of Mg is 24.3.

1.11 Germanium has the diamond cubic structure with interatomic spacing of 0.245 nm. Calculate the packing factor and density. (The atomic weight of germanium is 72.6.)

1.12 The basic unit (or mer) of polytetrafluoroethylene (PTFE) or Teflon is C₂F₄. If the mass of the PTFE molecule is 45,000 amu, what is the degree of polymerization?

1.13 Using the representation of the orthorhombic unit cell of polyethylene (see Figure E1.13), calculate the theoretical density. How does this value compare with the density values of polyethylene obtained in practice?

1.14 A pitch blend sample has five different molecular species with molecular masses of 0.5×10^6 , 0.5×10^7 , 1×10^7 , 4×10^7 , and 6×10^7 . Compute the number-averaged molecular weight and weight-averaged molecular weight of the sample.

1.15 Different polymorphs of a material can have different mechanical properties. Give some examples.

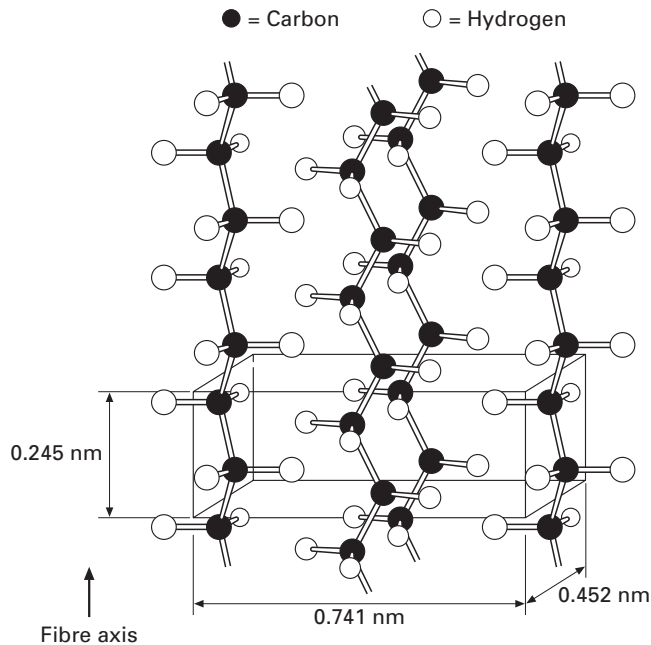


Fig. E1.13 Crystalline form of polyethylene with orthorhombic unit cell.

1.16 What are smart materials? Give some examples.

1.17 What are glass-ceramics? Explain their structure and properties. (Hint: Think of Corning ware.)

1.18 Explain how the scale of microstructure can affect the properties of a material. Use steel, an alloy of iron and carbon as an example.

1.19 For a cubic system, calculate the angle between

- (a) $[100]$ and $[111]$,
- (b) $[111]$ and $[112]$,
- (c) $[112]$ and $[221]$.

1.20 Recalculate the bicycle stiffness ratio for a titanium frame. (See Examples 1.1 and 1.2) Find the stiffness and weight of the bicycle if the radius of the tube is 25 mm. Use the following information:

Alloy: Ti–6% Al–4% V,

$$\sigma_y = 1,150 \text{ MPa},$$

$$\text{Density} = 4.5 \text{ g/cm}^3,$$

$$E = 106 \text{ GPa},$$

$$G = 40 \text{ GPa}.$$

1.21 Calculate the packing factor for NaCl, given that $r_{\text{Na}} = 0.186 \text{ nm}$ and $r_{\text{Cl}} = 0.107 \text{ nm}$.

1.22 Determine the density of BCC iron structure if the iron atom has a radius of 0.124 nm.

1.23 Draw the following direction vectors in a cubic unit cell:

$$\text{a } [100] \text{ and } [110], \text{ b } [112], \text{ c } [\bar{1}10], \text{ d } [3\bar{2}\bar{1}].$$

1.24 Calculate the stress generated in a turbine blade if its cross-sectional area is 0.002 m^2 and the mass of each blade is 0.5 kg . Assume that the rotational velocity $\omega = 15,000 \text{ rpm}$ and the turbine disk radius is 1 m .

1.25 Suppose that the turbine blade from the last problem is part of a jet turbine. The material of the jet turbine is a nickel-based superalloy with the yield strength, $\sigma_y = 1.5 \text{ GPa}$; it decreases with temperature as

$$\sigma = \sigma_0 \left[1 - \frac{(T - T_0)}{(T_m - T_0)} \right],$$

where $T_0 = 293 \text{ K}$ is the room temperature and $T_m = 1,550 \text{ K}$ is the melting temperature. Find the temperature at which the turbine will flow plastically under the influence of centripetal forces.

1.26 Calculate the lattice parameter of Ni(FCC) knowing that the atomic diameter of nickel is 0.249 nm .

1.27 A jet turbine blade, made of MARM 200 (a nickel-based superalloy) rotates at $10,000 \text{ rpm}$. The radius of the disk is 50 mm . The cross-sectional area is 20 cm^2 and the length of the blade is equal to 12 cm . The density of MARM 200 is 8.5 g/cm^3 .

- What is the stress acting on the turbine blade in MPa?
- If the room temperature strength of MARM 200 is equal to 800 MPa , what is the maximum operational temperature in kelvin?

The yield stress varies with temperature as:

$$\sigma = \sigma_0 \left[1 - \left(\frac{(T - T_0)}{(T_m - T_0)} \right)^m \right],$$

where T_m is the melting temperature ($T_m = 1,700 \text{ K}$) and T_0 is the room temperature; $m = 0.5$.

1.28 Generate a three-dimensional unit cell for the intermetallic compound AuCu_3 that has a cubic structure. The Au atoms are at the cube corners and the Cu atoms at the center of the faces. Given:

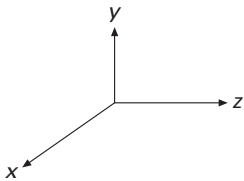
$$r_{\text{Cu}} = 0.128 \text{ nm A.N. } \text{Cu} = 63.55 \text{ amu}$$

$$r_{\text{Au}} = 0.144 \text{ nm A.N. } \text{Au} = 196.97 \text{ amu}$$

- Find the lattice parameter in nanometers.
- What is the atomic mass of the unit cell in grams?
- What is the density of the compound in g/cm^3 ?

1.29 Draw the following unit cells with the planes (one plane per cube with the coordinate axes shown below):

- $(\bar{1}01)$,
- $(\bar{1}\bar{1}1)$,
- $(0\bar{1}2)$,
- (301) .



Ex1.29

1.30 Show how the atoms pack in the following planes by drawing circles (atoms) in the appropriate spots:

- (111) in FCC,
- (110) in FCC,
- (111) in BCC,
- (110) in BCC.

1.31 BET is a technique for measuring the surface area of particles, which is of obvious importance in nanomaterials. Describe this technique. Don't forget to mention what the acronym BET stands for.

1.32 "Tin plate" is one of the largest tonnage steel products. It is commonly used for making containers. If it is a steel product why is it called tin plate?

1.33 Using Figure 1.7, list the important symmetry operations in the following crystal systems:

- (a) Triclinic,
- (b) Monoclinic,
- (c) Orthorhombic.

1.34 The only possible rotation operations that can be used to define crystal systems are rotations of type $n = 1, 2, 3, 4,$ and 6 . Using other values of n will result in unit cells which, when joined together, will not fill all space. Demonstrate this by giving a simple mathematical proof. (*Hint: consider two lattice points separated by a unit translation vector.*)

1.35 Calculate the APF (atomic packing factor) for BCC and FCC unit cells, assuming the atoms are represented as hard spheres. Do the same for the diamond cubic structure.

1.36 Draw the following crystallographic planes in BCC and FCC unit cells along with their atoms that intersect the planes:

- (a) (101),
- (b) (110),
- (c) (441),
- (d) (111),
- (e) (312).

1.37 A block copolymer has macromolecules of each polymer attached to the other as can be seen in Figure 1.22(c). The total molecular weight is 100,000 g/mol. If 140 g of A and 60 g of B were added, determine the degree of polymerization for each polymer. A: 56 g/mol; B: 70 g/mol.

1.38 Sketch the following planes within the unit cell. Draw one cell for each solution. Show new origin and ALL necessary calculations.

- (a) $(0\bar{1}\bar{1})$,
- (b) (102),
- (c) (002),
- (d) $(1\bar{3}0)$,
- (e) $(\bar{2}12)$,
- (f) $(3\bar{1}\bar{2})$.

1.39 Sketch the following directions within the unit cell. Draw one cell for each solution. Show new origin and ALL necessary calculations.

- (a) [101],
- (b) $[0\bar{1}0]$,
- (c) $[12\bar{2}]$,
- (d) [301],
- (e) $[\bar{2}01]$,
- (f) $[2\bar{1}3]$.

1.40 Suppose we introduce one carbon atom for every 100 iron atoms in an interstitial position in BCC iron, giving a lattice parameter of 0.2867 nm. For the Fe-C alloy, find the density and the packing factor.

Given:

Atomic mass of C = 12,

Atomic mass of Fe = 55.89,

$a(\text{Fe}) = 0.2867 \text{ nm}$,

Avogadro's number, $N = 6.02 \times 10^{23}$.

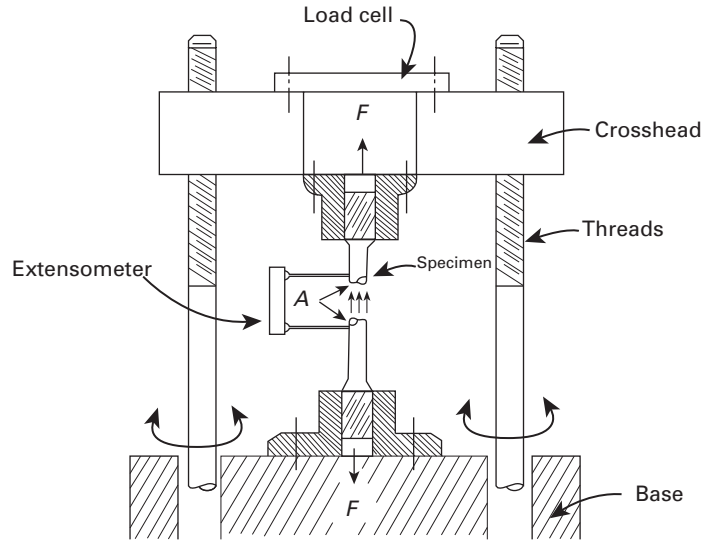
1.41 Determine the maximum length of a polymer chain made with 1,500 molecules of ethylene, knowing that the carbon bond length is 0.13 nm.

Elasticity and Viscoelasticity

2.1 Introduction

Elasticity deals with elastic stresses and strains, their relationship, and the external forces that cause them. An *elastic strain* is defined as a strain that disappears instantaneously once the forces that cause it are removed. The theory of elasticity for Hookean solids – in which stress is proportional to strain – is rather complex in its more rigorous treatment. However, it is essential to the understanding of micro- and macromechanical problems. Examples of the former are stress fields around dislocations, incompatibilities of stresses at the interface between grains, and dislocation interactions in work hardening; examples of the latter are the stresses developed in drawing, and rolling wire, and the analysis of specimen-machine interactions in testing for tensile strength. This chapter is structured in such a way as to satisfy the needs of both the undergraduate and the graduate student. A simplified treatment of elasticity is presented, in a manner so as to treat problems in an undergraduate course. Stresses and strains are calculated for a few simplified cases; the tridimensional treatment is kept at a minimum. A graphical method for the solution of two-dimensional stress problems (the Mohr circle) is described. On the other hand, the graduate student needs more powerful tools to handle problems that are somewhat more involved. In most cases, the stress and strain systems in tridimensional bodies can be better treated as tensors, with the indicial notation. Once this tensor approach is understood, the student will have acquired a very helpful visualization of stresses and strains as tridimensional entities. Important problems whose solutions require this kind of treatment involve stresses around dislocations, interactions between dislocations and solute atoms, fracture mechanics, plastic waves in solids, stress concentrations caused by precipitates, the anisotropy of individual grains, and the stress state in a composite material.

Fig. 2.1 Sketch of screw-driven tensile-strength testing machine.



2.2 Longitudinal Stress and Strain

Figure 2.1 shows a cylindrical specimen being stressed in a machine that tests materials for tensile strength. The upper part of the specimen is screwed to the crosshead of the machine. The coupled rotation of the two lateral screws causes the crosshead to move. The load cell is a transducer that measures the load and sends it to a recorder; the increase in length of the specimen can be read by strain gages, extensometers, or, indirectly, from the velocity of motion of the crosshead. Another type of machine, called a servohydraulic machine, is also used. Assuming that at a certain moment the force applied on the specimen by the machine is F , there will be a tendency to “stretch” the specimen, breaking the internal bonds. This breaking tendency is opposed by internal reactions, called *stresses*. The best way of visualizing stresses is by means of the method of analysis used in the mechanics of materials: The specimen is “sectioned,” and the missing part is replaced by the forces that it exerts on the other parts. This procedure is indicated in the figure. In the situation shown, the “resistance” is uniformly distributed over the normal section and is represented by three modest arrows at A. The normal stress σ is defined as this “resistance” per unit area. Applying the equilibrium-of-forces equation from the mechanics of materials to the lower portion of the specimen, we have

$$\begin{aligned}\sum F &= 0 \\ F - \sigma A &= 0 \\ \sigma &= \frac{F}{A}.\end{aligned}\tag{2.1}$$

This is the internal resisting stress opposing the externally applied load and avoiding the breaking of the specimen. The following

stress convention is used: Tensile stresses are positive and compressive stresses are negative. In geology and rock mechanics, on the other hand, the opposite sign convention is used because compressive stresses are much more common.

As the applied force F increases, so does the length of the specimen. For an increase dF , the length l increases by dl . The normalized (per unit length) increase in length is equal to

$$d\varepsilon = \frac{dl}{l},$$

or, upon integration,

$$\varepsilon = \int_{l_0}^{l_1} \frac{dl}{l} = \ln \frac{l_1}{l_0}, \quad (2.2)$$

where l_0 is the original length. This parameter is known as the *longitudinal true strain*.

In many applications, a simpler form of strain, commonly called *engineering* or *nominal strain*, is used. This type of strain is defined as

$$\varepsilon_n = \varepsilon_e = \frac{\Delta l}{l_0} = \frac{l_1}{l_0} - 1. \quad (2.2a)$$

In materials that exhibit large amounts of elastic deformation (rubbers, soft biological tissues, etc.) it is customary to express the deformation by a parameter called “stretch” or “stretch ratio.” It is usually expressed as λ :

$$\lambda = \varepsilon_e + 1.$$

Hence, deformation starts at $\lambda = 1$.

When the strains are reasonably small, the engineering (or nominal) and true strains are approximately the same. We will use subscripts t for true values and e for engineering values. It can be easily shown that

$$\varepsilon_t = \ln(1 + \varepsilon_e). \quad (2.2b)$$

The elastic deformation in metals and ceramics rarely exceeds 0.005, and for this value, the difference between ε_t and ε_e can be neglected.

In a likewise fashion, a *nominal* (or *engineering*) stress is defined as

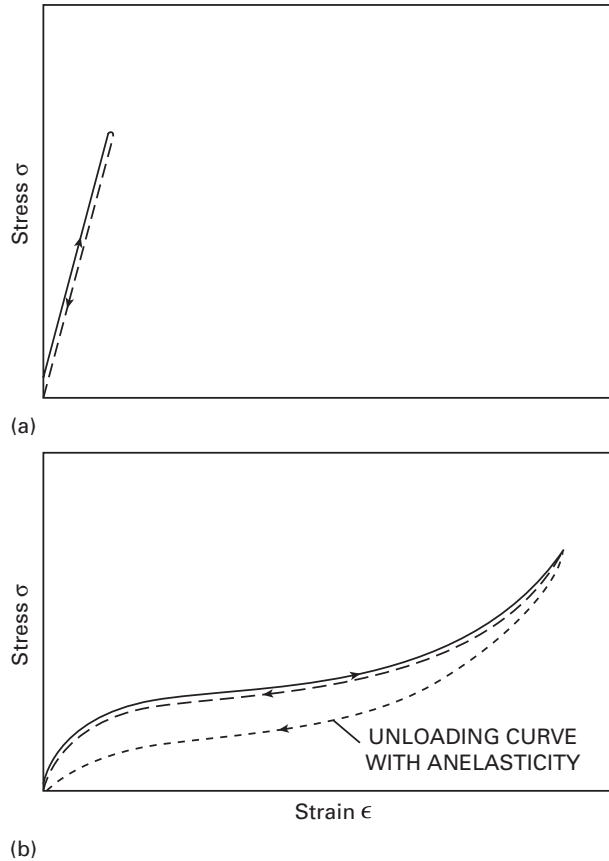
$$\sigma_e = \frac{F}{A_0}, \quad (2.2c)$$

where A_0 is the original area of cross-section.

The relationship between the true stress and the engineering stress is

$$\frac{\sigma_t}{\sigma_e} = \frac{A_0}{A}.$$

Fig. 2.2 Stress–strain curves in an elastic regimen. (a) Typical curve for metals and ceramics. (b) Typical curve for rubber.



During elastic deformation, the change in cross-sectional area is less than 1% for most metals and ceramics; thus $\sigma_e \cong \sigma_t$. However, during plastic deformation, the differences between the true and the engineering values become progressively larger. More details are provided in Chapter 3 (Section 3.1.2).

The sign convention for strains is the same as that for stresses: Tensile strains are positive, compressive strains are negative. In Figure 2.2, two stress–strain curves (in tension) are shown; both specimens exhibit elastic behavior. The solid lines describe the loading trajectory and the dashed lines describe the unloading. For perfectly elastic solids, the two kinds of lines should coincide if thermal effects are neglected. The curve of Figure 2.2(a) is characteristic of metals and ceramics; the elastic regimen can be satisfactorily described by a straight line. The curve of Figure 2.2(b) is characteristic of rubber; σ and ϵ are not proportional. Nevertheless, the strain returns to zero once the stress is removed. The reader can verify this by stretching a rubber band. First, you will notice that the resistance to stretching increases slightly with extension. After considerable deformation, the rubber band “stiffens up,” and further deformation will eventually lead to rupture. The whole process (except failure) is elastic. A